Tolga Özdemir

Computational toolkit for early-stage cost assessment and optimisation of BIPV façades

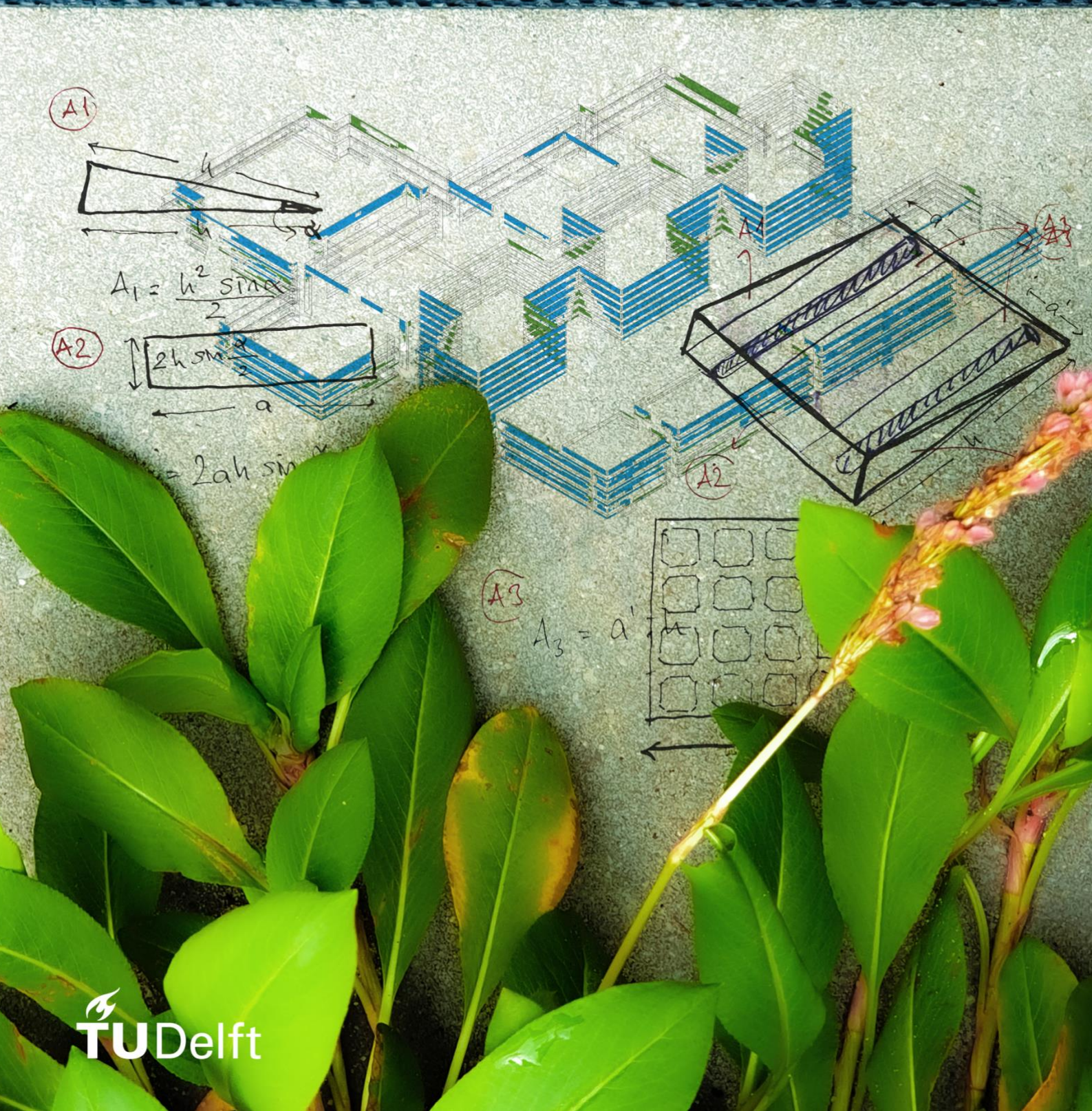

TU Delft

Computational toolkit for early-stage cost assessment and optimisation of BIPV façades

By

Tolga Özdemir

To obtain the degree of Master of Science
at the Delft University of Technology,
to be defended publicly on Monday July 6, 2020 at 13:30.

Student number:	4843959	
Thesis committee:	Dr. ir. P. Nourian,	TU Delft, supervisor
	Ir. A. Snijders,	TU Delft
	Ir. G. Coumans,	TU Delft

TU Delft

Acknowledgements

I would like to express my thankfulness to my graduation committee for their continuous support: Dr Ir. Pirouz Nourian, my supervisor: Ir. Annebregje Snijders, my tutor and Ir. Geert Coumans, my examiner. All I learnt was made possible by them.

My completion of this graduation work could not have been possible without the efforts of Prof. Dr Ir. Arch. Sevil Sarıyıldız. I cannot thank her enough for believing in me and encouraging me in the most challenging times.

Without the guidance of Prof. Dr Ayşe Zerrin Yılmaz, I would not have been in TU Delft in the first place. I would like to word my gratitude to my valuable professor for broadening my horizon.

Many thanks to Dr-to-be Gizem Yılmaz, for helping me connect my profession with engineering economics and optimisation; for spending time trying to understand my problems in work and pulling me on the right track.

Thanks to my friends Berk Ekici, Berra Şule Kılıç and Mehmet Kısa, for the good memories that made life in the Netherlands so much fun; Dilşad Dağtekin, Çağdaş Mıdıklı and Zeynep Oğuzhan, for being as close as an online call for constructive view exchanges; Gökhan Yüksel, for reminding me to think about the best move forward; Mert Keleş, for always being there for me, no matter how far we fall physically and for how long.

Everyday support of Ecem Tarancı made me keen to overcome the challenges that I face and remain peaceful while doing so. My special thanks to her.

Last but not least, I would like to thank my nuclear family sincerely: my father, for his teachings; my brother, for sitting coding with me; and my mother, for showing me what is more substantial in life and for her tremendous emotional support.

Table of Contents

List of Figures

List of Tables

Abbreviatons

AMC	Academisch Medisch Centrum
CHP	Combined heat and power
PV	Photovoltaic
BIPV	Building-integrated photovoltaics
BAPV	Building-applied photovoltaics
a-Si	Amorphous silicon
c-Si	Crystalline silicon
CdTe	Cadmium telluride
CIGS	Copper indium gallium selenide
GaAs	Gallium arsenide
OPV	Organic photovoltaic
EVA	Ethylene vinyl acetate
PVB	Polyvinyl butyral
TPSE	Thermoplastic silicone elastomer
AR	Anti-reflective
DC	Direct current
AC	Alternative current
PWM	Pulse-width modulation
MPPT	Maximum power point tracker
NPV	Net present value
LCoE	Levelized cost of electricity / energy
TVM	Time value of money

1. Introduction

1.1. Abstract

Reduction of energy consumption and to increase its generation is necessary, as the population lives in urban settlements consume three-quarters of global resources, and these numbers are continually growing. Building-integrated photovoltaic panels (BIPV) which would assist for the resolution of the problem can be applied by replacing the façade cladding with BIPV panels whenever possible. The optimum orientation of PV panels for the Netherlands is south with an angle of 37°, which maximises total electricity production. While the process is simple for new buildings and systems installed in areas with no orientation restrictions or horizon obstructions, the scenario becomes more challenging in urban settlements. As the premises cannot be reoriented in an urban context, solutions may be finding the best places to install BIPV panels on the façade and tilting them. This process can be deployed simultaneously with the building refurbishment that is needed to reach the current envelope insulation standards. Tilting can increase the energy yield, but this would increase the production costs and thus, initial investment costs. The balance between energy yield and added production costs can be found by locating the right panel in the right place on a limited budget. In this study, an early-stage computational design method to optimally allocate and reorient BIPV façade modules to reach a cost-effective and applicable solution is presented. The method was tested in a case setting of a concrete façade retrofit.

1.2. Context

Half of the global population lives in urban areas and consume 75 per cent of the world's resources, and these numbers are continually increasing. This necessitates the reduction of energy consumption and raising its generation. Urban environments face new challenges about the integration of photovoltaic (PV) systems onto the building envelope sustainably. Many buildings in the Netherlands are being refurbished, and their insulation properties are improved (Konstantinou, 2014). A concept to employ building integrated photovoltaic panels (BIPV) is to replace the façade cladding with BIPV panels whenever possible.

An aspect to take into consideration when designing a cost-effective BIPV system is the orientation and tilt of the panels as the energy yield would be maximum when the sun is directly perpendicular to them. The optimum orientation of the PV panel for the Netherlands is south with an angle of 37°, which maximises total electricity production. While the process is quite straightforward for new buildings and systems deployed in areas with no orientation restrictions or horizon obstructions, the scenario becomes more challenging in urban settlements (Freitas et al., 2015).

As the buildings cannot be reoriented in an urban context, a solution may be tilting the cladding panels attached to the façade. However, this would increase the initial investment costs as more material and labour would be needed. So, employing this strategy in the right place with right angles would assist in reaching a cost-effective solution.

1.2.1. Societal relevance

As much as renewable energy solutions are vital for ecological sustainability, there are challenges adopting them in urban settlements. Conventional energy is still cheaper in urban environments (Konstantinou, 2014). However, finding ways to benefit from PV energy as much as possible can change the trends of the energy source preference.

1.2.2. Scientific relevance

The optimum angles for PV panels have been investigated for the Netherlands, and there is adequate know-how about the fabrication of complex façades. Together with the existing solar modelling algorithms and financial assessment methods, this study aims to help early-stage design decisions.

1.2.3. Motivation

Many projects are being developed to promote renewable energy usage, but few of them can be realised due to cost-related challenges. The motivation of this study is to contribute to finding cost-effective BIPV solutions to apply in areas where renewable energy generation is less prevalent.

1.3. Objectives, deliverables and research questions

The main objective of this thesis is to deliver a computational design methodology for early-stage design development of BIPV-façade systems to reach a cost-effective and applicable solution, in combination with different cladding materials. The method was integrated and tested in the AMC Amsterdam case. Several sub-objectives are determined as follows:

- To discover the energy performance improvement options of the AMC external walls and the building's solar electricity generation potential.
- To discover façade system options for the BIPV retrofit of the concrete external walls of the AMC Amsterdam, allowing different façade cladding options.
- To elaborate on the relation between energy yield benefits and added costs of custom-made BIPV panels.
- To investigate the financial aspect of BIPV usage in combination with other façade materials, such as façades with vegetation.
- To deliver a computational design methodology to maximise the energy yield of BIPV panels by proper allocation and tilting on a limited budget.

The main research question and the sub-questions are as follows:

How can the cost-effectivity of an early-stage BIPV design be assessed and optimised computationally within the frame of the AMC case?

- Which measures can be taken to improve the energy performance of the AMC Amsterdam's external walls and what is the solar electricity potential of the building?
- Which façade systems can be used for BIPV retrofit to the AMC's concrete external walls, in combination with other cladding options?

- What may be the energy yield benefit compared to the added costs of custom-made BIPV-panels?
- What is the financial aspect of BIPV usage in combination with other façade materials, such as façades with vegetation?
- To what extent can the proposed computational design methodology maximise the profits on a limited budget?

1.4. Scope

This study is established mainly within the domains of Architecture and Computer Science, particularly optimisation. Since it involves a façade design to be cost-effectively produced and aims to gain maximum energy yield, it also makes use of the knowledge from the domains of Engineering Economics for financial assessment and Physics, for solar analyses. However, this information remains on the level of acknowledged data and assumptions. Within the domain PV technology, no electrical engineering problem will be addressed. A diagram showing how these domains intersect can be seen in Figure 1.

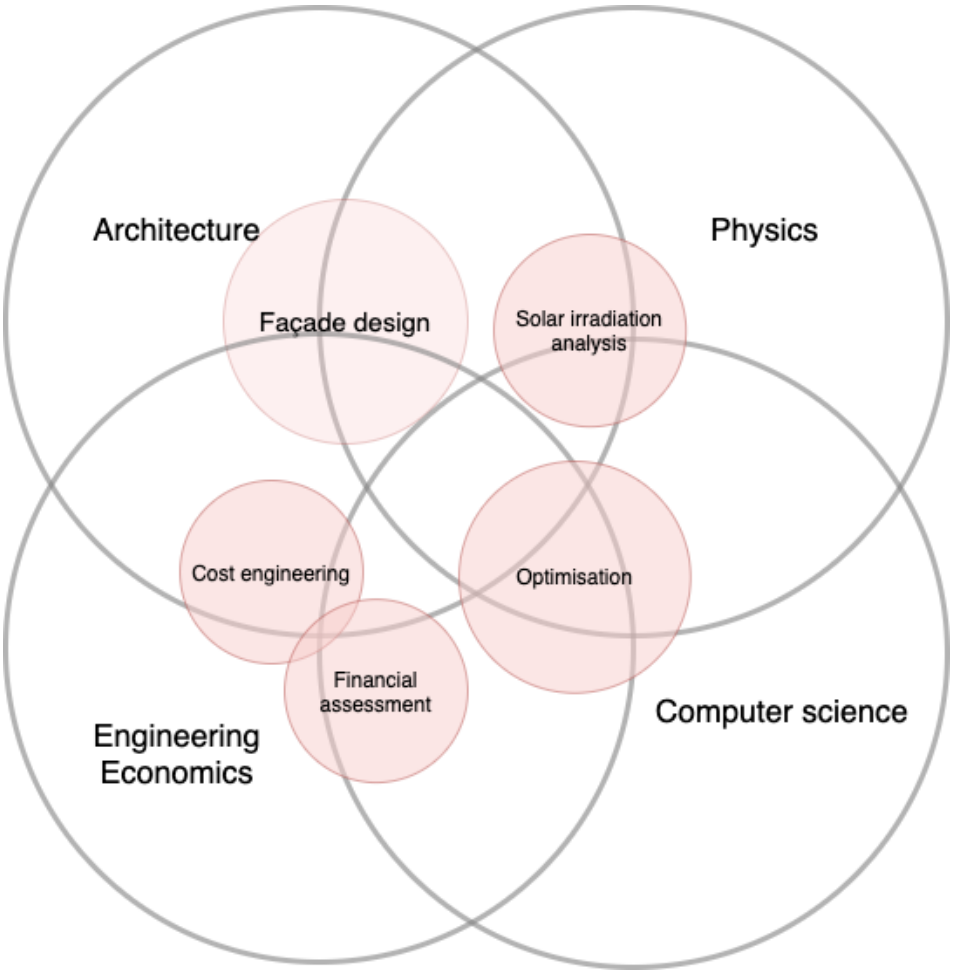

Figure 1: Diagram showing the relations of the research domains.

1.5. Problem statement

There is a need for adopting renewable energy generation strategies in urban settlements. A relatively simple way of doing so is replacing the façade claddings with BIPV panels

when improving the insulation properties of buildings. In urban settlements, it is not always easy to have PV panels optimally oriented to the South with a 37° tilt. The yield can be increased by minor rotations of the modules. However, this would increase the production costs and thus, initial investment costs. Furthermore, the façade system can allow other cladding options such as green façades. These aspects must be made clear for the investor to ensure applicability. We aim to deliver a methodology including analytic, design and computational assessment and optimisation components for the planning of cost-effective BIPV solutions.

1.6. Research methodology

Starting with a case study of the AMC Amsterdam in terms of façade thermal properties and energy generation potential, we defined and targeted the main problems in the context. A suitable design was made, which also constitutes the base for the optimisation problem. The prepared algorithm and scripts were used to test the scenarios to answer the research questions. Proper changes will be made according to the feedbacks, and the study will be documented. The flowchart of the research methodology can be seen in Figure 2.

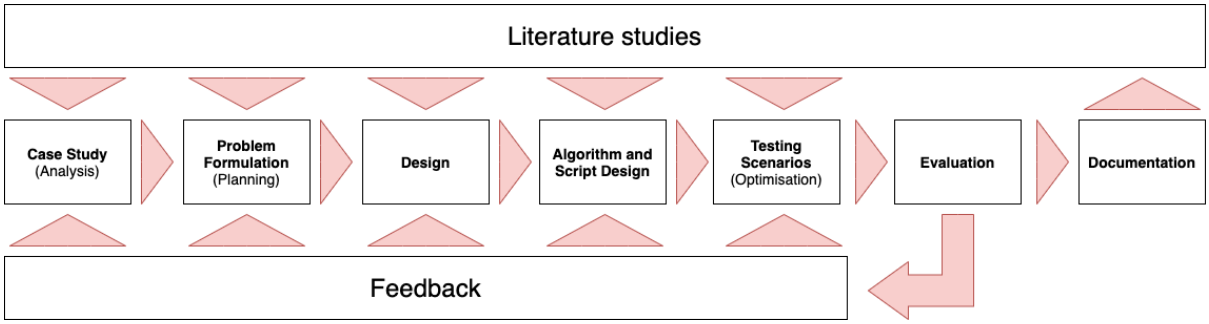

Figure 2: Flowchart of the research methodology.

1.7. Literature

This is the first phase of the literature review. The concepts of Performance-Based Design and Research by Design were investigated in Scopus and Google Scholar platforms with keywords such as "performance-based design", "performance approach".

The efficiency improvement which can be achieved through the orientation of photovoltaic systems was investigated with the keywords "BIPV" and "PV efficiency" with "orientation", "optimum angle" and "tilting". For a more comprehensive design base, the state-of-art applications in the building market were investigated both in the aforementioned platforms and also Google. The keywords such as "modularity", "standardisation", "flexibility" with "BIPV façades", "green façades" and even "restoration", "renovation" and "retrofit" were used.

"Engineering economics" textbooks, especially Engineering Economic Analysis (Newnan et al., 2004) from Oxford University Press, were consulted for a better understanding of the application.

1.8. Design methodology

The overall design process started with the analysis. In this phase, we analysed the thermal properties of the current façades and running a comprehensive solar irradiance analysis on the façades and the roofs. Compositions of different façades were investigated for a better understanding of the construction and to gain insight into whether any existing component can be kept. Based on the literature studies, we decided upon possible materials which can be used alongside BIPV and started collecting price information.

Followingly, we planned the design by elaborating on how the construction can be conducted and defining the basic design rules, such as the final façade materials and how the thermal improvement would be made. In the main design phase, we determined our standard grid dimensions, in which the panel options would fit. We elaborated on how the PV-cell layout in the modules may be and did a study on tilted panels to determine the tilting style. We also aimed to find a design base by interpreting currently used techniques and products for our design.

In the optimisation part, the remaining research questions were answered over scenarios. We calculated the performance of flat and tilted BIPV panels using the financial metrics net present value (NPV) and levelized cost of energy (LCoE). These calculations consider the time value of money (TVM). These were chosen as performance criteria to ensure that the proposed solutions are cost-effective. The diagram of the design steps is shown in Figure 3.

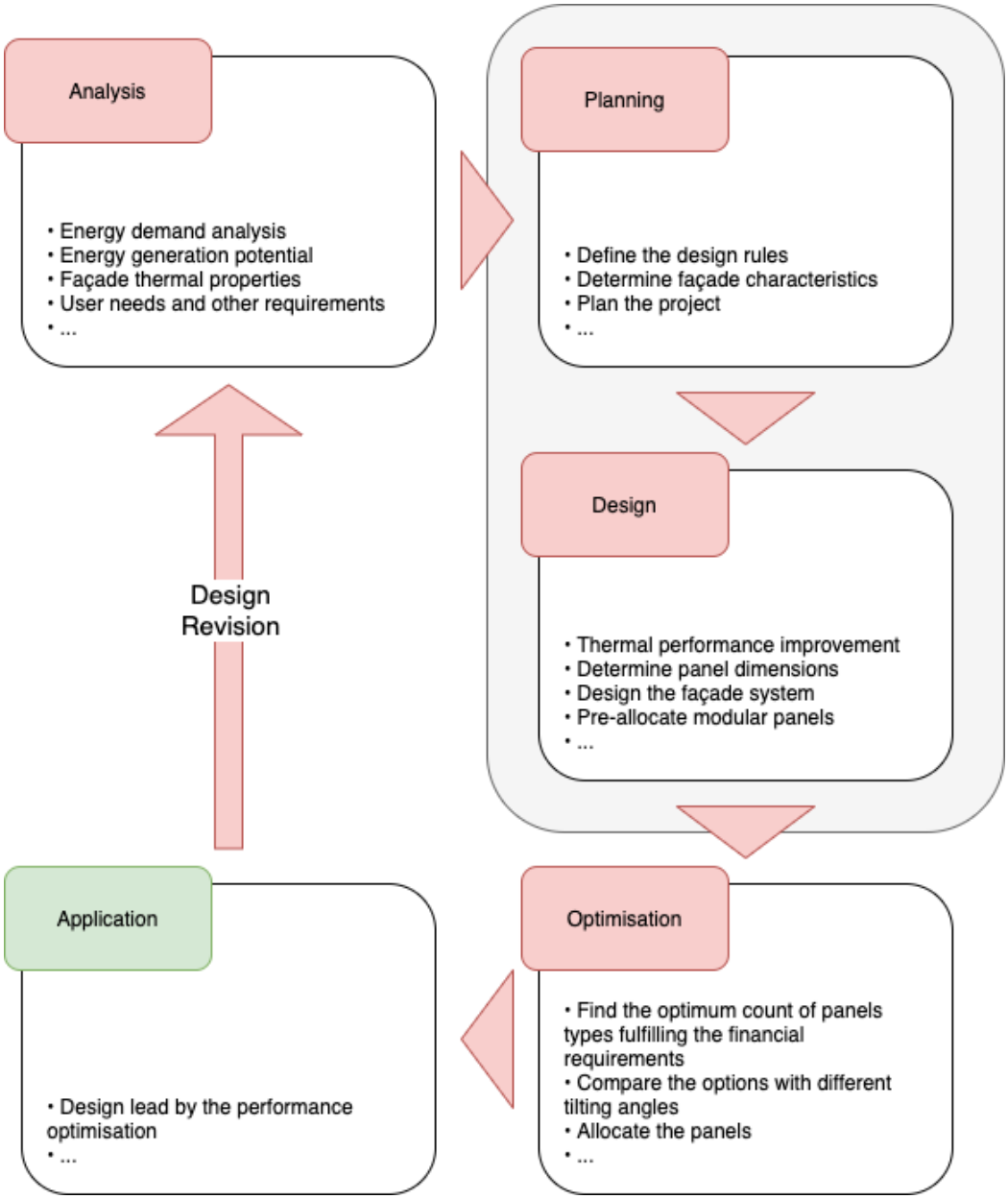

Figure 3: Steps of the proposed design methodology.

1.9. Research planning

Shortly before P2, the graduation topic had to be changed. So, the research planning was done by defining the crucial components of the contents and deadlines. No financial burdens were identified. The work breakdown structure (WBS) of the study can be seen in Figure 4.

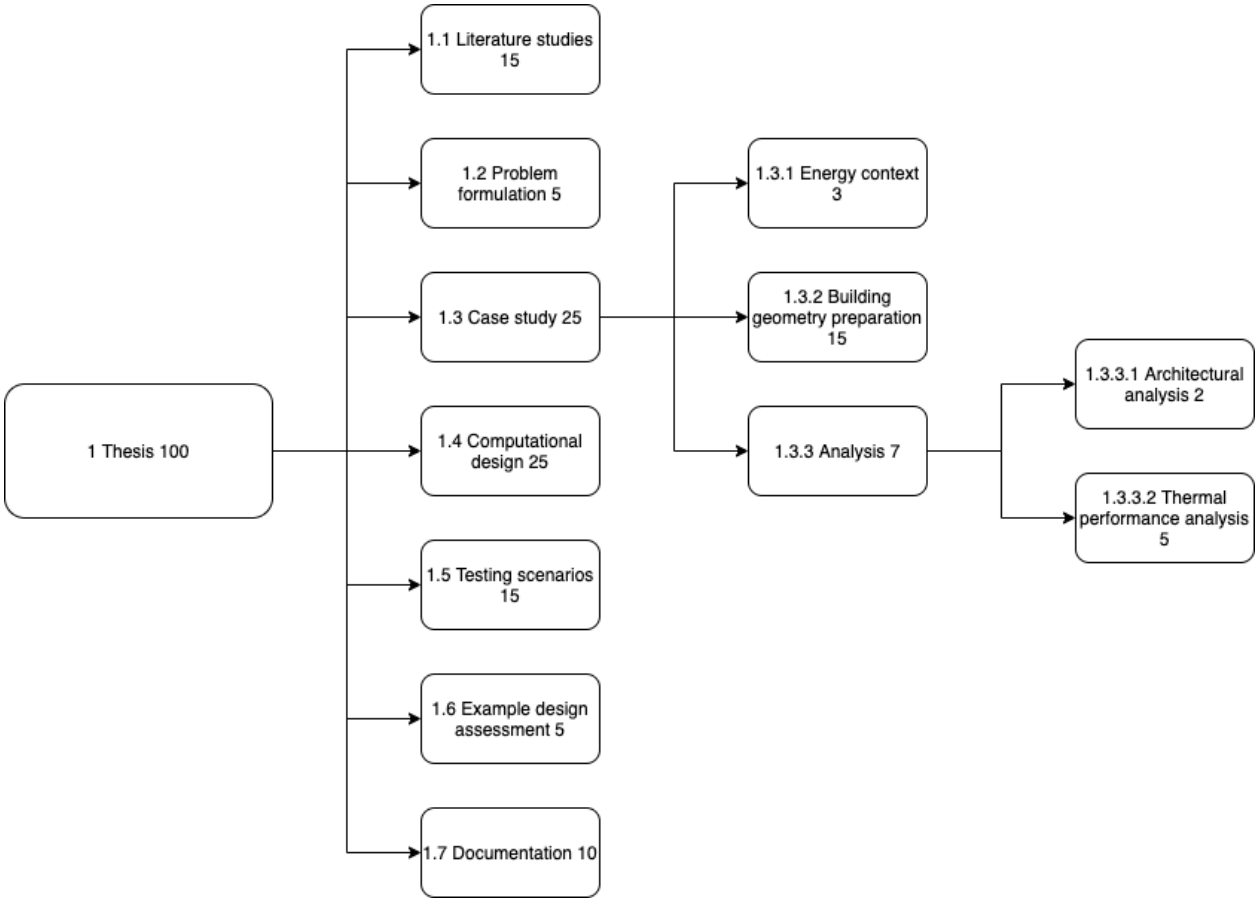

Figure 4: WBS of the study.

Literature studies and problem formulation were initiated together for a suitable proposal for P2. Until P3, literature studies continued with the case study. The computational design tool was prepared between P3 and P4 with further research on Engineering economics. The tool was tested with different scenarios before its introduction in P4. Between P4 and P5 the tool was improved, the results were compiled, and the documentation was made. The reflection of the tasks defined in the WBS on the academic calendar can be observed in Figure 5.

		P2									P3						P4						P5
Task name	%	2.10	3.1	3.2	3.3	3.4	3.5	3.6	3.7	3.8	3.9	3.10	4.1	4.2	4.3	4.4	4.5	4.6	4.7	4.8	4.9	4.10	4.11	5.1
1.1 Literature studies	15		1.1										1.1											
1.2 Problem formulation	5		1.2																					
1.3 Case study	25				1.3														Amendment					
1.4 Computational design	25										1.4									Amendment				
1.5 Testing scenarios	15													1.5						Amendment				
1.6 Example application	5																1.6							
1.7 Documentation	10																		1.7					

Figure 5: Time planning of the study.

2. Foundation knowledge

2.1. Performance-based design

Performance approach concentrates on the practical performance required for business processes and user needs. It concerns the determination of specifications and fitness for a

house, built asset or installation or a building product or service from the outset (Szigeti, 2005).

The concept includes two languages. There are a requirement and a capacity to meet that demand and execute it as necessary. The customer's language is required on the demand side, and the supplier's word is needed on the supply side. These languages are different, and it is essential to recognise this fundamental difference (Szigeti, 2005).

The interpretation of this concept to the AMC can be seen in Figure 6. The starting point of the project is the aim to make the AMC Amsterdam environmentally friendly and add architectural quality to it. Affordable, flexible and innovative solutions are needed to improve the properties of the external walls and contribute to the building's energy generation. Supplier side is expected to find solutions to at least these requirements, and this is we are investigating in this study.

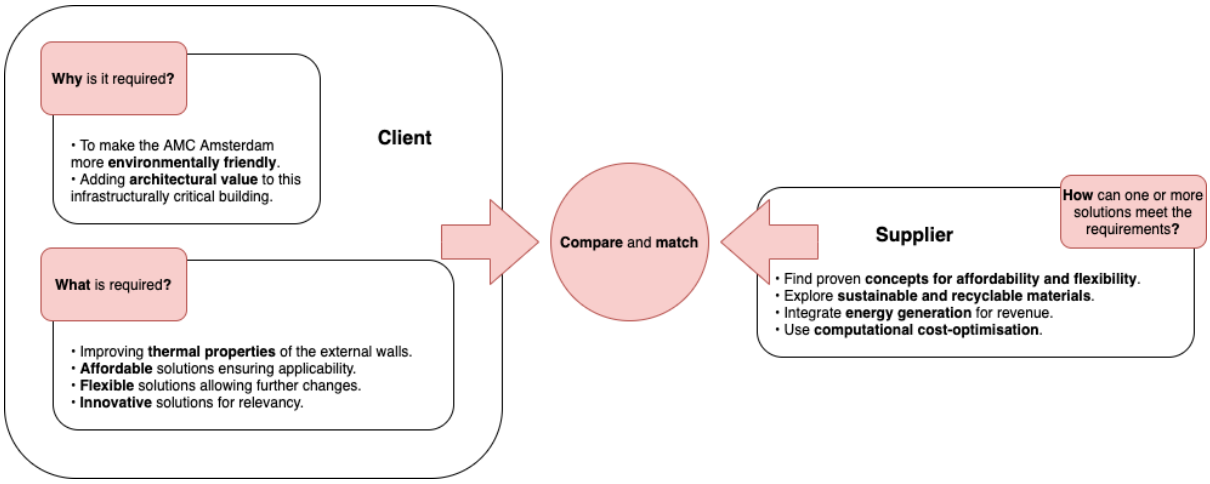

Figure 6: Performance approach in the AMC case.

2.2. Energy Context

2.2.1. Electricity in the Netherlands

The Netherlands generated 117,5 terawatts in 2018. While the most recent figures only cover the period up to 2015, World Bank data shows that the Netherlands produced 82 per cent of their electricity from oil, gas and coal sources that year. Over the past several years, however, the share of electricity generated from these sources has generally decreased. The EUR 8,63 cents per kilowatt-hour puts the average Dutch price somewhere between European industrial prices (Statista, 2019).

According to the Dutch Statistical Office, PV systems with a capacity of 2,4 GW were installed in 2018, bringing the total installed PV power to 6,9 GW at the end of the year. The total generated solar electricity was 5.2 TWh or 4,3 per cent of the net electricity generation (CBS, 2020).

The Netherlands has been enforcing the Net Metering policy since 2004. Net energy metering is an electricity billing mechanism that allows users who produce some or all of their own power to use that electricity at any moment, rather than when it is

generated. Net metering has been the key to the consistent growth of PV in recent years, and also the main driver in the early days of solar production. (Bellini, 2019). The Netherlands Government has announced that it will keep its net-metering program in its present form until 2023, with intentions to phase it out gradually by 2031 (Bellini, 2019).

2.2.2. Dutch Building Decree 2012

This decree contains the technical regulations that represent the minimum requirements for the buildings in the Netherlands. The requirements relate to safety, health, accessibility, energy efficiency and the environment (Business.gov.nl, n.d.).

When insulating a building, the decree makes a clear distinction between new construction and renovation. New construction is understood to mean all completely new homes to be built, but also all of the additions or extensions and renovations whereby at least 25 per cent of the surface of the integral building envelope is being changed or enlarged. If the building is renovated thoroughly, the new construction must meet the new-building requirement for insulation. If the renovation is of a smaller sort, the renovation rule shall apply. These requirements are less than for new construction. The improvement itself must meet the minimum R_c value of 1.3 m^2K/W. The minimum thermal resistance values stipulated for new construction and renovation in terms of façades, roofs and flooring are given in Table 1.

Table 1: : Minimum thermal resistance values according to the Dutch Building Decree 2012.

Type	**New construction**	**Renovation**
Façades	R_c 4.5 m^2·K/W	R_c 1.3 m^2·K/W
Roofs	R_c 6.0 m^2·K/W	R_c 2.0 m^2·K/W
Flooring	R_c 3.5 m^2·K/W	R_c 2.5 m^2·K/W

2.2.3. Building refurbishment

Refurbishment is a crucial step towards achieving the European Commission's energy and decarbonisation targets for 2030 which require at least 40 per cent reduction in greenhouse gas emissions from 1990 levels, at least 32 per cent renewable energy share and at least 32.5 per cent increase in energy efficiency (European Comission, 2014). The EU also aims to be climate-neutral by 2050, which mean no greenhouse gas emissions (European Comission, 2018).

Early design stages are particularly important, as decisions taken at this point will decide the success or failure of the design. Although the first design decisions may have a more significant impact on lower costs and effort, most of the existing procedures concentrate on post-design assessment. The integration of all factors during the initial design phase is complicated, particularly in terms of energy-efficient design.

There are two main approaches to which the external wall refurbishing strategies can be categorised: to remove the existing façade partially or to replace entirely, or wrapping

building in additional layers (Konstantinou, 2014). Considering that AMC Amsterdam should remain functional even during the construction process, this thesis is focused on the latter.

2.3. Engineering economics

This section constitutes the base of the engineering economics knowledge used in the study, which will be detailed depending on the photovoltaic energy field.

2.3.1. Cash flow diagram

Cash flow is the sum of money reported in a project's financial records as receipts or disbursements. A cash flow diagram shows cash flow as arrows on a timeline scaled to cash flow magnitude, where expenses are down arrows, and revenues are up arrows.

When making the investment, an investment transaction begins with negative cash flow and continues with positive cash flows when earning paybacks. An exemplary cash flow diagram template is given in Figure 7 (Engineering ToolBox, 2009). In this diagram, the upward arrows show the positive cash flows or payback, and the downward arrows indicate the negative cash flow or investing.

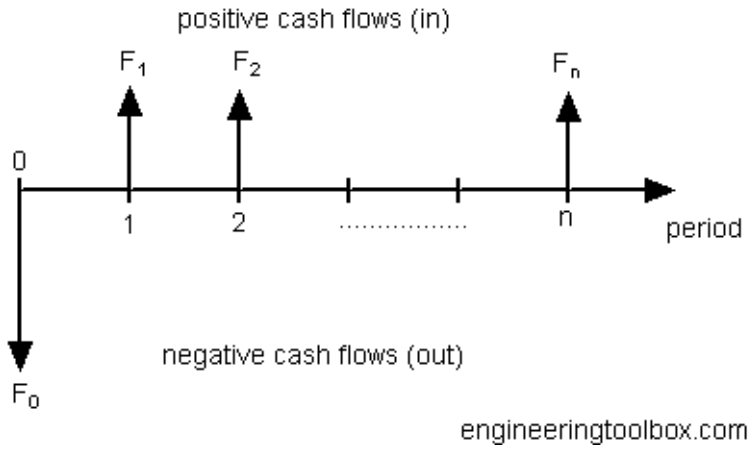

Figure 7: Example cash flow diagram (Engineering ToolBox, 2009).

2.3.2. Time value of money (TVM)

Time value of money (TVM) is the idea that money currently available is worth more than the same amount in the future, due to its possible earning capacity. This finance principle holds that cash will earn interest, and the faster it is received, the more it is worth. TVM is sometimes referred to as discounted value. The most fundamental formula of TVM is (Newnan et al., 2004):

$$FV = PV \times [1 + i]^t$$

Where;

FV	Future value of money
PV	The present value of money

i interest rate

t number of years

2.3.3. Net present value (NPV)

Net present value (NPV) is defined as the difference between the present value of cash in- and outflows over a period of time. In capital budgeting and investment planning, NPV analyses the feasibility of a planned investment or project. However, the calculation is based upon several projections, so there is a strong possibility for errors (Gallo, 2014). The following formula calculates NPV (Mao, 2006):

$$NPV = \sum_{t=1}^{n} \frac{R_t}{(1+i)^t}$$

Where;

R_t net cash inflow-outflows during a single period t

i interest rate

t number of years

2.3.4. The Fisher Effect

The time value of money contains several losses, such as the possibility of default, which is the probability that the borrower would not be able to pay the loan back, the possibility of change in the taxation or the regulations, and the loss in the purchasing power under inflation. Nominal interest considers all of these loss factors. Instead, real interest rate measures the recompense for expected losses due to default and regulatory changes, not including the inflation compensation factor (Agarwal, 2019). Real interest rates are preferred for a risk-free investment.

The Fisher Effect is a theory in economics that states the relationship between inflation, real interest rates and nominal interest rates. The Fisher equation in financial mathematics and economics estimates this effect (Agarwal, 2019):

$$r = \frac{1+i}{1+\pi} - 1$$

Where;

r Real interest rate

i Nominal interest rate

π Inflation rate

2.3.5. Economies of scale

In microeconomics, the economy of scale is the relation between the size of an industry and a product's lowest possible cost (Britannica, 2005). Typically, a decrease in the average value of a commodity is achieved when a factory increases production. This reduction is called the economy of scale. Increased supply of labour, improved productivity, advanced infrastructure, and discovery of new tools or better application of existing ones can all increase output and contribute to the economy of scale. Alternatively, diseconomy of scale can occur when a raise in output causes an increase in the average cost. Long-run average and marginal costs (LRAC and LRMC) are illustrated in Figure 8 (Diagram by District 2013, distributed under a CC BY-SA 4.0 license).

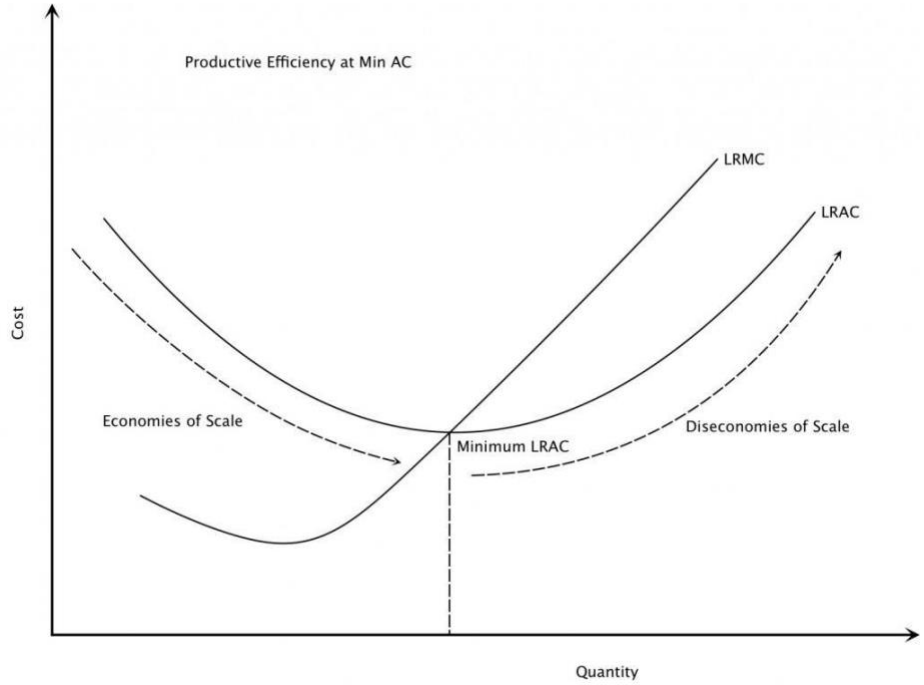

Figure 8: Illustration of economies and diseconomies of scale (Diagram by District 2013, distributed under a CC BY-SA 4.0 license).

2.4. PV systems

2.4.1. Components of a PV system

2.4.1.1. Solar array

A PV Array consists of PV modules which are fixed PV-cell accumulations. The whole electrical power generation unit is a PV array. It consists of various PV modules. The most important component of any solar photovoltaic system is the PV module, which consists of different interconnected PV-cells. PV-modules are combined into strings to fulfil various vitality needs, as shown in Figure 9.

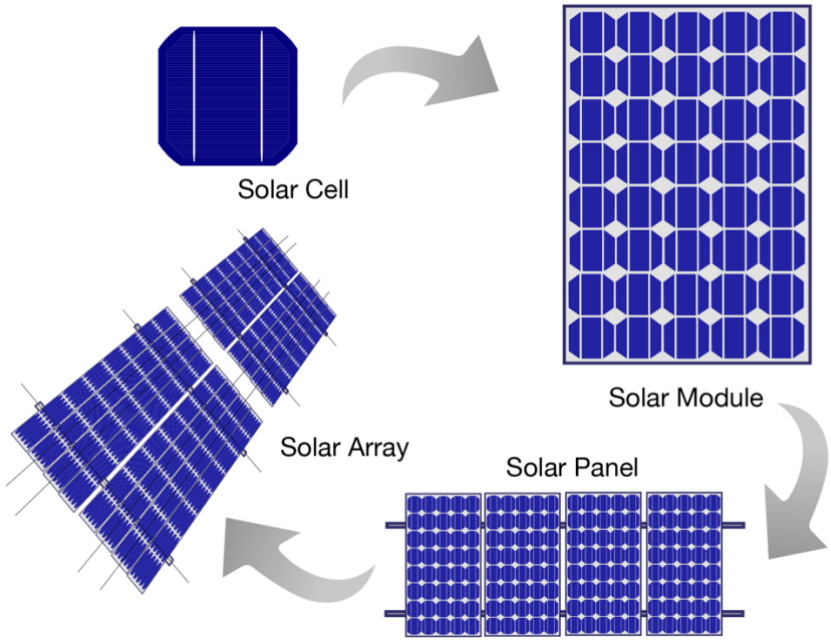

Figure 9: The relation between PV-cell -module and -array.

2.4.1.2. Mounting

A PV system array can be mounted on rooftops, typically with a distance of a few centimetres and parallel to the roof surface. The system is positioned with an angle if the rooftop is horizontal. Ground-mounted PV systems are usually large photovoltaic power plants of a utility-scale type. The PV array consists of solar panels, which are held in place by racks or frames connected to mounting supports on the ground.

2.4.1.3. Cabling

A solar cable is an interconnecting cable used in the generation of photovoltaic electricity. Solar cables are used to interconnect solar panels and other electrical components of the photovoltaic network. Solar cables are designed to be UV-resistant and weather-resistant and can be used within a large temperature range and are usually put outdoors (Odersun, 2011). Different jurisdictions will have specific rules on grounding solar power systems for the safety of electrical shocks and lightning.

Solar modules have two connecting cables with plug connectors. This makes it easy to join the modules. The requirements to be met for PV module cables are substantially higher for DC cables than for AC cables due to the related safety regulations (Odersun, 2011).

2.4.1.4. Tracker

The solar tracking system reorients the solar panel throughout the day. Based on the type of tracking system, the panel either points straight to the sun or to the brightest portion of an overcast sky. Trackers greatly improve performance early in the morning and late in the afternoon, increasing the total power supplied by the machine by 20–25 per cent for a single axis tracker and 30 per cent for a single axis tracker (MECASOLAR, 2017). Trackers

are beneficial in regions where a large amount of direct sunlight is provided. Tracking in diffuse light is essentially pointless (Al-Mohamad, 2004). Tracking systems have two key reasons for improving performance. Firstly, its surface has more irradiance when the solar module is perpendicular to the sun than when it is inclined. Besides, direct light is more effectively used than indirect light (Mills, 2015).

2.4.1.5. Inverter

An inverter transforms the DC coming from the PV-modules to the grid-compatible AC. It also monitors and optimises the processing and documentation of critical operational data.

Depending on their capacity, inverters can be used centrally for the whole system, or for each array or even for each module. Inverters should be placed where they can stay cool or properly ventilated.

BIPV systems are split into several modules or subsystems with the same environmental effects and production capacities. Thus, central inverter models are not always possible. The inverter must be chosen specially to match the appropriate section sizes, for each section of the system to have its own maximum power point tracker (MPPT). MPPT ensures that the solar generator consistently runs within an optimal output range (Odersun, 2011).

2.4.1.6. Battery

Still being costly, PV systems commonly use rechargeable batteries for surpluses to be used when there is no solar exposure. Batteries used for grid storage can even balance the electrical grid by preventing peak loads and are vital in the smart grids, since they recharge during low-demand periods and supply their stored energy to the grid when the electricity is demanded more (Fan et al., 2020).

Both pulse-width modulation (PWM) and MPPT charge controller systems are tused for charging solar system batteries. It is commonly accepted, that MPPT can overtake PWM in a cold and temperate environment, while in a subtropical and tropical climate, both controllers give about the same results (Victron Energy, 2020).

2.4.1.7. Metering

Net metering

The meter can work in both directions in the net metering system. The electricity generated by the PV system (S_g) either supplies direct power to the loads or is transmitted to the grid to move the meter backwards, thereby lowering the total number of units that the meter counted (Figure 10) (GSES, 2013).

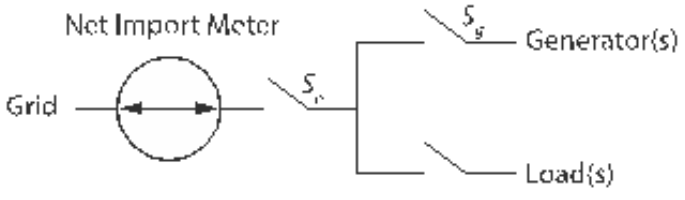

Figure 10: Net-metering diagram 1 (GSES, 2013).

Where information on the export and import of electricity was needed, a dual metering system was introduced. Two mechanical meters can be mounted in this arrangement with I that allow them to work only in one direction (Figure 11) (GSES, 2013). The energy produced by the PV system exported to the network during the day is measured by the export meter in this arrangement while the import meter measures the exact amount of energy received from the grid. Users can be encouraged to increase self-consumption by maintaining the export price of solar electricity at reasonable levels.

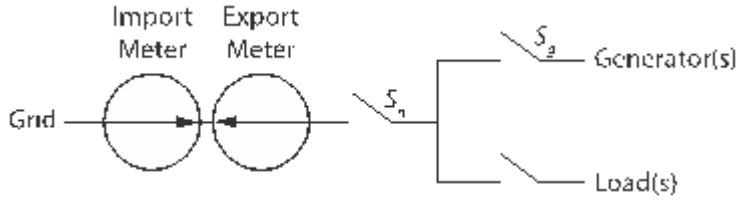

Figure 11: Net-metering diagram 2 (GSES, 2013).

Gross metering

This method of calculation measures the electricity generation and supply separately. This calculation allows the company to charge customers independently of production, generation and net consumption at various rates, by calculating the number of solar units produced and the total of units consumed. This is determined by two distinct meters or by double calculation (Figure 12) (GSES, 2013). However, all generated electricity is sold to the grid in this mode of arrangement, and users have no incentive to raise self-consumption.

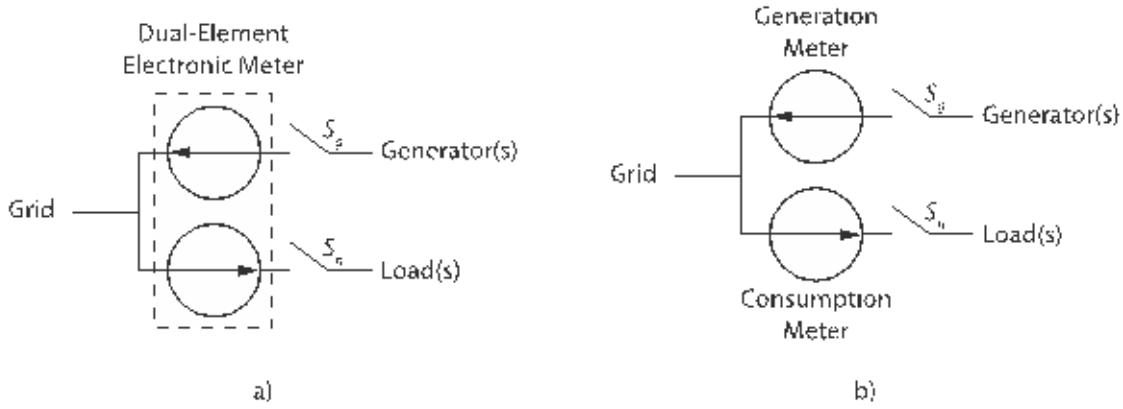

Figure 12: Gross metering diagram (GSES, 2013).

2.4.2. PV-cell types and their efficiencies

PV-cells are made of semiconductor materials that transform light into electricity. Silicon is the most popular semiconductor in the PV-cell manufacture (U.S. Department of Energy, n.d.).

Most of the currently available PV-panel options are made of monocrystalline, polycrystalline (multi-crystalline) or thin-film PV cells. These solar panels differ in the way they are made, the size, the efficiency, the prices, and the installations that are best suited to each (EnergySage, 2020).

Different from monocrystalline and polycrystalline PV-cells, thin-film panels are made from a variety of materials, such as amorphous silicon (a-Si), cadmium telluride (CdTe), Copper gallium indium di-selenide (CIGS), conductive organic polymers or small organic molecules (OPV). The efficiency ratings of these PV-cell types are given in Table 2 (Green et al., 2019).

Table 2: PV-cell efficiency ratings (Green et al., 2019).

PV-cell type		Cell efficiency (per cent)	Module efficiency (per cent)
Monocrystalline PV-cells		26,7±0,5	24,4±0,5
Polycrystalline PV-cells		22,3±0,4	19,9±0,4
Thin-film PV-cells	a-Si	10,2±0,3	-
	CdTe	21,0±0,4	18,6±0,5
	CIGS	23,4±0,5	19,2±0,5
	GaAs	29,1±0,6	25,1±0,8
	OPV	11,2±0,3	8,7±0,3

Scientists developed a cell type with 34.5 per cent efficiency (da Silva, 2016) in Australia. Earlier, cells with 44.7 per cent efficiency had been developed, that makes the aspirations of scientists to cross the 50 per cent mark much more viable (Fraunhofer ISE, 2013).

2.4.2.1. Monocrystalline and polycrystalline PV-cells

Monocrystalline and polycrystalline PV-modules contains cells made out of silicon wafers. For the construction of a mono- or polycrystalline module, wafers are arranged on a glass or back sheet, covered with a glass sheet and put together.

Made from the same material, monocrystalline and polycrystalline modules have different silicon characteristics. Monocrystalline cells are made from a single silicon crystal. Instead, polycrystalline cells are made up of silicone crystal bits mixed together in a furnace and then sliced into wafers (Marsh, 2018).

2.4.2.2. Thin-film solar panels

The most common type of thin-film technology is CdTe. To make this type of thin-film screen, manufacturers put a layer of CdTe between transparent conductive layers that capture sunlight. This form of thin-film PV-cell also has a glass coating on the top for safety (Nunez, 2017).

Thin-film solar panels can also be made of a-Si which is close to the monocrystalline and polycrystalline panel structure. They are made of non-crystalline silicon placed on top of glass, plastic or metal (Richardson, 2019a).

CIGS are another common type of thin-film technology. CIGS panels all four components are mounted within two conductive materials (i.e. glass, plastic, aluminium or steel) and electrodes are mounted on the front and back of the coating to collect electric currents (Richardson, 2019b).

Gallium Arsenide (GaAs) is an expensive technology. It is mainly used on spacecraft and is intended for the flexible, mass-scale application of PV energy in extreme environments (Richardson, 2019b).

Finally, organic photovoltaic (OPV) cells employ conductive organic polymers or small organic molecules to generate electricity. A few particles of thin organic vapour or solvent are collected in an organic photovoltaic cell and placed between two electrodes to bear electrical current (Green et al., 2019).

2.4.3. Grid-connection

2.4.3.1. Grid-connected PV systems

Plants that are linked to the public grid via a feeding point and can feed the electricity generated into this grid are known as networked plants. They can supply either all the electricity generated or only the excess power that is not required on-site. Consequently, according to its specifications, the plant operator can determine whether to store electricity produced in batteries, use it directly or sell it to the power supplier. The grid-connected plants with their own usage can be run with special inverters efficiently (Odersun, 2011).

2.4.3.2. Grid-independent PV systems

PV plants without public grid connection are called stand-alone off-grid PV plants or island systems. The plant owner uses all the electricity generated. In fact, this implies an intermediate battery-based storage of solar electricity (Odersun, 2011).

2.4.3.3. Hybrid PV systems

PV plants hybrid with other energy conversion technologies is considered hybrid systems. Typical installations include wind power plants, diesel generators, biogas plants, fuel cells or micro-hydro-power plants. Such combined networks have the benefit of providing a constant and reliable energy supply. Therefore, if one of the plants breaks down, power is still supplied continuously. In fact, the plants supply electricity continuously over the course of the day or year (Odersun, 2011).

2.4.4. Performance of the c-Si PV-systems

2.4.4.1. Propagation of Uncertainty and Performance Ratio

In order to manage the financial risk of investment in photovoltaics, the uncertainties of the solar energy yield calculations are critical. The yield estimate is subject to the uncertainty in the PV simulation chain of each vector. The solar resource is the first and

most significant part. In addition to uncertainties related to the assessment and estimation of solar energy, attention must also be given to long-term resource fluctuations (Richter et al., 2015). These uncertainties can be classified, as shown in Table 3 (Richter et al., 2015).

Table 3: Uncertainties classification (Richter et al., 2015), relative uncertainty values (Thevenard & Pelland, 2013).

Group	Uncertainty
Solar resource	Climate models (4%) Solar insolation variability (5%) Transposition to the plane-of-array (3%)
PV modelling	Module rating (3%) PV cell degradation Shading Snow, dirt and soiling (3,5%) Other (temperature rise, spectral losses, reflection etc.) (5%)
Other field related uncertainties	Inverter and transformer losses (1%) AC and DC cabling

The industry uses different performance models to predict how much energy a photovoltaic system can generate. The underlying mathematical formulas, methodology and amount of data or assumptions for the simulation can change the models drastically. Moreover, there is inherent uncertainty with large amounts of input parameters such as irradiation, temperature, panel position, module and inverter efficiency, user-defined values for external losses such as soiling, mismatch and cabling. These must be properly compensated for and combined. Even the best possible algorithms result in uncertainty of ±3.75 per cent to ±5 per cent, given the uncertainty of a PV array model by ±3 per cent, irradiation model uncertainty by ±2 per cent and inverter uncertainty by ±1 per cent, when other field-related uncertainties are neglected (Richter et al., 2015).

In Germany, the mean performance ratio (PR) value was calculated as 0.84 after the investigation of around 100 PV systems with PR ratios between 0,7 and 0,9 (Reich et al., 2012). A good system is considered to have a PR value of more than 0,84. When combining the uncertainties in Table 3 by summation in quadrature (NDT Resource Center, 2011), ($\sqrt{4^2 + 5^2 + 3^2 + 3^2 + 3{,}5^2 + 5^2 + 1^2}$), an overall uncertainty of 9,7 per cent is found. So, the PR was considered as 0,84±0,08. This calculation suggests a possibility of 0.92 PR value (W. G. J. H. M. Van Sark et al., 2012).

2.4.4.2. Module efficiency

The efficiency of the solar panel refers to the amount of sunlight converted from solar panels to electricity. Solar panel efficiency, also known as the conversion rate, is one of the main factors when buying solar panels since this means the amount of solar energy gained from the system. A high-efficiency panel also means less space than lower efficiency panels, making it favourable for the systems with limited space. Conversion rates can vary according to production quality, technology and materials used (Infinite Energy, 2019). Effective module life is typically more than 25 years. Many major producers give contracts of 20 years or more for a high percentage of initial rated power production (Florida Solar Energy Center, 2014). After 20 years of use, panels produce 80 per cent or more of their rated power. The thumb rule is that panels degrade by approximately 1 per cent per year. However, there are studies which proof 0,4 per cent degradation rate for PV cells (Lombardo, 2014).

2.4.4.3. Shading

The electrical output of the photovoltaic cell is highly sensitive to shading. Even when a small part of a cell, module or array is shaded, and the remainder is under illumination, the output drops significantly by the internal shortcut when the electrons change their direction via the module's shaded portion (Sathyanarayana et al., 2015). The situation of how shading lowers the maximum amount of power that the system can generate also called as the maximum power point (MPP) is shown in Figure 8 (Alternative Energy

Tutorials, 2018). In the figure, three series-connected 0.5 V PV-cells are described under a solar irradiance of 1kW/m2.

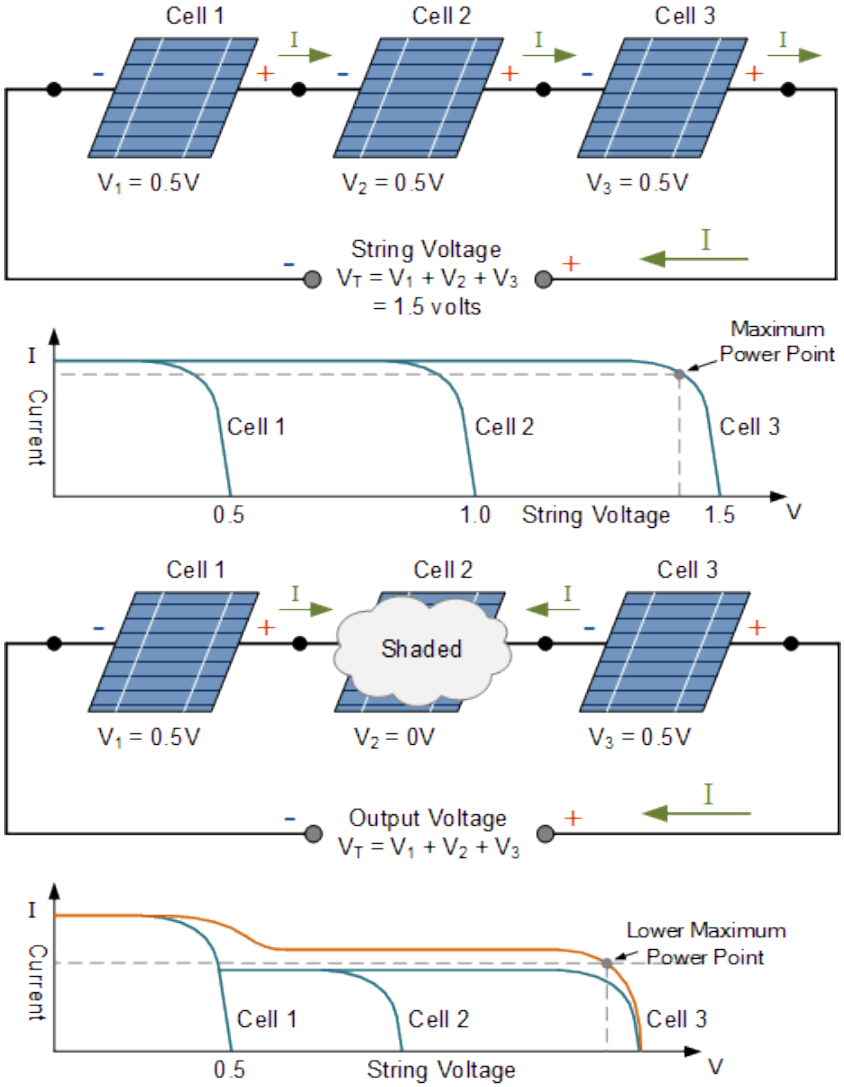

Figure 13: Shading of a single cell in a string causes a significant reduction in the MPP (Alternative Energy Tutorials, 2018).

If the current taken from the cell series is smaller than the current which the shaded cell would release, the string produces a small current. If the other cells have enough voltage in a band, then a current is forced into the cell by breaking the connection in the shaded section. The shaded cell consumes energy, turning it into heat instead of contributing to the power generated by the plate. Because the reverse voltage of shaded cells is greater than the forwarding voltage of the illuminated cells, a shaded cell can consume the power of the other cells in a string, which influences the output excessively (Eicker, 2005). Dirt and dust will lower the efficiency of the solar module by approximately 5 per cent (Infinite Energy, 2019).

In fact, hotspot heating occurs when there is one low-current PV-cell in a string of at least multiple high-current solar cells. Heating from hot spots leads to destructive effects, such as cell or glass breaking, solder burning or cell degrading, as shown in Figure 14

(Skyrobot Inc., n.d.). Hotspot heating leads to destructive effects, such as cell or glass cracking, melting of solder or degradation of the solar cell.

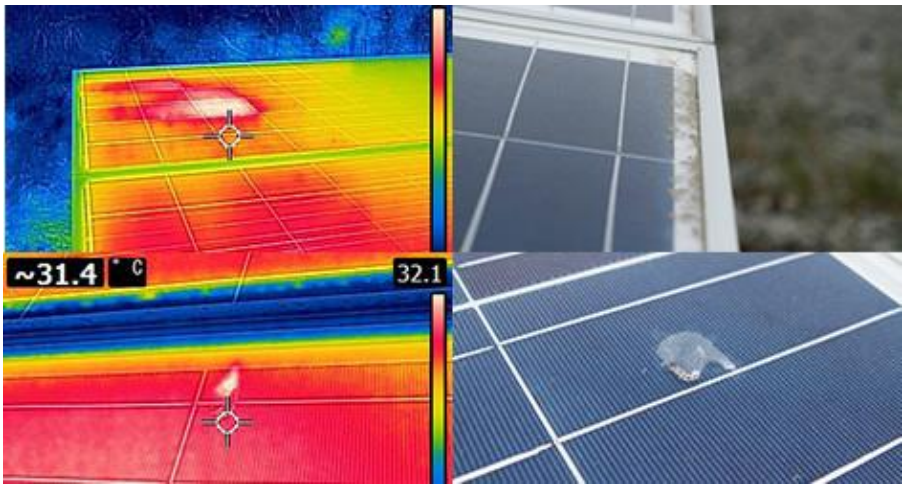

Figure 14: The damaging effects of hotspot heating (Skyrobot Inc., n.d.).

The damaging effects of the hotspot can be overridden by bypass diodes. Bypass diodes are connected to the cells in parallel but with opposite polarity. Each solar cell will be forward-biased under normal operation, and thus the bypass diode will be reverse biased and will be an open circuit in turn. However, if a solar cell is reverse-biased due to a short-circuit current mismatch between several cells in a string, the bypass diode conducts, allowing the current from the good solar cells to flow in the outer circuit rather than biasing each good cell forward, as shown in Figure 10 (Alternative Energy Tutorials, 2018). The overall reverse bias across the weak cell is reduced to about one drop in the diode, thereby reducing the current and preventing heating at the hotspot.

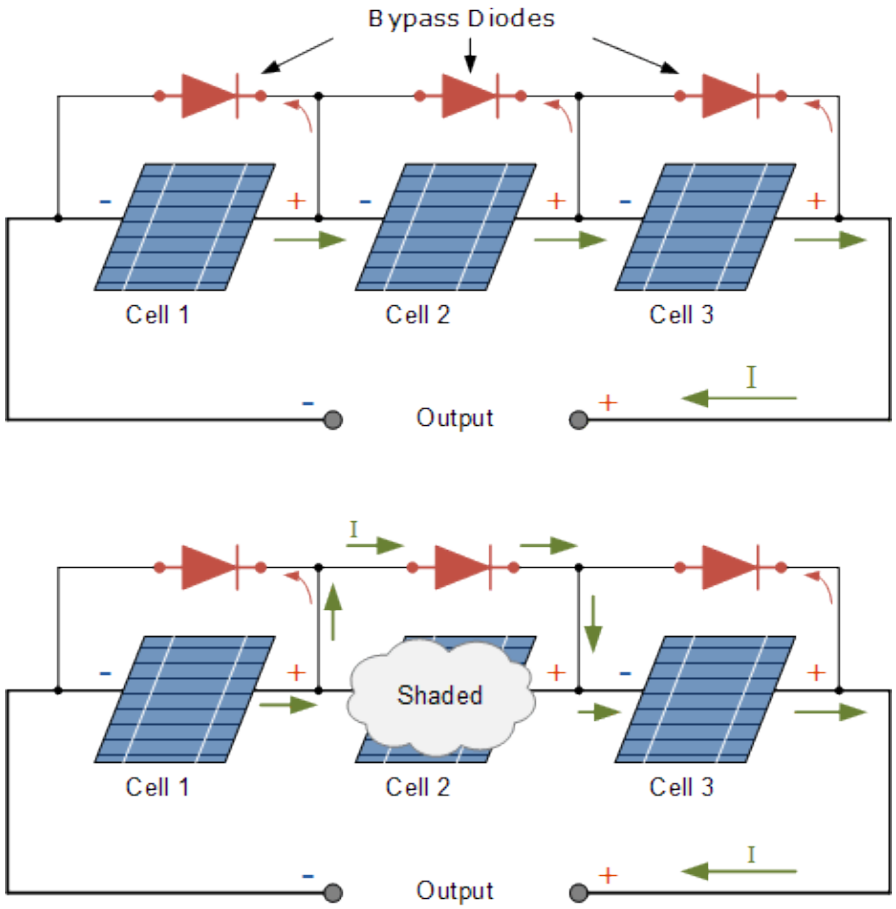

Figure 15: Bypass diodes prevent hotspot heating by preventing the current run through the shaded PV-cell (Alternative Energy Tutorials, 2018).

In reality, the bypass diode per solar cell is too costly, and instead, the bypass diode is typically located across strings of solar cells. The voltage across the shaded cell is equal to the forward bias voltage of the other cells in series that share the same bypass diode plus the bypass diode voltage (Alternative Energy Tutorials, 2018).

2.4.4.4. Temperature

Intense temperature increases will harm the solar cells and material, thereby reducing the lifespan of the panels. Semiconductor proprieties in solar pans change at higher temperatures. A mild current increase, but a significant reduction in voltage occur (Infinite Energy, 2019). It is usually determined how much power drop the panel will have when the temperature increases by 1°C or above 25°C in the product spec sheet.

2.4.4.5. DC-AC inversion losses

The efficiency of an inverter shows how much DC power is converted into AC power. Power can be lost as heat, and some electricity is also used to maintain the inverter in power mode. High-quality sine wave inverters have a 90-95 per cent efficiency. Low-quality sine wave inverters are usually less efficient at 75-85 per cent. Besides, high-frequency inverters are generally more efficient than low-frequency inverters (Fedkin & Dutton, 2018).

2.4.4.6. Half-cut cells

Half-cut solar cells are regular silicon-wafer PV-cells which are cut in half by a laser cutter. These cells provide a range of benefits over conventional cells. Half-cut solar cells have improved performance and endurance. Efficiency-wise, half-cut cells can increase the efficiency of the panel by a few per cent. In addition to improved production numbers, half-cut cells are more mechanically resilient than their conventional equivalents. As being smaller in size, they are more resistant against fractures (Marsh, 2018).

One type of PV power loss is resistive losses or power lost during current transport. PV-cells carry current using the thin metal ribbons crossing their surface. These ribbons also connect the cells to the adjacent cells. Running current through the ribbons causes a certain loss of energy. By splitting PV-cells in half, the current produced by each cell is halved (Marsh, 2018).

Half-cut cells are more resistant to shading effects than traditional solar cells. The cells are wired together in series in conventional solar panels which are designed with complete cells. In series wiring systems, if one cell in a row is shaded and does not generate energy, the whole line of cells will stop producing power. The half-cut panel has six cell strings instead of 3 cell strings like a standard PV-module. Under favour of the bypass diodes shown in red in Figure 16 (Brakels, 2018), a small shade spot on a panel will knock one whole-cell string out of action but will not affect the others. The effect of partial shade is less serious because the half-cut panel has more lines.

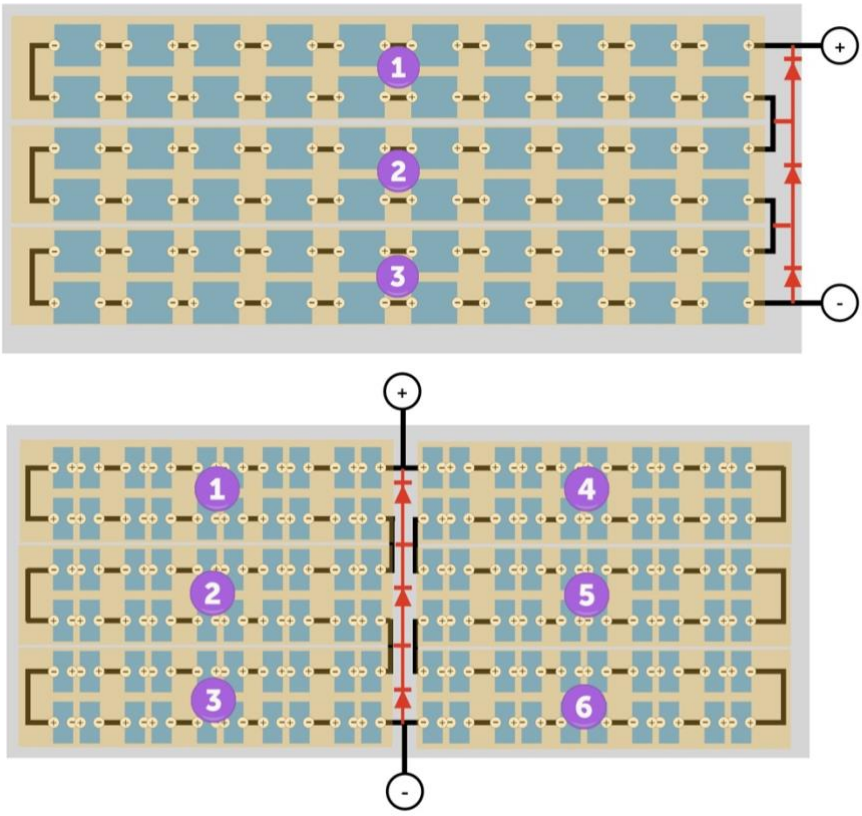

Figure 16: Comparison of 3-string full cell panel and 6-string half-cut cell panel, bypass diodes shown in red (Brakels, 2018).

Because of these advantages, solar panels made of half-cut solar cells can provide faster payback periods for proprietors installing PV-systems. Particularly for installations where shading and limited installation area are constraining elements, half-cut cells make the upfront cost of installing a solar panel even more worthwhile.

2.4.5. Scale of system

Photovoltaic systems are generally categorised into three distinct market segments: residential-, commercial-, and utility-scale systems. Their power varies from a few kilowatts to a hundred megawatts. The average home system is around 10 kilowatts and is mounted on a sloping roof, while commercial systems can reach a megawatt-scale and are typically mounted on low-slope or even flat roofs (Goodrich et al., 2012).

The dimension of the PV-modules also depends on the scale of the system. While standard PV-modules consist of 60 of 156 mm by 156 mm cells, The commercial-scale PV-modules have 72 cells. The average 72-cell module size is 99 cm by 199 cm (Matasci, 2018).

2.4.6. Economics of PV systems

2.4.6.1. The annual energy output of the system

The global formula to estimate the electricity generated in output of a photovoltaic system is (Saur News Bureau, 2016):

$$E = A \times r \times H \times PR$$

Where;

E	Energy (kWh)
A	Total PV module area (m2)
r	PV module efficiency (per cent)
H	Annual irradiance of PV modules
PR	Performance ratio

For the calculations in the study, irradiance data collected from the Ladybug analysis was used, and the performance ratio was taken 0.84 (Reich et al., 2012) with an uncertainty of ±0.08 calculated with the input from (Thevenard & Pelland, 2013).

2.4.6.2. Payback time

Payback time can be defined as the time needed to compensate the cost of an investment. It can be calculated with the formula, where a uniform annual return is considered (Newnan et al., 2004):

$$payback\ time = \frac{initial\ investment}{annual\ return}$$

In practice, more factors are taken into account than this simple formula, which increases the complexity of the calculation. If a significant period of time is in question, the

purchasing power of the capital changes due to inflation, also the change in the value of money has to be taken into account, which is. Another aspect that needs to be considered is renewable energy policies. Subsidies and feed-in tariffs may have an effect on initial investment and savings.

2.4.6.3. Self-consumption

Self-consumption is defined as the local usage of PV electricity to reduce the amount of electricity purchased from other producers (Masson et al., 2016). Depending on the PV-system size and the local load profile, self-consumption ratios may vary between a few per cent to a theory-based maximum of 100 per cent.

Using the generated PV electricity on-site, rather than exporting it into the grid is named as direct consumption (Smets et al., 2016). Direct consumption can be done in several ways. Limiting the PV system size to make sure that the peak power produced is always lower than the peak power consumed is an undesired option. Other techniques are energy storage in various ways like batteries or power-to-heat-to-power storage (PHPS) (Bellini, 2020).

Various measures can be taken to encourage direct consumption. Simple net metering, which treats a prosumer equally of terms of consumption and production, does nothing to promote self-consumption, as it actually pays back the prosumer retail cost of energy to the grid. Nevertheless, the adjustment of feed-in tariffs to be lower than retail energy is a popular scheme adopted by countries such as Germany and Italy to promote direct use in PV systems (Smets et al., 2016).

2.4.6.4. Compensation schemes

In buildings with PV systems installed, the electricity consumer becomes a prosumer, who sells the surplus electricity to the grid. There are different schemes to compensate for the electricity exported for PV system owners. The Netherlands have been applying the net-metering scheme since 2014 and will continue it until 2023 when the country gradually abandons the system until 2031 (Bellini, 2019).

Net-metering

Earlier analogue electricity meters can work bidirectionally. If energy is drawn from the power grid, the electricity count is raised. Oppositely, when the PV system produces more than used in the building, energy is fed to the grid. In this situation, the electricity count is reduced. In the end, only the net cost of energy has to be charged. Lately, smart digital electricity meters are put to use. Such meters differentiate between energy produced from the grid and electricity supplied to the grid. This network not only allows the control of the amount of electricity supplied to the grid by the PV network but also enables the grid provider to adjust its tariff structure. For example, the price of electricity also involves a certain charge for the use of the electricity grid. Such a tax may also be imposed on electricity supplied to the grid by the PV system (EnergySage, 2019).

Feed-in tariffs

The system of feed-in tariffs requires the electricity generated by the PV system to be sold to the grid provider at a fixed price. Either two analogue electricity meters, one of which measuring the power consumed from the grid and the other measuring energy supplied to the grid, or one smart meter are needed for such a device. There are two types of feed-in tariffs, gross and net. In the gross feed-in tariffs, all of the electricity generated by the system is sold to the grid and all the electricity consumed is purchased from the grid. On the other hand, for net feed-in tariffs, actual power usage is subtracted from PV power generation, and only surplus electricity is sold to the grid (Kenton, 2020).

Feed-in tariffs make it possible to promote the development of renewable electricity systems, such as PV, where feed-in tariffs are above the price of electricity. On the flip side, if they are placed slightly below the grid electricity level, self-consumption can be induced, as discussed below.

2.4.6.5. Levelized cost of electricity

LCoE is defined as the cost per kWh of the electricity generated by an electric power plant. It is used to compare the lifetime costs of the various technologies for generating electricity. Calculating the LCoE can become very difficult, depending on the number of factors that are to be taken into account. In a simple case, the following formula can be used to test the LCoE (Smets et al., 2016):

$$LCoE = \frac{sum\ of\ costs\ over\ lifetime}{sum\ of\ electricity\ produced\ over\ lifetime} = \frac{\sum_{t=1}^{n} \frac{I_t + M_t + F_t}{(1+r)^t}}{\sum_{t=1}^{n} \frac{E_t}{(1+r)^t}}$$

Where;

n	the lifetime of the system
I_t	investment expenditures in the year t
M_t	operational and overhaul expenditures in the year t
F_t	fuel expenditures in the year t
E_t	the electrical energy produced in the year t
r	discount rate

The LCoE for PV-system can vary a lot between different projects, based on location and the initial capital required for the system. The LCoE is a reliable predictor of the cost-effectiveness of technology for the energy provider. It is also an indicator for determining the price of electricity, which must be above the LCoE to make a profit. The supplier also cannot quote the electricity price independently from the policy factors, as it is strongly influenced by feed-in tariffs, discounts and other incentives (Smets et al., 2016).

2.4.6.6. Grid parity and socket parity

The terms grid parity and socket parity are used to examine whether the PV-electricity is compatible with electricity generated by other facilities. A clear distinction between the two principles makes for a well-founded assessment of the economic viability of electricity generated by PV. Grid parity is the point that the expense of PV power is considered equal to the cost of other systems for generating electricity. In comparison, the level at which a PV system's LCoE is equal to the amount the consumer pays out of the grid for electricity is called the socket parity. The operators of large-scale PV power plants must equate their system's LCoE with the cost of generating other sources of electricity, ignoring subsidies and other opportunities (Smets et al., 2016).

The definition of grid parity can be applied in theory also to other renewable technologies. There is, however, a significant difference between PV and other renewable technologies such as wind and hydropower. Wind and hydroelectricity projects can typically only be funded by corporations, but for home users, they are no alternative. PV, on the other hand, can be scaled down to the level of a single module, so that a house owner with his small, scalable PV system on his roof can become an electricity generator. The demand for residential power also often requires grid maintenance fees as well as taxes, which has an effect on the socket parity.

The installed volume may change over time, as the volume of the deployed PV-systems has risen significantly over the past decade. As capital costs decline with increasing volumes, the price of PV generated electricity is expected to decline in the future. This situation can be observed in Figure 17.

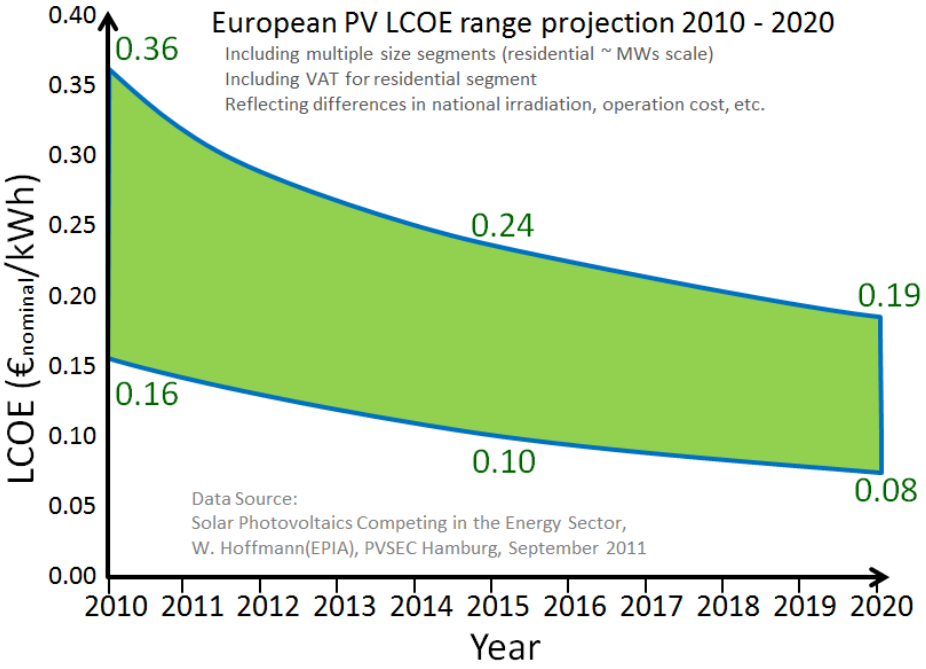

Figure 17: Graph showing the drop in the PV LCOE in Europe.

2.5. Building Integrated Photovoltaics

2.5.1. Requirements in building and solar power station applications

The requirements for PV modules with the six aspects of design, safety, reliability, performance ratio, efficiency and cost can be represented in a radar diagram which can be observed in Figure 18 (Palm et al., 2018). Only a qualitative ranking is possible, given the complexity of the factors such as safety and reliability. Performance and cost are the primary market drivers for standard PV, dominated by solar farm applications, with design aspects having the lowest priority. Parameters such as colour, finishing, transparency and size are of primary importance for BIPV implementations in contrast with design. It is crucial to make PV products a building material recognised by planners, architects and clients.

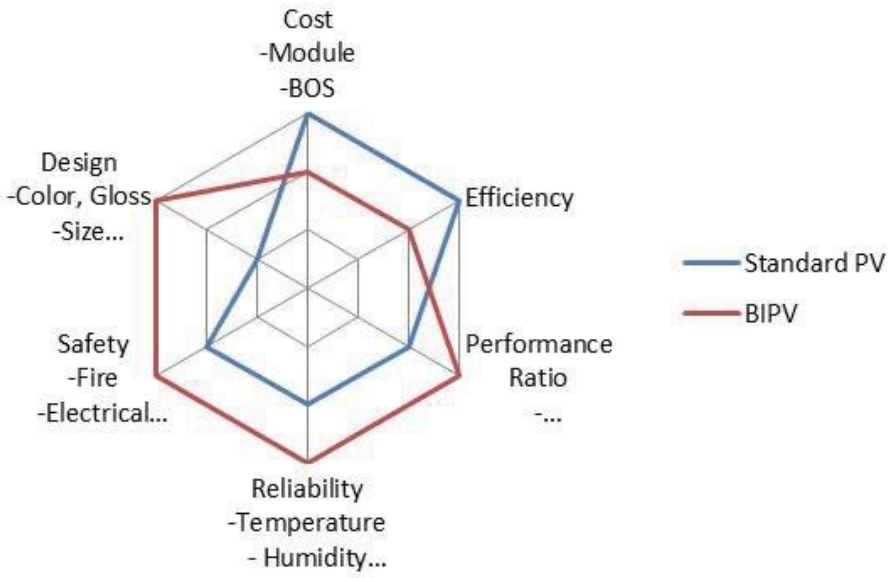

Figure 18: Requirement comparison for standard PV and BIPV (Palm et al., 2018)

Fixing orientation and the existence of neighbouring buildings or other objects can affect the BIPV's performance ratio. Shading tolerance, low light intensity performance or non-optimal sunlight incident angles are much more important, and the BIPV module needs to be well digested. In addition, in a power plant with modules also mounted in the optimum angle and very rarely shaded these requirements are practically non-existent. Buildings are not built for the sole purpose of generating electricity, and therefore BIPV modules should be adequate to replace classic façade materials while delivering the best possible electrical output at every spot of the building envelope. The classic building material should be the benchmark for durability factors, rather than traditional PV. Additionally, in some building applications, standard stress parameters such as wind and temperature may be more extreme compared to ground-mounted power plant modules. There are often more stringent safety requirements too. The comparison may also be viewed in a different way as well; namely, the difference in greenfield criteria and

building integrated PV may be used for an adapted development strategy. The additional specifications for BIPV can be met through smart design and partly customisable add-on functionality using a suitable base product produced in mass production (Palm et al., 2018).

2.5.2. Definition of BIPV and BAPV

BIPV and BAPV systems are not consensually defined. Architecturally, technically or financially, it varies greatly with context and perspective. Some definitions are broader, including partially- integrated systems, and systems embedded in architectural designs, while others are narrower with specific integration level requirements. The incorporation of PV systems into the shading devices is asserted to be an intermediate solution between BIPV and BAPV (Peng et al., 2011). Many interpretations, however, restrict BIPV to modules that replace a part of the building envelope such as roofs and façades (Sinapis & Donker, 2013), excluding therefore systems with modules built into external shading tools.

A BIPV system based on the technical functions is defined in this report. The modules in a BIPV device must substitute a traditional building material or part, or be inseparable from it, and thus serve a role in addition to generating electricity. Systems where PV-modules are incorporated into shading devices and balcony railings are also considered BI- and if the PV modules do not meet the BIPV specifications, a system is considered to be in the building BA- category.

2.5.3. Coloured BIPV modules

2.5.3.1. Solar transmittance

The working principle of PV-cells is based on the photovoltaic effect, which a potential difference generation at the meeting point of two different materials due to electromagnetic radiation. Albert Einstein found out that this effect can be explained by assuming that the light includes well-defined energy amount, called photons. The energy of such a photon is calculated by the formula (Smets et al., 2016):

$$E = h \times v$$

Where;

E Energy

h Planck's constant

v Frequency of the light

The solar direct transmittance is the percentage of incident solar radiation that the material directly transmits. This is the effective driver for the photovoltaic generation. For better efficiency of the modules, the solar direct transmittance should be high. Tempered glass, polyacrylic acids, fluorinated ethylene-propylene, non-opaque polyester and polycarbonate can be used as upper plates of PV-modules. Recently, low-iron ultra-clear tempered textured flat glass is typically used, which has a micro-pyramid structure

on the surface and an anti-reflection coating to improve absorption of scattered light and reduce light pollution the modules may cause (Wang, 2018). The upper plates of the PV-modules are usually 3,2 mm thick. The transmittance shall reach above 0,91 for c-Si cells (Wang, 2018) for performance. However, BIPV application prioritises not only the efficiency of the modules but also their appearances. In the next subsections, several products in the BIPV market will be given.

2.5.3.2. Anti-reflective coated PV-cells

Plain c-Si has high levels of reflection of around 30 per cent. Both monocrystalline and multi-crystalline PV cells contain anti-reflective (AR) coatings with an optimised thickness to improve their efficiencies. This coating causes the cells appear in the blue colour, as is common in multi-crystalline PV cells. Variations in the thickness of the AR coating transition the blue to other colours, also affecting the output of the PV-cells (Honsberg & Bowden, 2019b) of which examples can be seen in Figure 19.

Figure 19: Multi-crystalline wafers coated with silicon nitride (Honsberg & Bowden, 2019a).

Many colours can be obtained by changing the thickness of the coating material such as silicon nitride (Henrie et al., 2004), resulting in a reflection in the visible spectrum as seen in Figure 20 (Honsberg & Bowden, 2019a). PV-cells with modified colour based on the AR coating can be bought directly from the supplier of the cells. Cell manufacturers are, however, usually unable to produce small quantities at reasonable price levels for individual customers. Currently, the approach is not very popular (Masson et al., 2016).

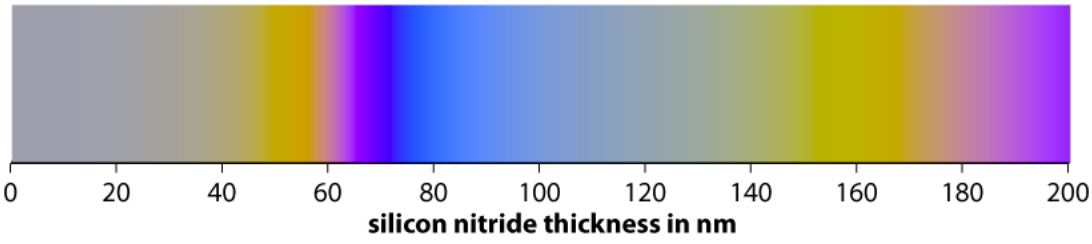

Figure 20: Colour of silicon nitride films as a result of film thickness under fluorescent light (Honsberg & Bowden, 2019a).

2.5.3.3. Coloured semi-transparent thin-film PV-modules

Semi-transparency of PV-modules can be obtained by partially removing the semiconductor layer to increase the light transmissivity. Degree of transparency can be manipulated by different levels of abrasion. Eventually, shading and energy generation can be combined in a windowpane. A possible application is in buildings with glass façades where the surface to install BIPV is very large, so there is no need for high-efficiency (Masson et al., 2016).

2.5.3.4. PV-modules with printed interlayers and solar filters

Interlayer sheets with desired colours or patterns can be laminated with the unit. It is possible to use traditional film printing techniques or translucent inks. Because of these key advantages, in the immediate future, this technique could attain a large market share. One such technology includes laminating a selective scattering filter in front of the sensor, which scatters the entire visible spectrum while transmitting infrared light, as shown in Figure 21. With this technology, any solar technology based on crystalline silicon can be used for the production of white or coloured modules. However, this application results in a significant efficiency drop (Solaxess, n.d.).

Similar technology is used for integrating images PV panels. Partial print patterns are often used to mask the structure of the solar cells while maintaining a high transmittance (Mittag et al., 2017). Coloured enamels absorb significant parts of the spectrum which increases the operating temperature of the module. The transparent, light-scattering design of the enamels used requires sophisticated measuring equipment to obtain optical data on printed glass panes accurately.

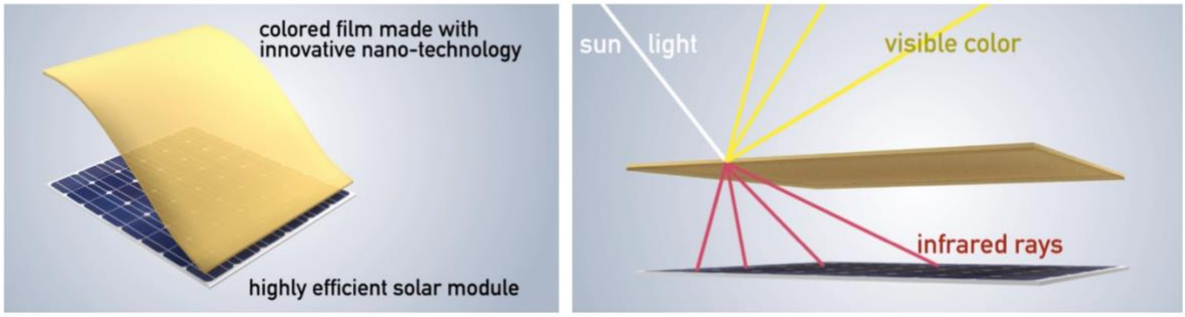

Figure 21: Selective film applied on the c-Si PV-module (Solaxess, n.d.).

2.5.3.5. PV-modules with coloured encapsulants

ethylene-vinyl acetate (EVA) is the most popular encapsulant in the PV industry, but no major producer of EVA provides coloured interlayer films. Coloured polyvinyl butyral (PVB) encapsulants are used in safety glass within the glazing industry. Thus, PVB is a technically feasible encapsulant for PV modules (Kutter et al., 2018).

2.5.3.6. PV-modules with modified front glass

Researchers previously presented a spectrally selective photonic structure inspired by the Morpho butterfly that shows angle-independent saturated colours and low glare (Bläsi et al., 2017). With this technology, colours can be obtained with low losses. The

photonic structure applied to the front glass reflects narrow bands of the incident spectrum and shows no significant absorbance, with a solar transmittance of 86-90 per cent (SwissINSO, n.d.).Another technology involves colour-coating the glass layer with an even-thickness layer, avoiding significant shading losses with a solar transmittance of 83-88 per cent (Mertin et al., 2011).Sandblasting technique onto the front glass surface, creates milky white patterns on the module surface, resulting in a reduction of solar transmittance by 29 per cent (Agea-Blanco et al., 2018).

2.5.4. BIPV Design

Typical solar panels are composed of a glass front-plate, a thin polymer interlayer and a thin polymer back sheet. Thin-film modules or crystalline silicon (c-Si) PV-modules designed for use in integrated building applications often include an additional glass back-plate. One purpose of this layer is to protect the photoelectric semiconductor from environmental influences, such as moisture. However, as opposed to modules with thin polymer back sheets, modules in laminated glass construction demonstrate increased stability and strength properties (Schulze et al., 2009).

PV-cells are usually made of brittle and thin silicon wafers, so they are embedded in a compliant polymeric encapsulant. Materials like ethylene-vinyl acetate (EVA), polyvinyl butyral (PVB) or thermoplastic silicone elastomer (TPSE) are some polymers that can be used for encapsulating solar cells in (Schulze et al., 2009).

PV-modules must endure mechanical loads such as scattered snow loads or wind strain. In addition, they are subject to non-stationary thermal conditions, including daily or year-round temperature cycles. The severity of the loads transmitted to the solar cell may be large enough to cause failures in the form of microcracks and lack of functionality of the array. Adequate design of solar modules for proper operation over a long period is therefore necessary (Schulze et al., 2009).

2.5.4.1. Crystalline silicon PV-modules

The average size of crystalline silicon (c-Si) PV-module used in a rooftop solar installation is approximately 165 cm by 99 cm. These modules are made up of individual PV-cells, which are 156 mm by 156 mm. The layers of o generic c-Si PV-module is shown in Figure 22 (Schulze et al., 2012). Most PV-modules for rooftop solar installations are made up of 72 solar cells. There is some difference depending on manufacturers and models. Custom designs for BIPV panels are also possible.

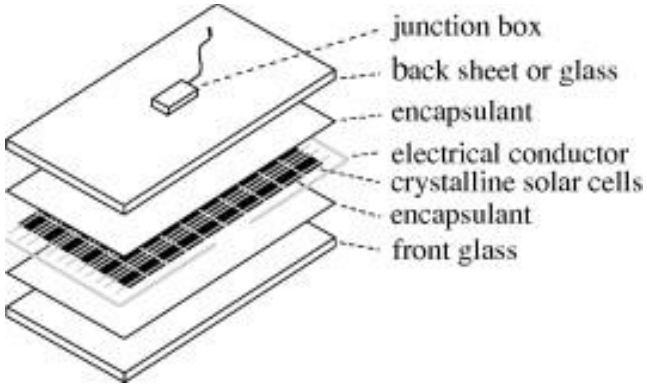

Figure 22: Layers of a generic c-Si PV-module (Schulze et al., 2012).

BIPV facade systems replace traditional rain-screen and provide. Each façade is tailor-made providing extensive design freedom in dimensions, shapes, finish and colours while standardised products are available (Onyx Solar, n.d.). The system is passively ventilated to keep the cells cool as production decreases with higher temperatures of the cells. This ventilation is provided by a minimum 5 cm gap, which can go up to 35 cm. The preferred minimum panel side length is 21 cm when consisting of a single row. The module size can go up to 200 cm by 400 cm (Onyx Solar, n.d.). The installed weight is around 13 kg per square meter (SolarLab, n.d.).

2.5.4.2. Thin-film PV-modules

Thin-film PV-modules can be customised to adapt to the needs of each project. The layers of a generic thin-film PV-module is shown in Figure 23 (Schulze et al., 2012). By spanning a range of material, length and colour, these modules allow a degree of freedom in planning and designing solar-active elements of a building envelope.

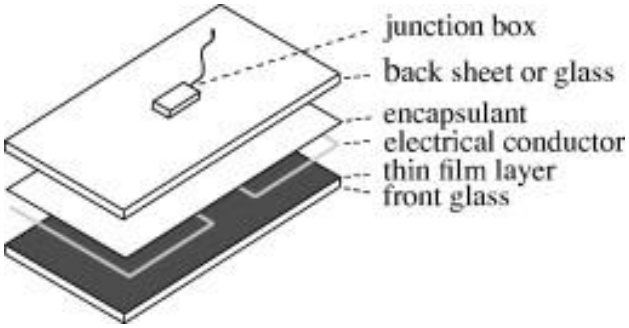

Figure 23: Layers of a generic thin-film PV-module (Schulze et al., 2012).

Non-transparent thin-film PV-modules can be used with ventilated façade systems as part of an energy-efficient and sustainable building envelope. The module size can go up to 200 cm by 400 cm (Onyx Solar, n.d.).

2.6. Façades with vegetation

Studies show that the nature view is beneficial to people's health by decreasing stress and relieving pain (Ulrich, 1984). This effect is proposed to be a result of evolution (Kaplan, 1995; Ulrich, 1984). It is concluded in one of the studies that the patients felt more relaxed when passing a corridor with features of natural daylight and view to exterior gardens (Edgerton et al., 2010).

The environmental benefits of greenery in the façades are, but not limited to, increasing the thermal performance of buildings, improving air quality, mitigating the urban heat island effect (Cheng et al., 2010), reducing noise pollution, improving the water sensitivity of the urban design, increasing urban biodiversity (McCarthy et al., 2001) and urban food production. Examples of façades systems with vegetation are shown in Figure 24 (Hollands & Korjenic, 2019).

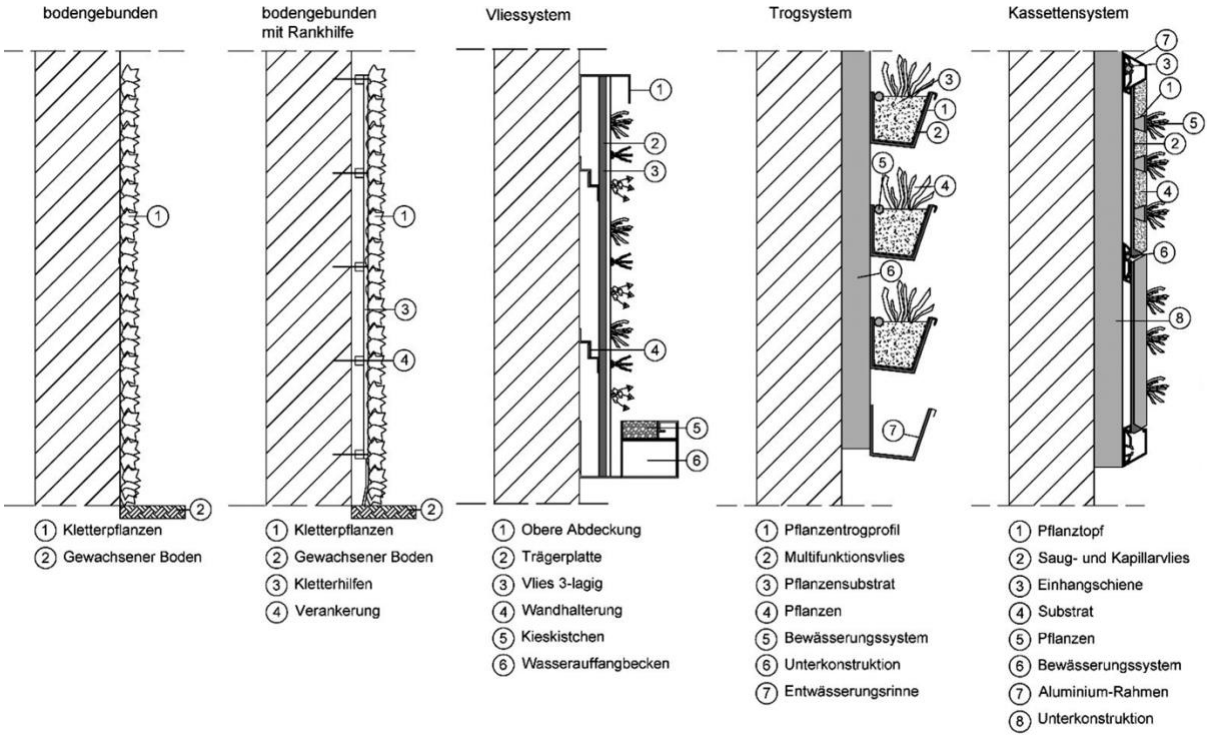

Figure 24: Example of façade systems with vegetation (Hollands & Korjenic, 2019).

2.6.1. Green façades

Green façades are systems in which climbing or hanging plants are grown using special supporting construction to cover an area (Pérez et al., 2011). The first two systems shown in Figure 24 are examples of this group. The plants can be placed directly on the ground, at the bottom of the structure, or in planters on the façade. Green façades are based on the use of climbing plants without the complexity and technification of the living wall systems (Pérez et al., 2011). The ecological advantages of the green façades, namely, savings in electricity, thermal insulation and building safety, are not so evident as with living walls (Weinmaster, 2009).

2.6.2. Living walls

Living walls are made of pre-vegetated panels, vertical modules, or planted blankets that are fixed vertically to a structural wall or frame. The panels and geotextile felt provide support to the plants. There are many commercially available living-wall systems, and they can be categorised in terms of different parameters. The study classifies living walls into three systems: trellis, modular panels and felt layer systems. This designation shall be based on the characteristics of the planter (Loh, 2008). Modular systems, like the one designed as a master thesis at the Delft University of Technology, is shown in Figure 25 (Wagemans, 2016).

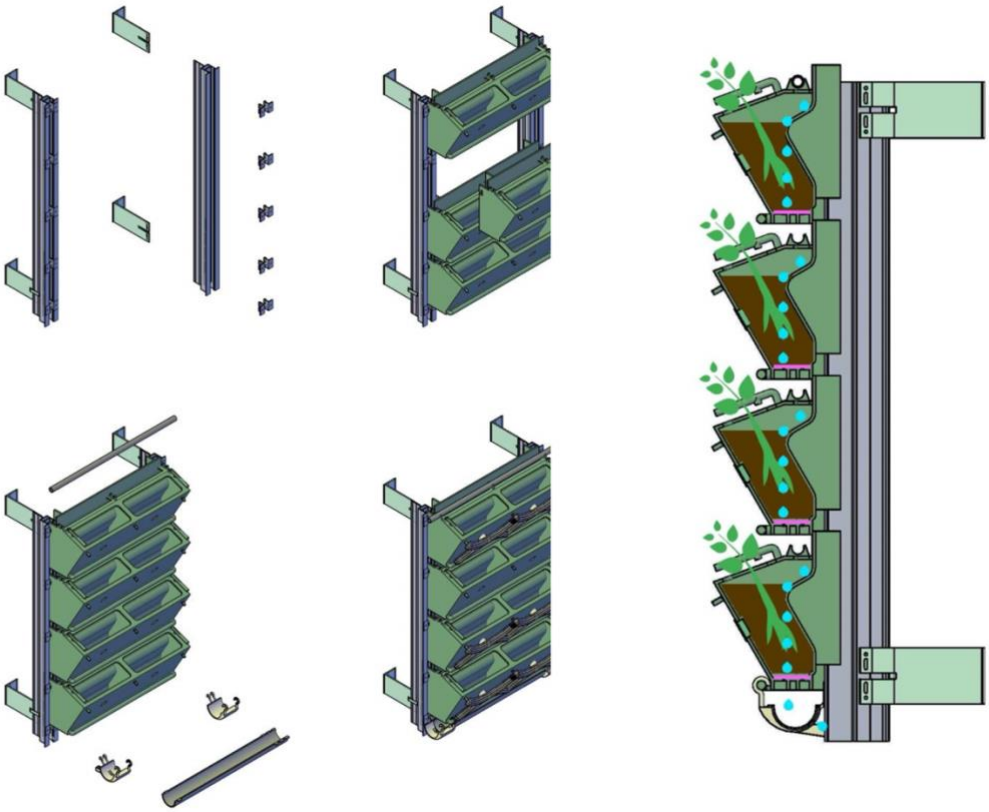

Figure 25: A modular living wall design (Wagemans, 2016).

2.6.3. Moss walls

Growing moss on façade panels is another option to have vegetation on the façades of building in an urban context. Two options to have moss covered façades are moss mats and biological concrete panels. Moss mats were primarily designed to serve as a roof covering, but these mats can also be used for the facades with a few minor changes. The biological concrete, unlike existing vertical garden systems which require complex supporting structures, the supports the growth of organisms on its own surface, without special maintenance requirement (Chairunnisa & Susanto, 2018).

2.6.4. Economic valuation of façades with vegetation

When considering the economic effects, an entire life cycle from installation to operation and disposal must be considered. To assess the value of costs and benefits over the entire life cycle, as well as monetary benefits, are incurred at different times during the observation period. Using the NPV method, these deposits and withdrawals are made comparable, since for each payment their value is determined at the beginning of a project. The NPV depends on various factors and is decisively influenced by the interest rate used.

2.7. Ventilated façade

The ventilated wall system is considered to be an important façade technology to provide protection against humidity and temperature. A ventilated wall consists of multiple layers supplying natural ventilation through the facade. This removes excess of humidity and

plays a vital role in keeping the building cool in summer. The façade also controls heat loss to keep the building warm in winter. These situations are described in Figure 26 (Marazzi Engineering, 2019). The thermal properties of the system are based on the chimney effect principle, obtained by leaving a several centimetres deep air gap between the exterior wall of the building covered with a layer of insulation and the outer panels.

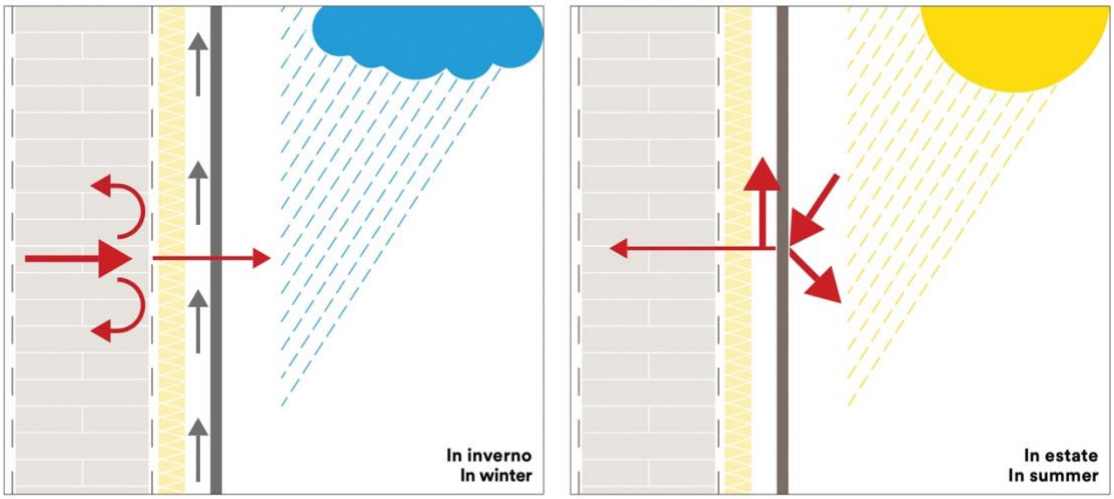

Figure 26: Ventilated façade behaviour in winter (left) and in summer (right) (Marazzi Engineering, 2019).

The ventilated facade consists of three basic components, which are thermal insulation applied to the exterior of the wall, substructure supporting outer facing and outer facing separated from insulating layer by a cavity several centimetres in-depth as shown in Figure 27 (Marazzi Engineering, 2019).

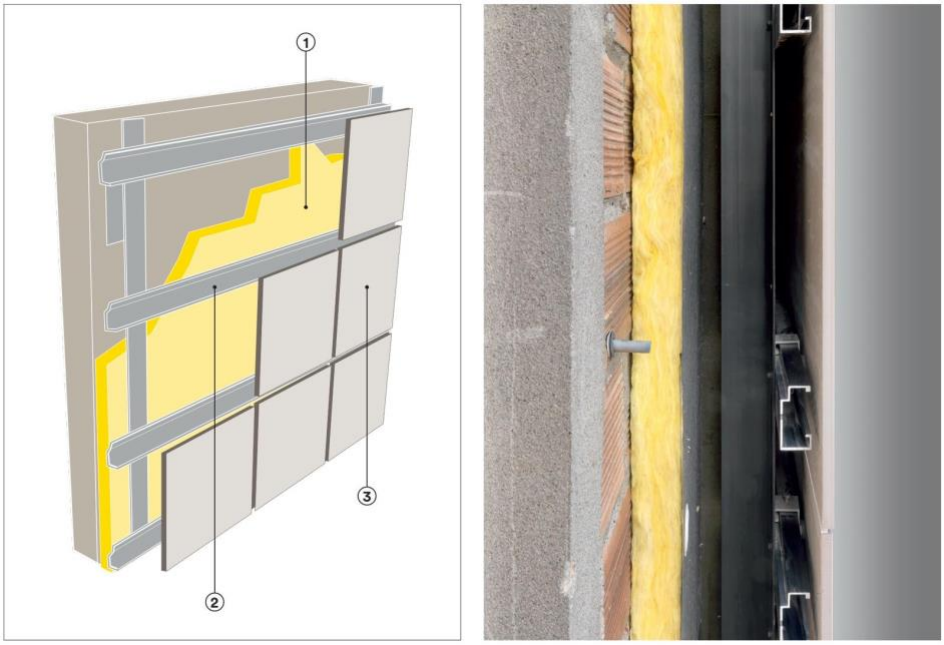

Figure 27: Ventilated façade layers (left): insulation (1), supporting substructure (2), façade cover (3) and a photograph of a ventilated façade system (right) (Marazzi Engineering, 2019).

2.7.1. Visible anchoring system

The visible anchoring system comprises façade panels fixed to the supporting substructure via screws, hooks or other fasteners, which are visible from the exterior. It is relatively cheap, efficient. The assembly with the hooks is done by driving the panels horizontally, fed from the side. Hooks are mostly used for façades with ceramic or stonework cladding, of which the diagram can be seen in Figure 28 (Marazzi Engineering, 2019).

Figure 28: Visible anchoring system (Marazzi Engineering, 2019).

2.7.2. Concealed anchoring system

In the concealed anchoring system, the façade panel is anchored to the load-bearing substructure by clamps fixed to the back of the panel with special screw anchors, or by means of slots integrated into the panels. The substructure consists of vertical profiles with wall brackets and crosses members riveted or screwed to the profiles. Since the tiles are not punctured by screws or rivets, no dirt can accumulate underneath, and the tile remains clean. The traditional systems of this type of system usually require a bottom to top or top to bottom installation as the panels are fixed via screws from one side after being hung. Examples of this system can be seen in Figure 29 (IPEX, 2020).

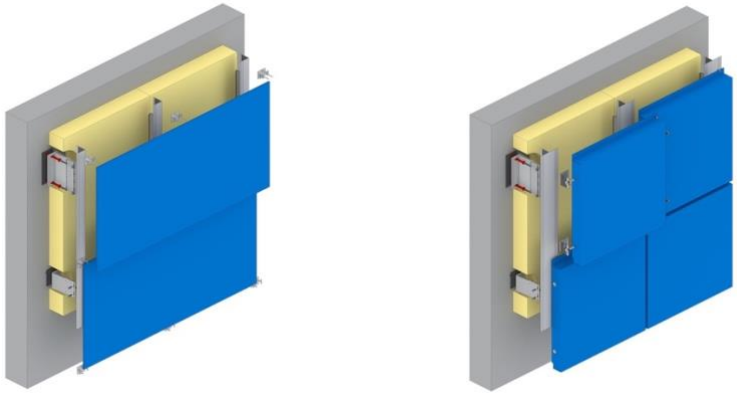

Figure 29: Examples of concealed anchoring system (IPEX, 2020).

Another solution for individual repairs of the panels is available for a thin-film BIPV-system product. After the panels are placed, they are secured via clamps tightened from between the panels. A plan drawing of this system with an installation diagram is shown in Figure 30 (Avancis, 2019b).

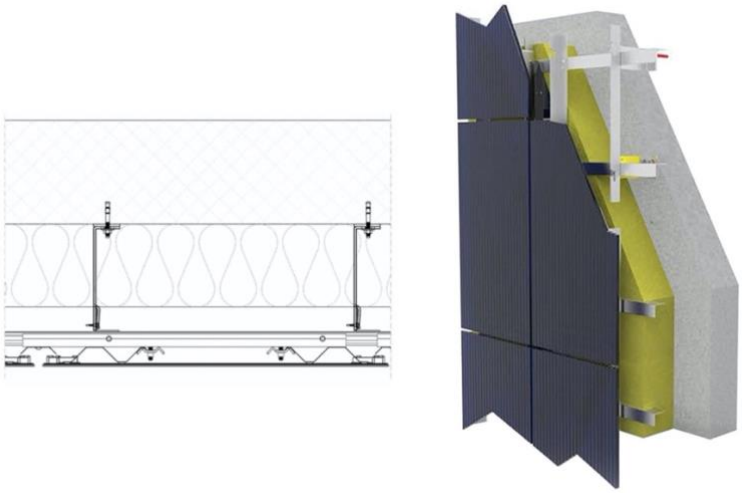

Figure 30: Example BIPV ventilated façade plan drawing (left) and façade installation diagram (right) (Avancis, 2019b).

2.7.3. Click system

This system is a click-fit ventilated façade solution which is relatively easy to install. They can be installed retrospectively without any additional effort in areas where the panels cannot be installed directly, because of scaffold anchors, missing panels or for other reasons. This feature can be used for maintenance or replacement of the BIPV modules in a non-destructive manner, without the need to dismantle the entire facade surface. A diagram showing the system components is shown in Figure 31 (Kalzip, 2019).

Figure 31: Façade composition with the click system (Kalzip, 2019)

3. Analysis

During the analysis stage of the AMC Amsterdam, the BIM-model of the building, which had been supplied by Delft University of Technology Faculty of Architecture and the Built Environment, was used to determine functions, investigated façade properties and extract 3D geometries. AMC's location and axonometric views of the model can be observed in Figure 32.

Figure 32: AMC's location and axonometric perspectives from the South-East and North-West.

3.1. About the AMC

The AMC in Amsterdam is the largest academic hospital in the Netherlands and comprises of about half a million square meters of floor area. The design dates back to the end of the seventies and is from the Dutch architects of Mourik and Duintjer. In addition to buildings, covered streets and squares, the complex also includes the medical faculty of the University of Amsterdam (TU Delft, 2018).

3.2. Functions and user needs

The building has three main users with their own requirements and wishes: A safe, clean and efficient work environment for doctors and nurses, recovery area for the patient and a working environment for education and research in the university (TU Delft, 2018). The functional distribution is shown in Figure 33

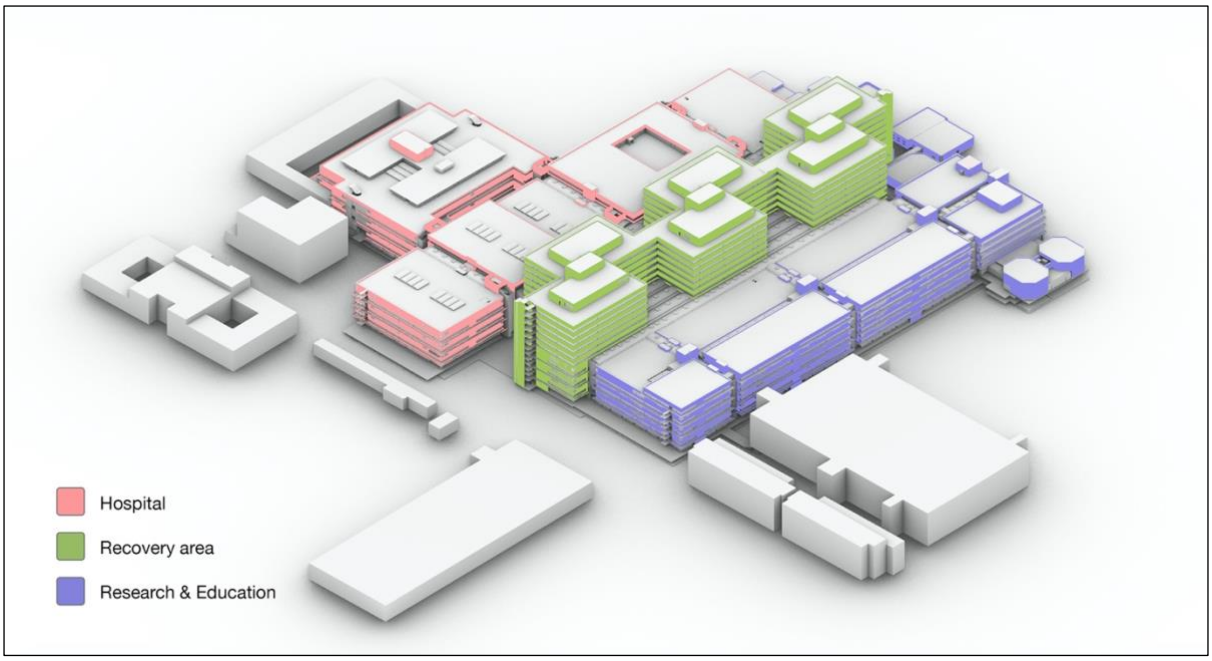

Figure 33: Building functions.

3.3. Energy usage

AMC is currently producing a large part of its energy need with its own combined heat and power (CHP) plant. In this thesis, only the electricity part will be considered. Every year it produces 112.353 MWh electrical energy at the CHP plant. The purchased net electricity is 12.981 MWh. These add up to 125.334 MWh. A breakdown is given in Table 4 (TU Delft, 2018).

Table 4: Breakdown of electricity use in the AMC.

Sort	**Amount**
Ventilation	20.988 MWh
Lighting	17.490 MWh
Appliances	38.102 MWh
Medical and research equipment	48.754 MWh
Total	125.334 MWh

Amsterdam's near-future climatic ambitions are being CO2- and energy-neutral, fossil-free and circular in all terms of materials. Large-scale, far-reaching renovations are envisioned as well as aesthetically and historically integrated PV panel maximisation (Van den Dobbelsteen, 2018).

3.4. Façade

3.4.1. Façade types in the building

There are many façade cladding types used in the building, such as concrete, steel sheets and sandwich panels. These façade types were investigated, and their components were tried to be revealed to determine the retrofitting options. This step was made using the BIM-model, the photographs of the building and the common knowledge about the relevant cladding type. The illustration of which parts of the façade was taken as type samples can be seen in Figure 34.

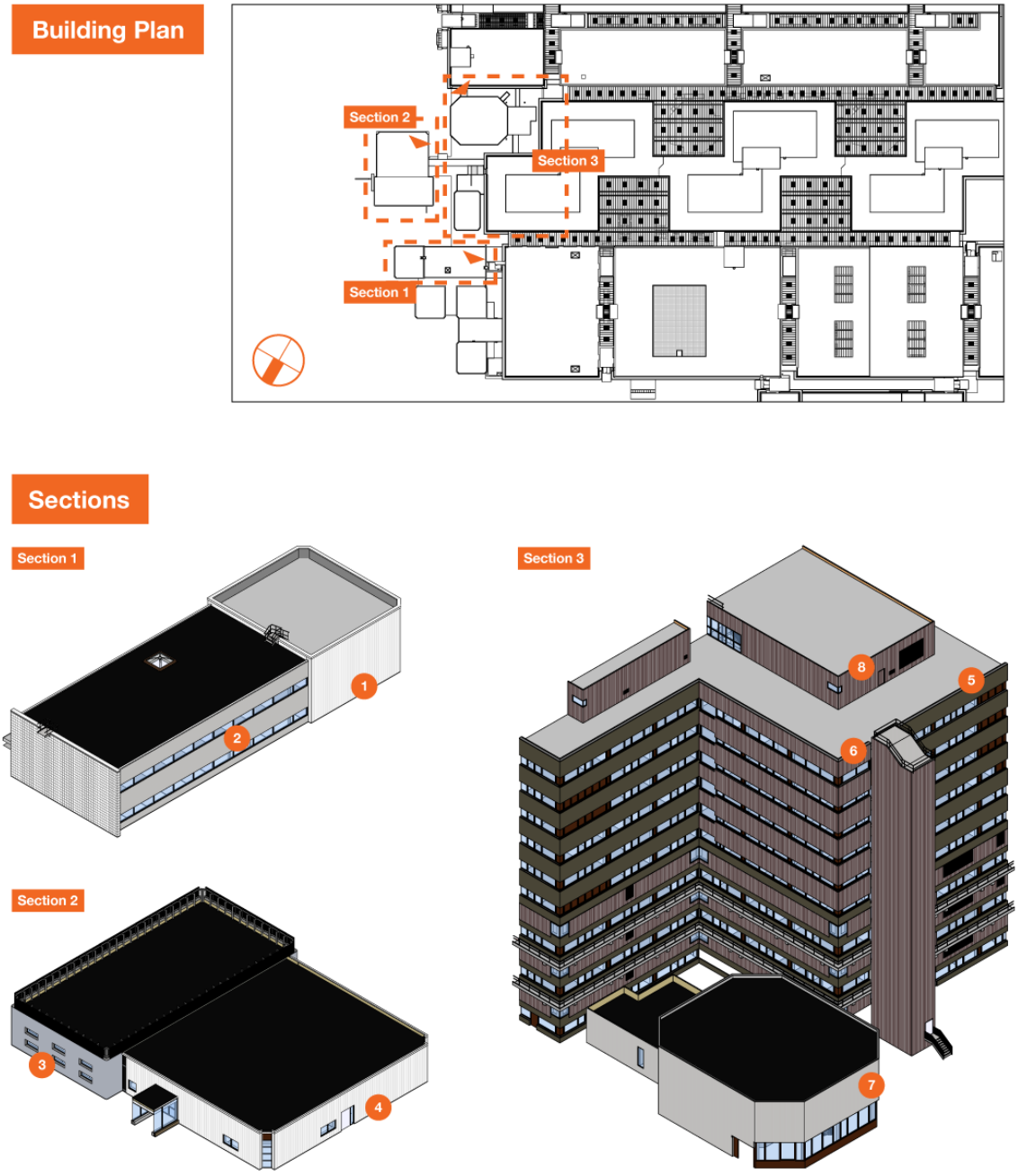

Figure 34: Different façade types (1 to 8) and their position in the building.

The BIM-model was used as a base for the materials and their thicknesses. However, not all the components can be seen in the model, especially the substructures. Generic components were used for the illustration in Figure 35. This illustration may not reflect the absolute reality. It can be useful when designing, considering that some of the components may be kept for avoiding unnecessary costs.

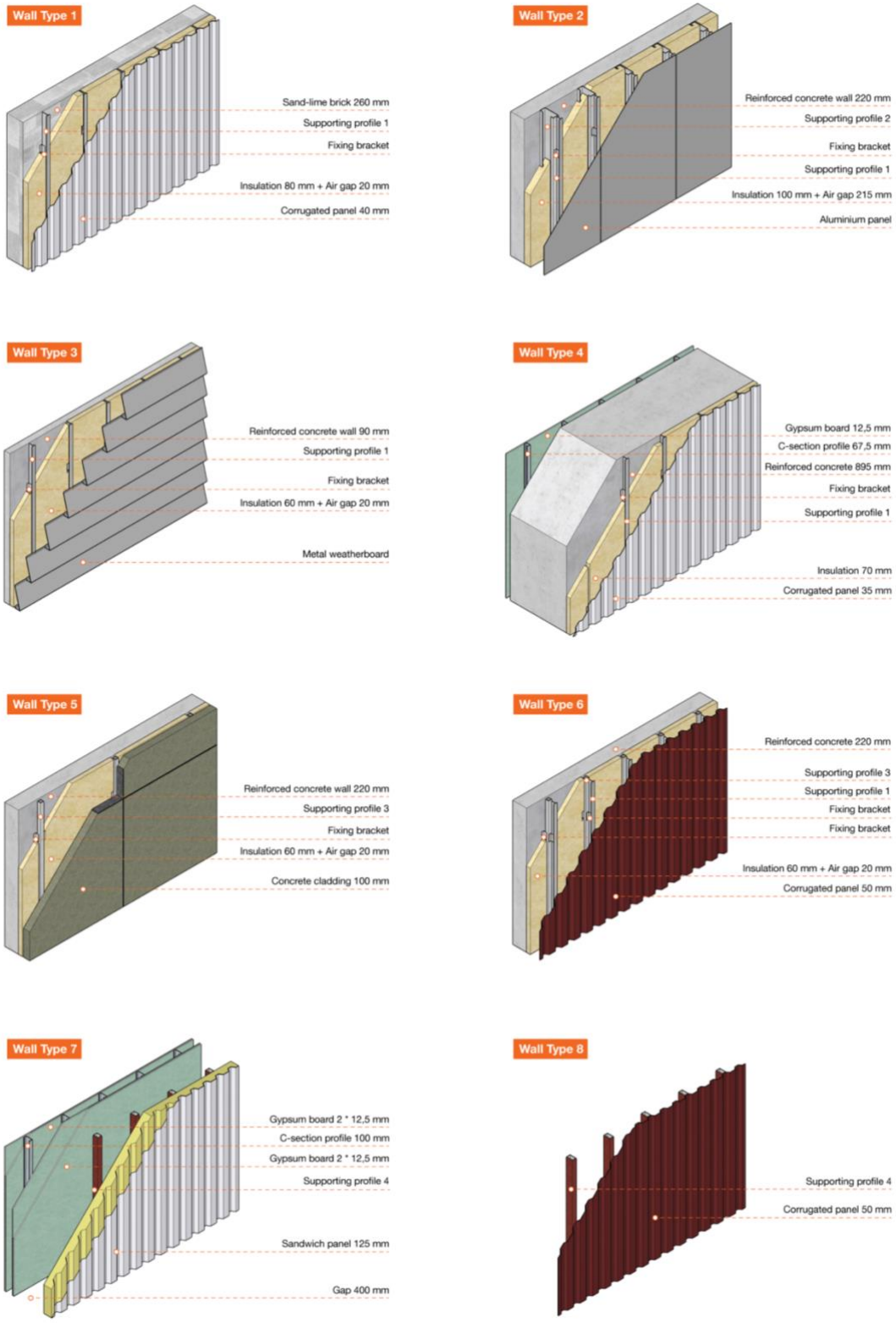

Figure 35: Components of the façades. Materials and layer thicknesses were taken from the BIM-model, but the substructures were interpreted.

3.4.2. Façade thermal properties

At the AMC, both low-rise and high-rise buildings have a horizontal articulation in the facade, which can mainly be read from the concrete elements. In low-rise buildings, continuous concrete balconies occur on user layers, whereas concrete bands characterise the technical layers. The high-rise building consists of a concrete façade cladding that alternates with strips of glass (TU Delft, 2018).

DGMR Bouw calculated the R-value of the low-rise and high-rise buildings considering the following factors (2016):

- The ageing of materials results in lower insulation value.
- At the low-rise building, the effect of the unheated installation space causes a greater heat loss
- The concrete strip on the façade loses much heat due to thermal bridges.

As a result, measures must be taken on the thermal insulation to ensure that the façade meets the requirements described in NEN 1068. Additionally, measures must be taken on the thermal bridges in the façade to ensure that they meet the requirements in accordance with NEN 2778 and NEN-EN ISP 10211-2 (DGMR Bouw, 2016).

In Figure 36, steady-state thermal simulation results of AMC low-rise and high-rise parts can be seen, in which an inside temperature of 18°C and an outside temperature of 0°C was taken (DGMR Bouw, 2016).

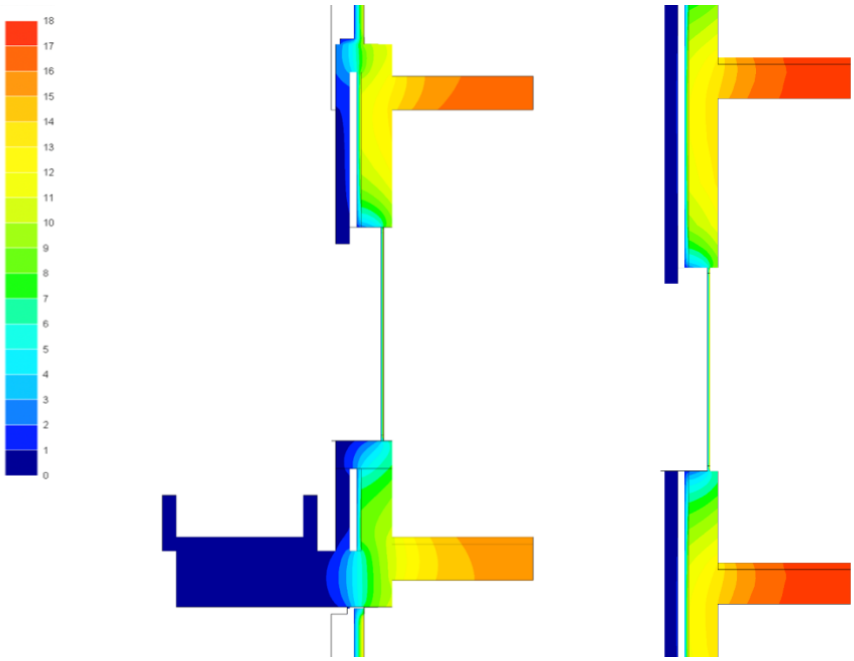

Figure 36: Steady-state thermal simulation results of AMC low-rise (left) and high-rise (right) (DGMR Bouw, 2016).

The specific R_c value is given as 0,56 m^2K/W for low-rise building and 0,61 m^2K/W for the high-rise building. Additionally, the same report asserts that the temperature factor, which can be used as an indicator for good quality becomes 0,3 at the points where the

window frames are connected to the parapet, even though the minimum number that can be accepted is 0,5 (DGMR Bouw, 2016). This situation can also be approached as a thermal bridge problem. The suggested options are moving the frame to the inside or adding an insulation layer to inside or outside.

3.5. PV electricity generation potential

The 3D geometry of the building extracted from the BIM-model was imported to Sketchup to draw simpler façade geometries for simpler calculation. The simplification process comprises the alignment of façade faces of different depths to the outermost one and cleaning the edges of coplanar faces.

Surrounding buildings were not included in the building drawings. So, we used the site plan drawing to create 3D geometry of the surrounding buildings and arranged the heights and the vertical articulations by an eyeball estimate, looking at Google Street Views. Trees are thought to have an effect as well. However, they were excluded from the analysis. The plan view of the analysis setting is given in Figure 37.

Figure 37: The plan view of the solar analysis setting.

The most favourable blocks in terms of PV energy yield were to be selected through an overall annual radiation analysis to design a façade system onto consequently. We conducted this analysis using Ladybug for Grasshopper. Amsterdam 062400 (IWEC) weather file was used. The BIM-model had been created with no geographic angle, so were the exports. Thus, we adjusted the North by the input of 150° in Grasshopper.

The breakdown can be observed in Table 5 with their favourability rating obtained by the formula $Total\ radiation \div (Area \times 100)$. The total radiation on the façades of blocks A, B, C, D, E, F, G, H, J, K, L, M and Z was calculated to be 14.710 MWh. The total radiation on the roofs was calculated to be 32.800 MWh. The annual insolation of all the envelope

surfaces of the AMC is around 47.500 MWh, which can result in 9.500 MWh/year electricity revenue with a high-efficiency conversion of 20 per cent. This is still far less than the 125.334 MWh annual electricity usage, or even less than the 12.981 MWh net electricity purchase of the building.

Table 5: Façade insolation breakdown with ratings.

Block	**Area** (m_2)	**Radiation** (kWh)	**Preference** Radiation / (Area * 100)
A	4.962,8	1.099.000	2,2
B	1.641,6	356.477	2,2
C	2.686,9	570.624	2,1
D	2.102,4	319.169	1,5
E	2.491,1	770.953	3,1
F	6.787,2	2.416.200	3,6
G	5.185,6	1.994.000	3,8
H	7.590,0	2.756.000	3,6
J	3.832,3	1.092.600	2,9
K	2.961,5	964.672	3,3
L	2.961,7	806.890	2,7
M	4.637,3	1.562.415	3,3

Isometric perspectives of the building geometry with the radiation analysis result reflected on the façades, from the South can be seen in Figure 38 and the North in Figure 39. The insolation of the roof can be observed in Figure 40.

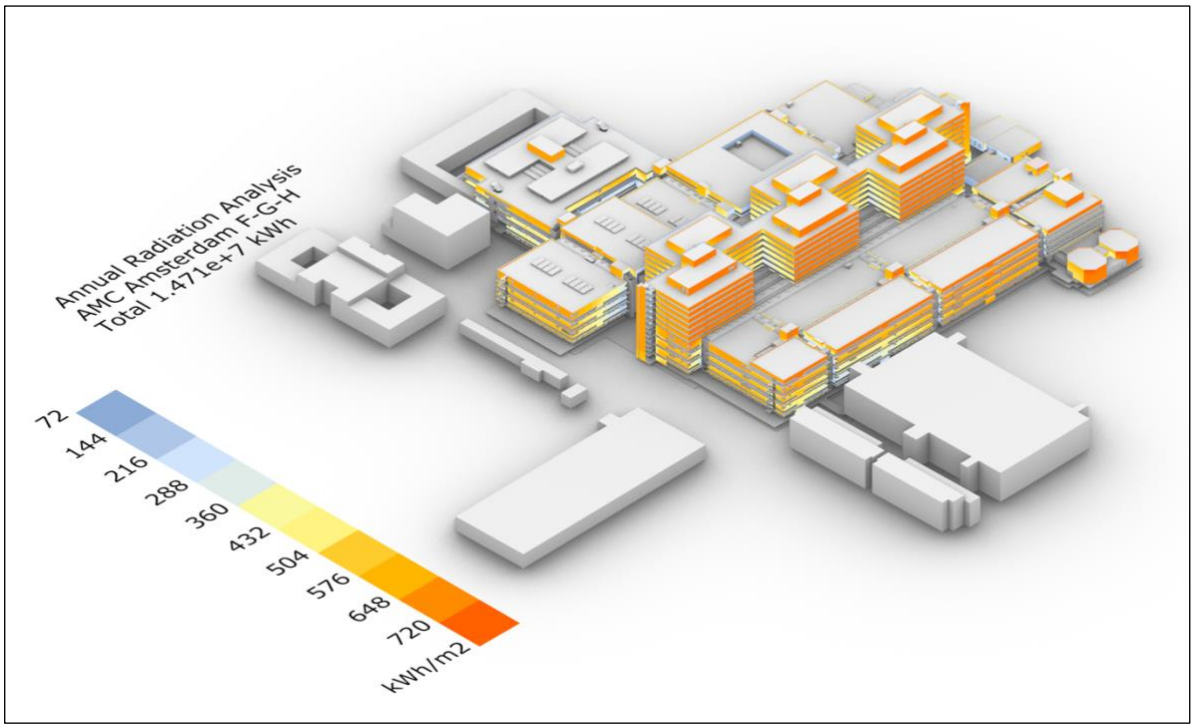

Figure 38: Façade insolation analysis result (view from the South).

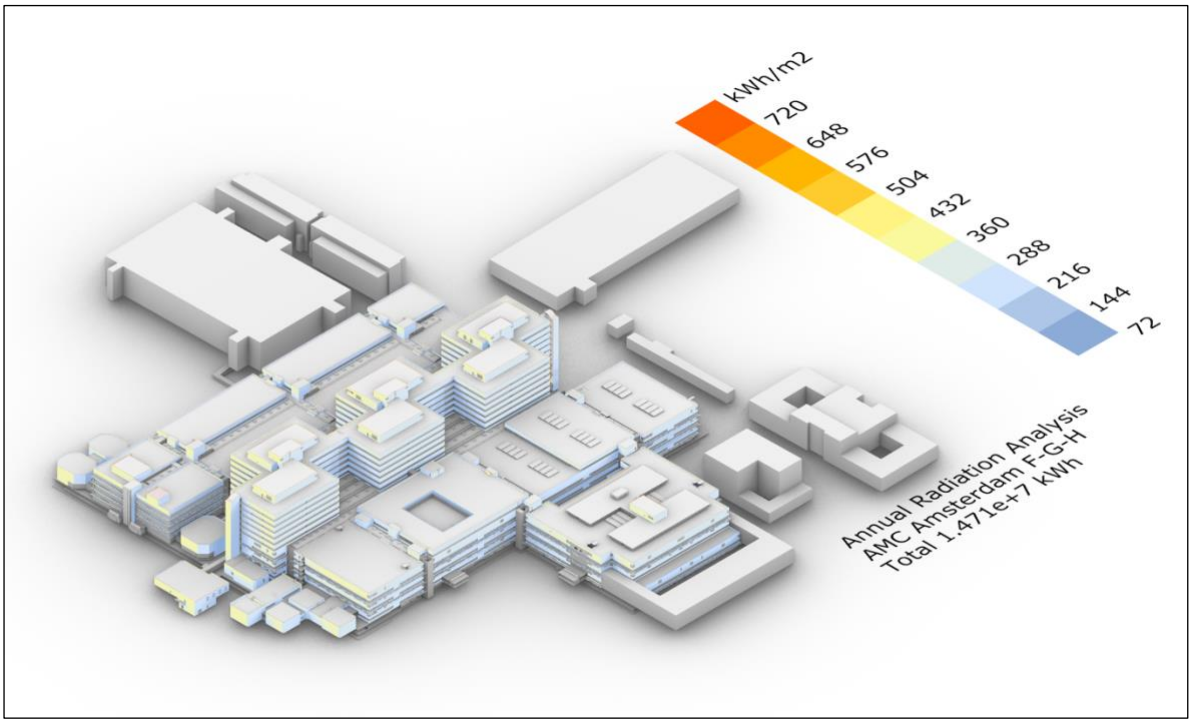

Figure 39: Façade insolation analysis result (view from the North).

By looking at the results, it can be seen that the solar exposure of façades of the lower blocks of the AMC building is mostly obscured by the surrounding buildings, which are located in the South. The trees were not included in this analysis.

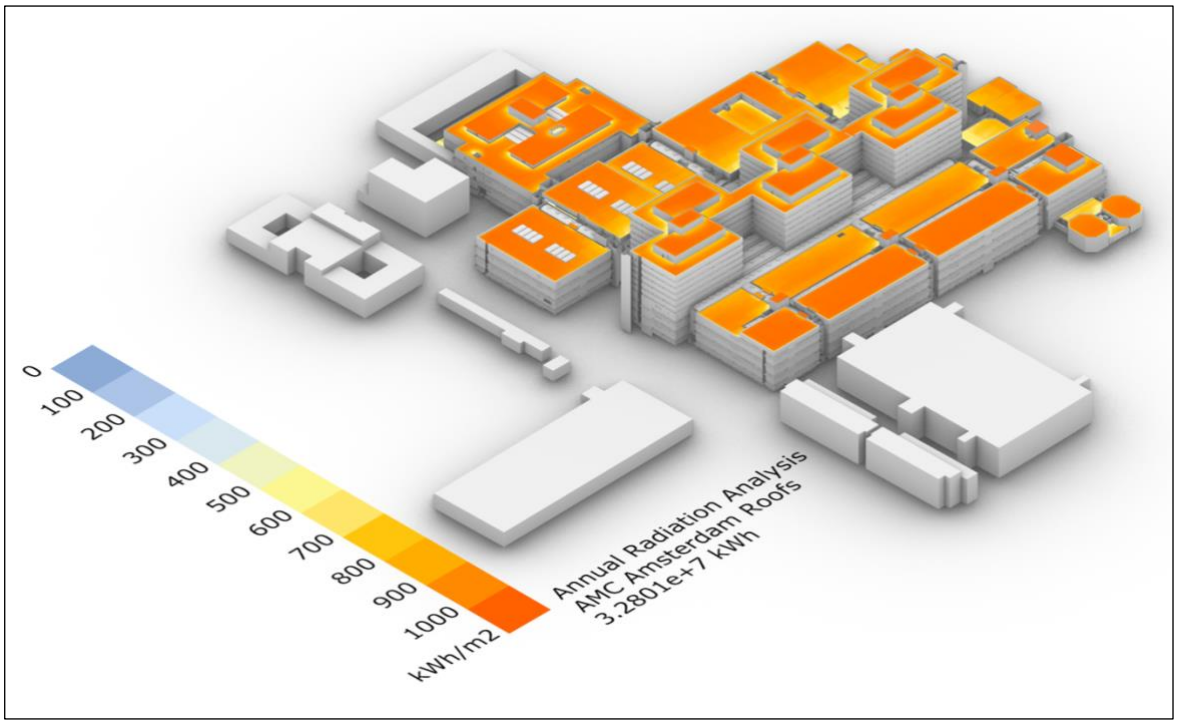

Figure 40: Roof insolation analysis result (view from the North).

3.6. Trade-off between energy and water management

Flat roofs of the buildings carry great potential to add quality and functional areas to the buildings. However, since the roof area is relatively small compared to the total construction area, how this space will be used is an aspect to be thought of carefully. As seen in the PV-energy potential analysis, the roof is more beneficial compared to the façades. Nevertheless, green roofs are another beneficial option for this large concrete building in terms of avoiding huge amount of water run-off, contributing to the micro-climate management and also supplying good views for the in-patients and the staff in the bed tower. In fact, the Netherlands government is planning to develop projects with green roofs and no connection for rainwater connection, in favour of local area planning (Government of the Netherlands, 2016). As seen in Figure 41, if the rooftops, which can be seen from the bed tower, are covered with greenery, around 20 per cent of the whole roof area can be used for energy generation.

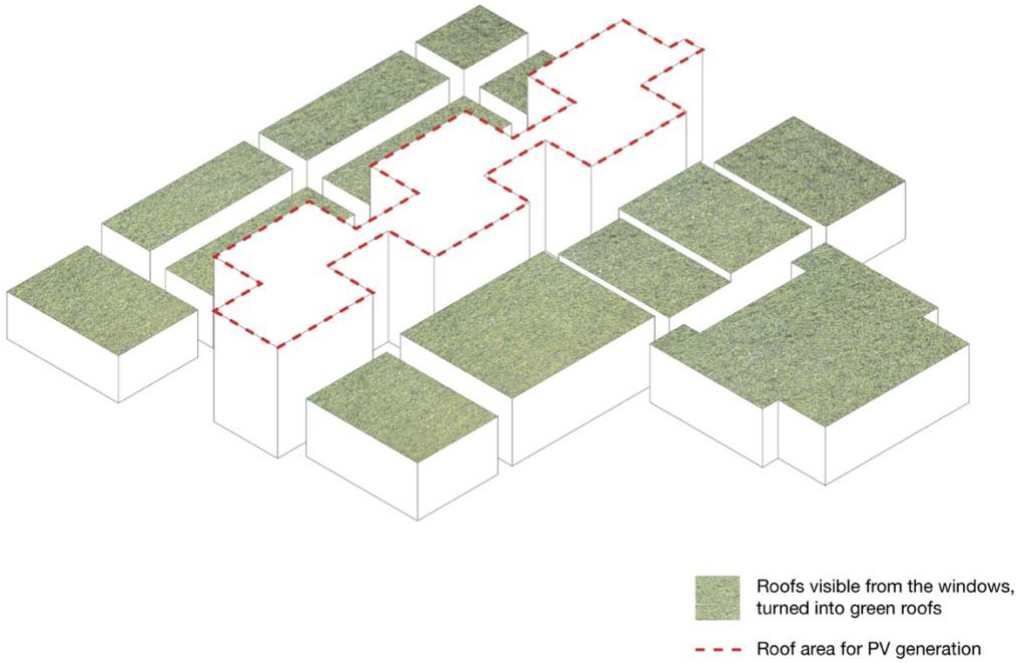

Figure 41: If the roof visible from the bed towers are turned into green roofs, very small are is left for energy generation.

3.7. Cladding with standard PV-modules

As a reference for assessing the design, the building façade was cladded with standard 72-cell PV-modules. These panels a dimension of 199 cm by 99 cm. 31.673,41 m2 of façade area was cladded with 10446 panels, which makes 65 per cent of the whole façade. The distribution of the panels is shown in Figure 42. This percentage can be increased by decreasing the module size, which would result in a finer level of panelling.

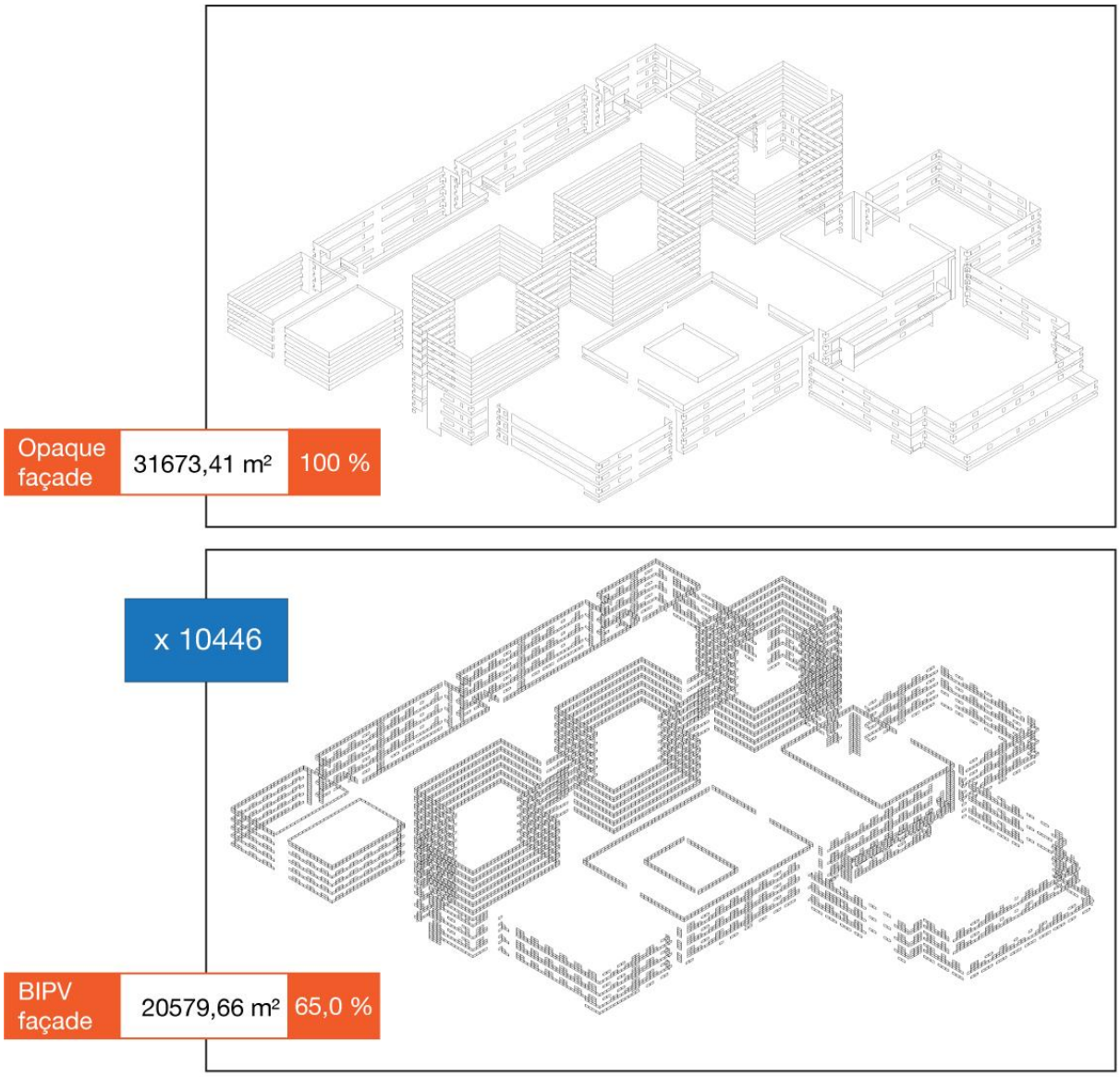

Figure 42: Distribution of standard PV-module son the opaque walls of AMC.

4. Design

4.1. Design rules

4.1.1. Project vision

The analysis of the AMC showed that the renovation of the building is necessary, as the thermal properties of the façades do not meet the standards anymore, due to decaying and its outdated technology. So, the project starts with the assumption of the façade of the low-rise and high-rise buildings with concrete wall core would be completely replaced.

In the project planning, it was envisaged that the façade can cladded with different types of interchangeable panels, so that the façade acts like a flexible solar farm or an expandable surface for greenery. This ensures the possibility of investment for PV installation or living walls at any point over the building's lifespan and also easy maintenance. A diagram of the envisaged application process, which is independent from the research process is given in Figure 43.

The process starts with the research about the concept. In the first step of the application, the balconies, which are prefabricated detachable pieces are dismantled to be able to create a reachable working surface. Then the existing façade is peeled off. The next step is to anchor the fixing brackets on the façade, installing the insulation layer and the supporting substructure before installing the new panels. If special panels like BIPVs or living walls are to be used, their infrastructure should be set up beforehand. The balconies, either as they are or renewed and cladded with special panels depending on the strategy, can be then put back to their place. In time, if the investing conditions change, the installation can be altered.

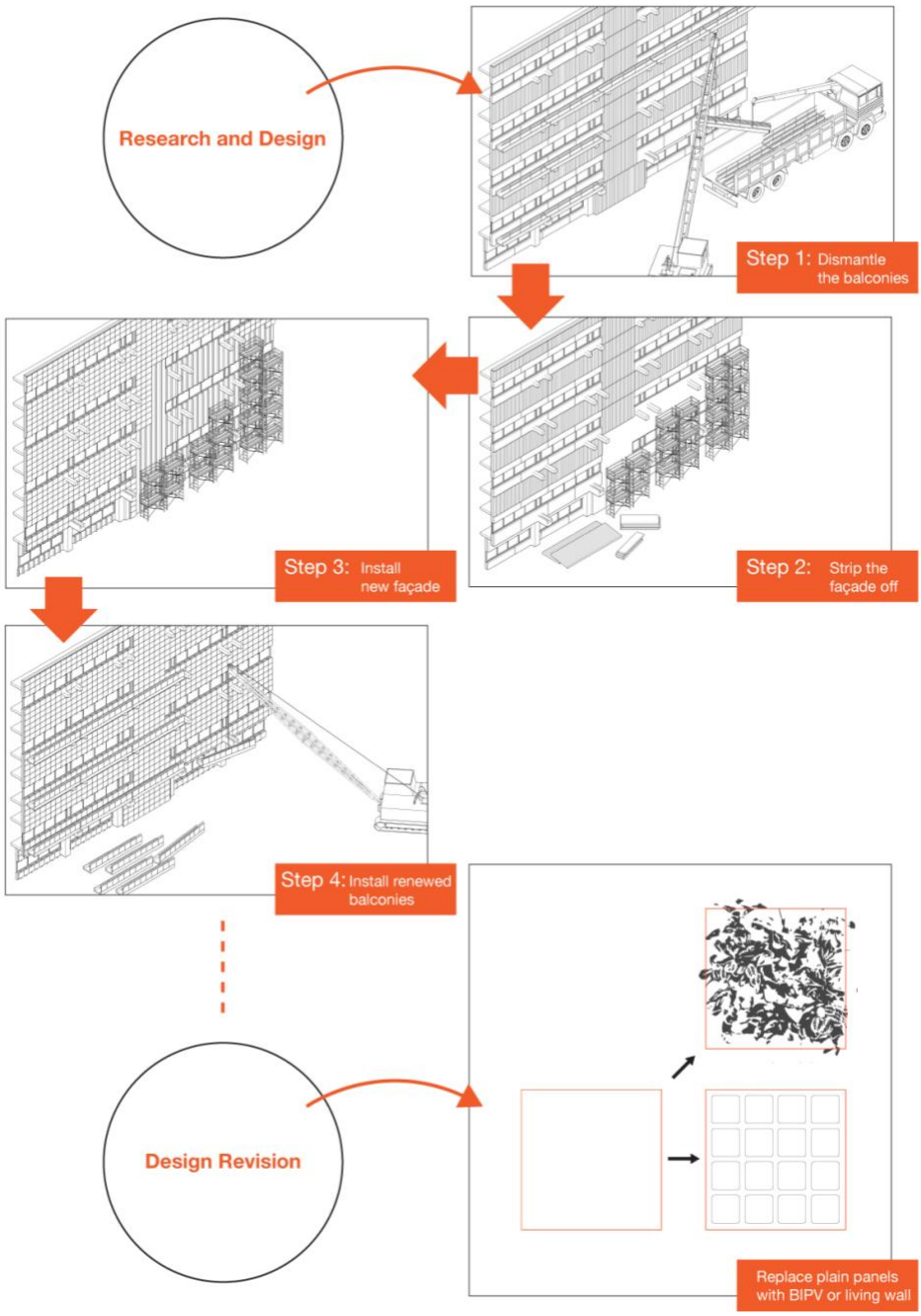

Figure 43: Diagram showing the project planning.

4.1.2. Façade materials

A set of possible façade options were investigated as the project vision involves interchangeable façade panels applied all over the building. Plain façade covers were chosen to constitute the base as they are cheaper and would not need as much maintenance.

For such a façade restoration, metal cladding is a suitable option for its durability and low maintenance requirement (Architizer Editors, n.d.). We compared several material

options for the façade panels, regarding their embodied energy and CO_2 footprint, alongside their appearance. These materials are aluminium, zinc, copper, titanium and stainless steel. Additionally, for a similar appearance as the building has at the moment, fibre cement was also added to this comparison.

A comparative chart was prepared using CES EduPack 2019 (Granta Design, 2019) except for concrete and fibre cement (Milne & Reardon, 2013). Figure 44 and Figure 45 give an overview of the considered materials and their environmental impact. In practice, these materials would require different designs, and as a result, the quantity might change, especially comparing metals with concrete. Titanium is the least preferable option due to its high environmental impact. Aluminium has a high embodied energy and carbon footprint as well. Zinc and copper were considered too expensive, as the main aim of this study is to offer a cost-effective solution.

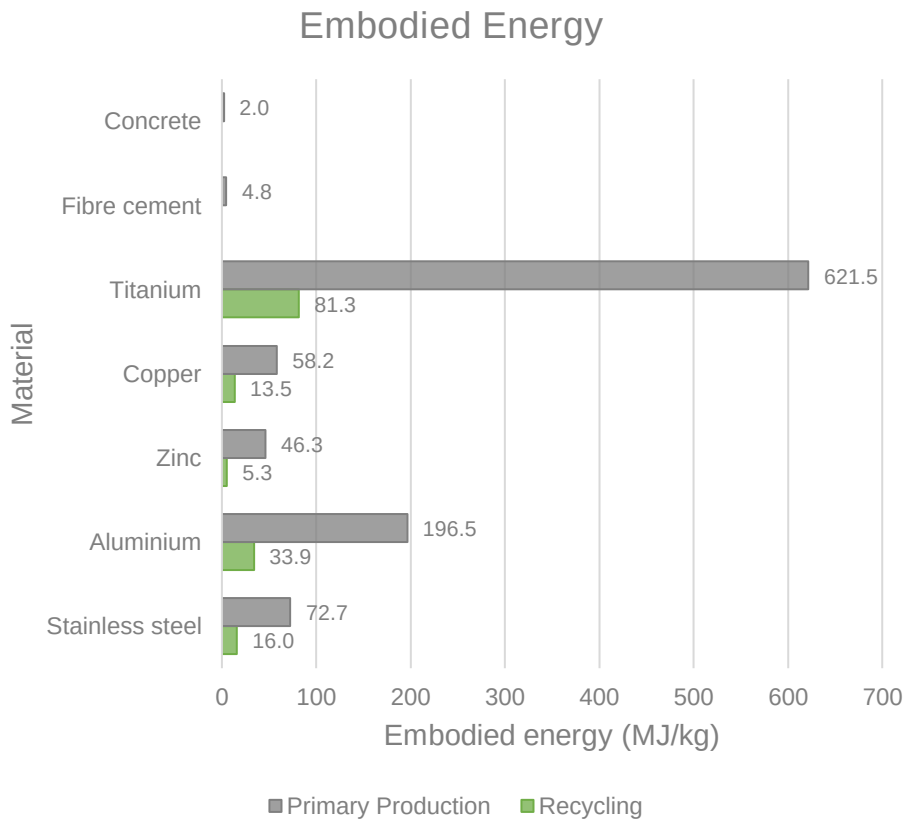

Figure 44: Material options, embodied energy comparison.

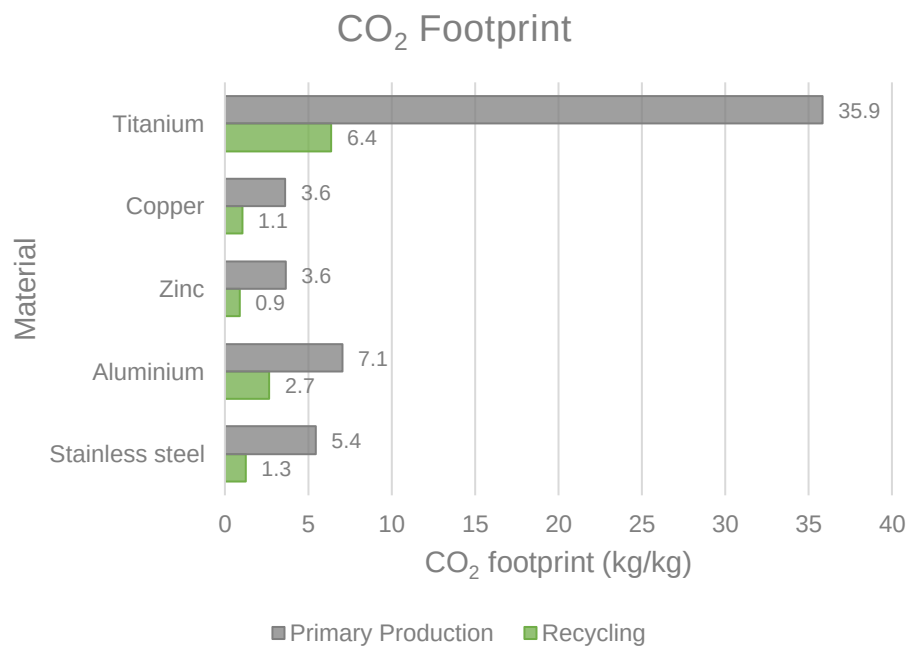

Figure 45: Material options, CO_2 footprint comparison.

Figure 46 shows that fibre cement has a significantly low embodied energy. To have insight, we compared façade claddings mad of 10 mm fibre cement and 2 mm steel. Considering the density of steel 8005 kg/m2 and fibre cement 1650 kg/m2, the embodied energy of the steel façade becomes 256,16 MJ/m2 and the fibre cement becomes 79,2 MJ/kg. The downside of this material is that it is not fully recyclable, and its end-of-life use is mostly landfill.

The infrastructure and incentive for recycling steel exist, and when steel is recycled, it is not downgraded. After being formed into ingots, the material can be put again to the production process. Usually, a hot rolling process transforms the ingots into plates (Montanstahl, 2017). This gives flexibility regarding material use, and material savings gain favour.

Considering the positive effect of economies of scale in such a large building, the façade types were kept at minimum. The three panel types; stainless steel, BIPV and living wall panels are shown in Figure 46 (Living wall reference: ANSglobal, https://www.ansgroupglobal.com).

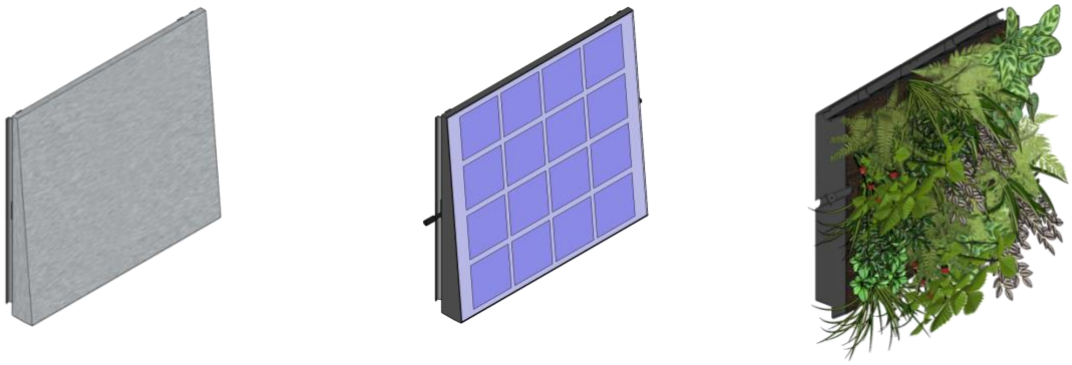

Figure 46: Stainless steel, BIPV and living wall panels.

4.1.3. Insulation

In the cavity walls, all types of heat transfer occur; conduction, radiation and convection. Air is a good insulator that increases the thermal resistance of the wall construction. Unfortunately, the air in a cavity structure does not remain still. There is a flow, and even if the cavity is not ventilated, a large amount of heat resistance in the air is reduced significantly by radiation and convection (van der Linden, 2013).

Giving an exact value for the heat resistance for any particular cavity is not possible. Calculations are generally made using an average value obtained by measurements. If there is a well-ventilated layer of air in construction, R_c value can be calculated by counting only the specific heat resistances of the layers that are situated on the inside of the air layer (van der Linden, 2013). We used this approach, calculating the amount of insulation layer needed.

When dealing with the construction of the same thickness throughout, the heat resistance can be calculated for every layer. The total heat resistance can be found by adding up the resistance values of the individual layers (van der Linden, 2013):

$$R_c = R_1 + R_2 + R_3 + \cdots$$

Where;

R_c : the heat resistance of the total construction in m^2K/W

$R_1, R_2, R_3, \ldots$: the heat resistance of the individual layers in m^2K/W

When calculating the amount of insulation needed, two approaches are possible depending on the Building Decree 2012: either aiming the new building insulation level of R_c=4,5 m^2K/W or stick by the renovation insulation level, which is R_c=1,3 m^2K/W.

We took the concrete core of the AMC façades as a base. These are 220 mm thick concrete walls. We calculated the thermal resistance of these walls with the following formula (van der Linden, 2013):

$$R = \frac{d}{\lambda}$$

Where;

R : the heat resistance of the total construction (m2K/W)

d : the thickness of the layer (m)

λ : heat conduction coefficient (W/mK)

Considering the heat conduction coefficient of concrete 0,9 W/mK, the thermal resistance of the wall core was calculated as:

$$R_{core} = \frac{0{,}22\ m}{0{,}9\ W/mK} = 0{,}24\ m^2K/W$$

The insulation can be applied to the inside, to the outside, or both. In the case that insulation is applied to the interior, one 12,5 mm thick gypsum board and 15 mm of plaster would be used. The thermal resistance of these layers is as follows:

$$R_{gypsum\ board} = \frac{0{,}125\ m}{0{,}17\ W/mK} = 0{,}73\ m^2K/W$$

$$R_{plaster} = \frac{0{,}15\ m}{0{,}2\ W/mK} = 0{,}75\ m^2K/W$$

Insulation material can be chosen from a variety of options. Every application and every insulation goal require its own specific insulation material. For insulating walls, the materials given with their preferable properties in Table 6 can be used (De Isolatieshop, n.d.).

Table 6: Possible insulation materials and their properties (De Isolatieshop, n.d.).

	Mineral wool	**Glass wool**	**PIR**	**EPS**	**XPS**
Lambda value, λ (W/mK)	0.033 - 0.040	0.032 - 0.040	0.022 - 0.027	0.036	0.034 - 0.036
Fire resistance	Very good	Good	Bad	Bad	Bad
Heat insulation	Good	Good	Very good	Fair	Fair
Sound insulation	Very good	Very good	Fair	Fair	Fair
Flexibility	Very good	Very good	Fair	Fair	Fair
Recyclability	Very good	Very good	Fair	Very good	Very good

Mineral wool was selected because of its precedence in fire resistance and recyclability. The thickness of the insulation layer was calculated with the following formula, which is a conversion of the thermal resistance formula above (van der Linden, 2013):

$$d = R \times \lambda$$

The higher bound for the thermal conductivity of mineral wool is 0.040 W/mK in Table 6. Thus, the required minimum thickness of the insulation layer of the construction with interior insulation was calculated as 111,2~120 mm. The required minimum thickness of the insulation layer without interior insulation is 170,4~180 mm. 180 mm insulation is difficult to achieve only on the outside, as the current total thickness of the construction attached to the core is already 180mm. The additional thickness on the outside may cause a clash with the balconies and using only interior insulation may cause a significant decrease in the room area. So, a combination of options shown in Figure 47, which was prepared based on DGMR Bouw's analysis (2016), is recommended.

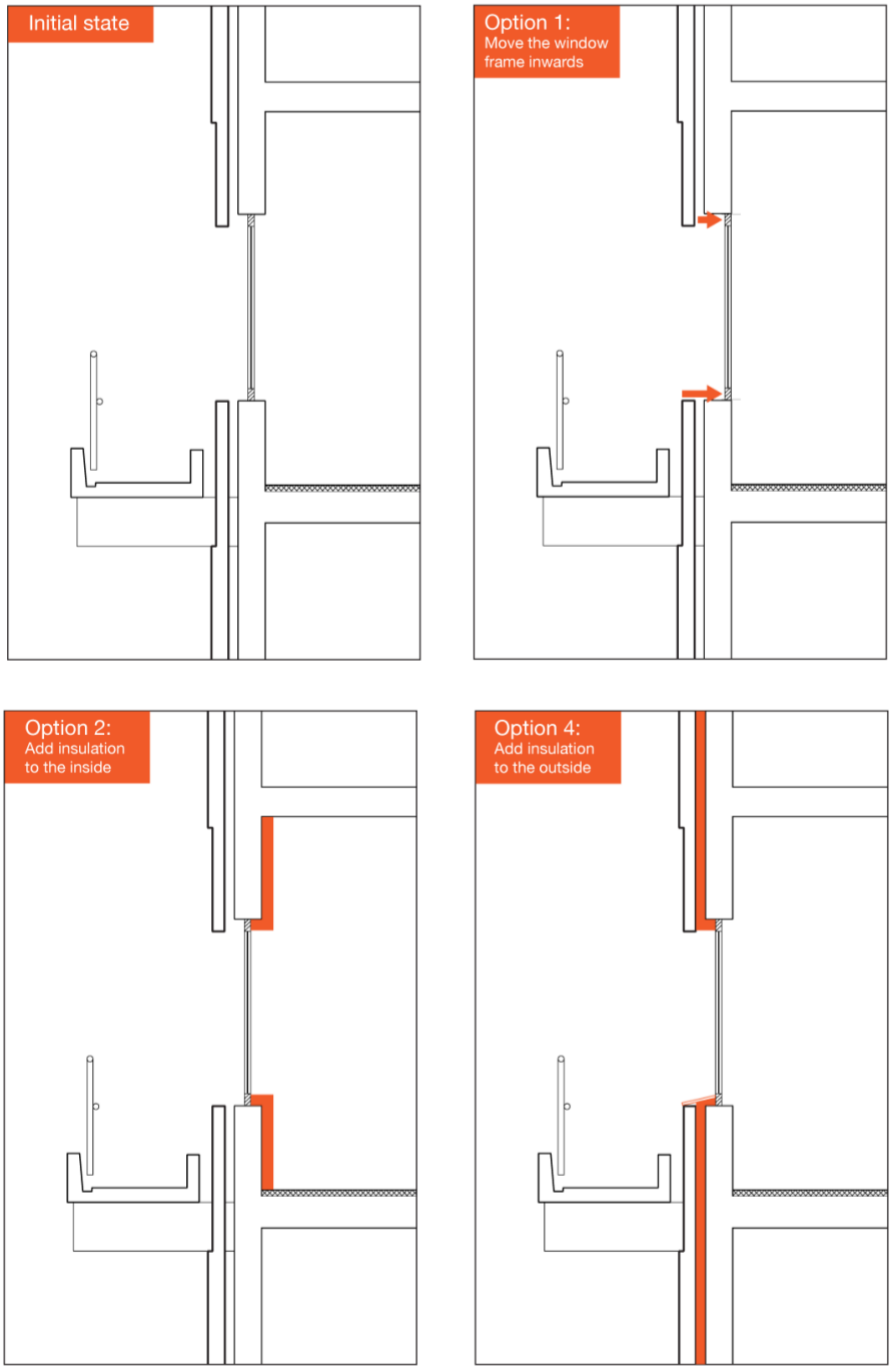

Figure 47: Initial state of the façade and the options for thermal improvement.

4.2. BIPV-module design

4.2.1. Determining module size

AMC Amsterdam was built with the concepts of modularity and flexibility. Even though the complex comprises buildings with different shapes and sizes, several design decisions ensure the usage of standardised components. The aim of the analysis of the dimensions is to increase the 65 per cent area that can be cladded with identical panels. One aspect that played a crucial role in the panel size is the span. The building is built on a square grid,

and the distance between the columns is 780 centimetres centre-to-centre all over the building.

This feature of the building was considered when determining the side-lengths of the grid, in which the modules are to fit. The width of the grid was set to 78 centimetres. An illustration showing the spans and how the modules are fit regarding this can be seen in Figure 48.

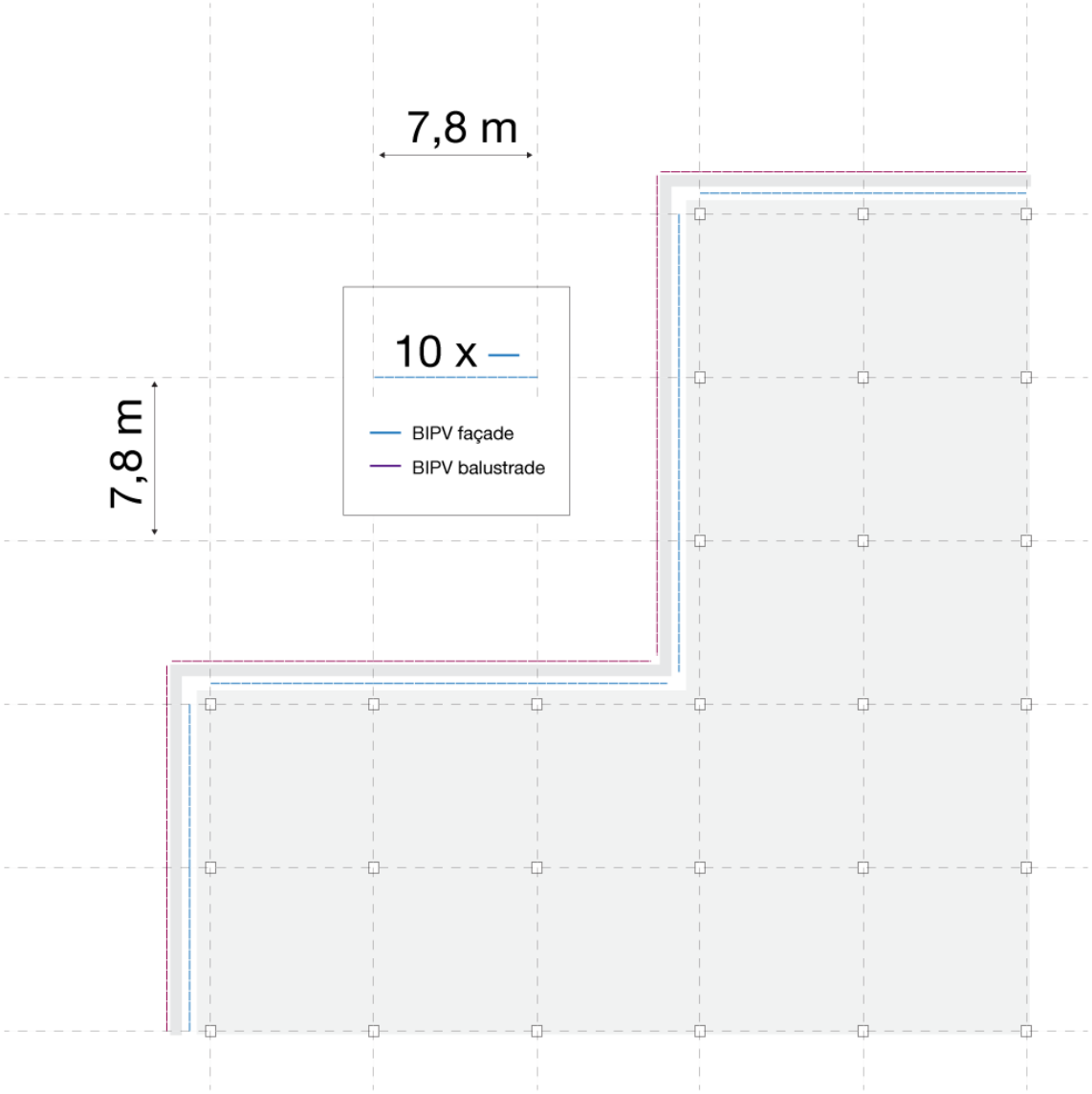

Figure 48: An illustration of how the panel widths were determined.

Additionally, the façades of the blocks C, G and K were examined to find a rule regarding the vertical dimensions. Unfortunately, we found no dimensions that fit all the different façades without waste. However, we saw that the window heights are the same and 143 centimetres all over the complex, regardless of the block. At the same time, some of the parapets have the same height. So, the height of the grid was determined as 71,5 centimetres. Eventually, the overall grid size became 71,5 cm x 78 cm. Parts of the façades

taken from the blocks C, G and K, can be observed in Figure 49, Figure 50 and Figure 51, with relevant dimensions.

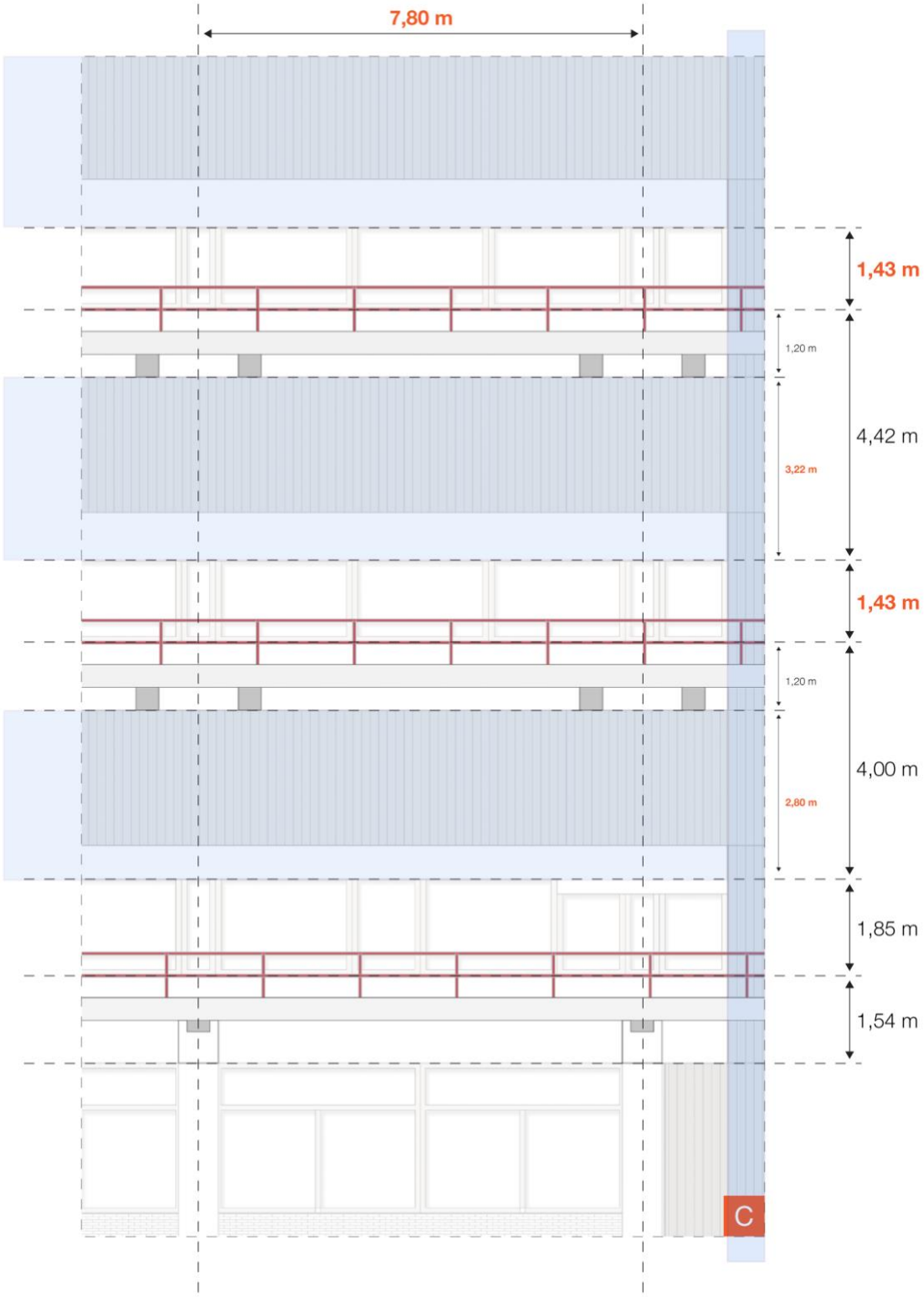

Figure 49: Partial elevation of block C with its dimensions.

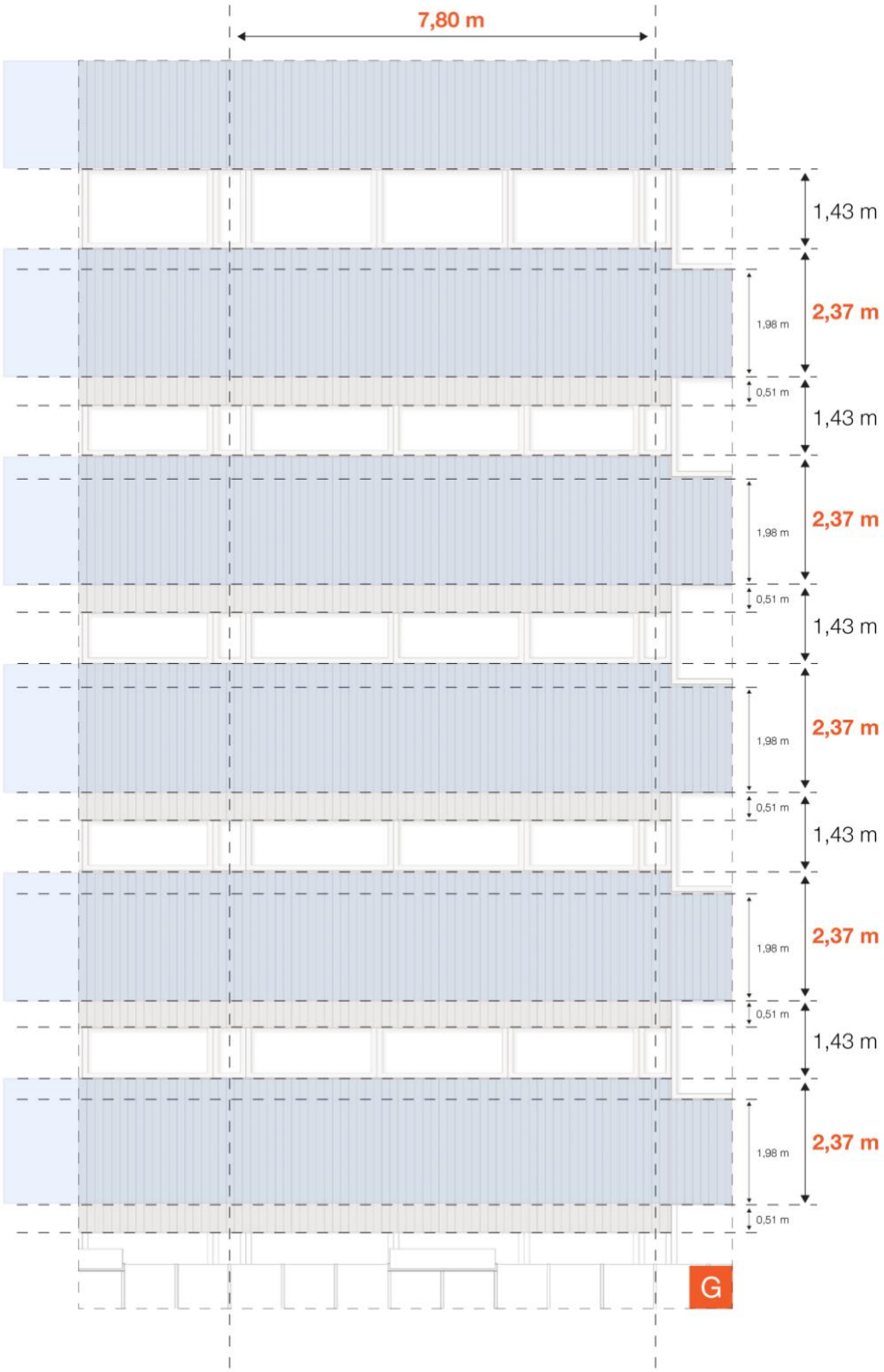

Figure 50: Partial elevation of the block G with its dimensions.

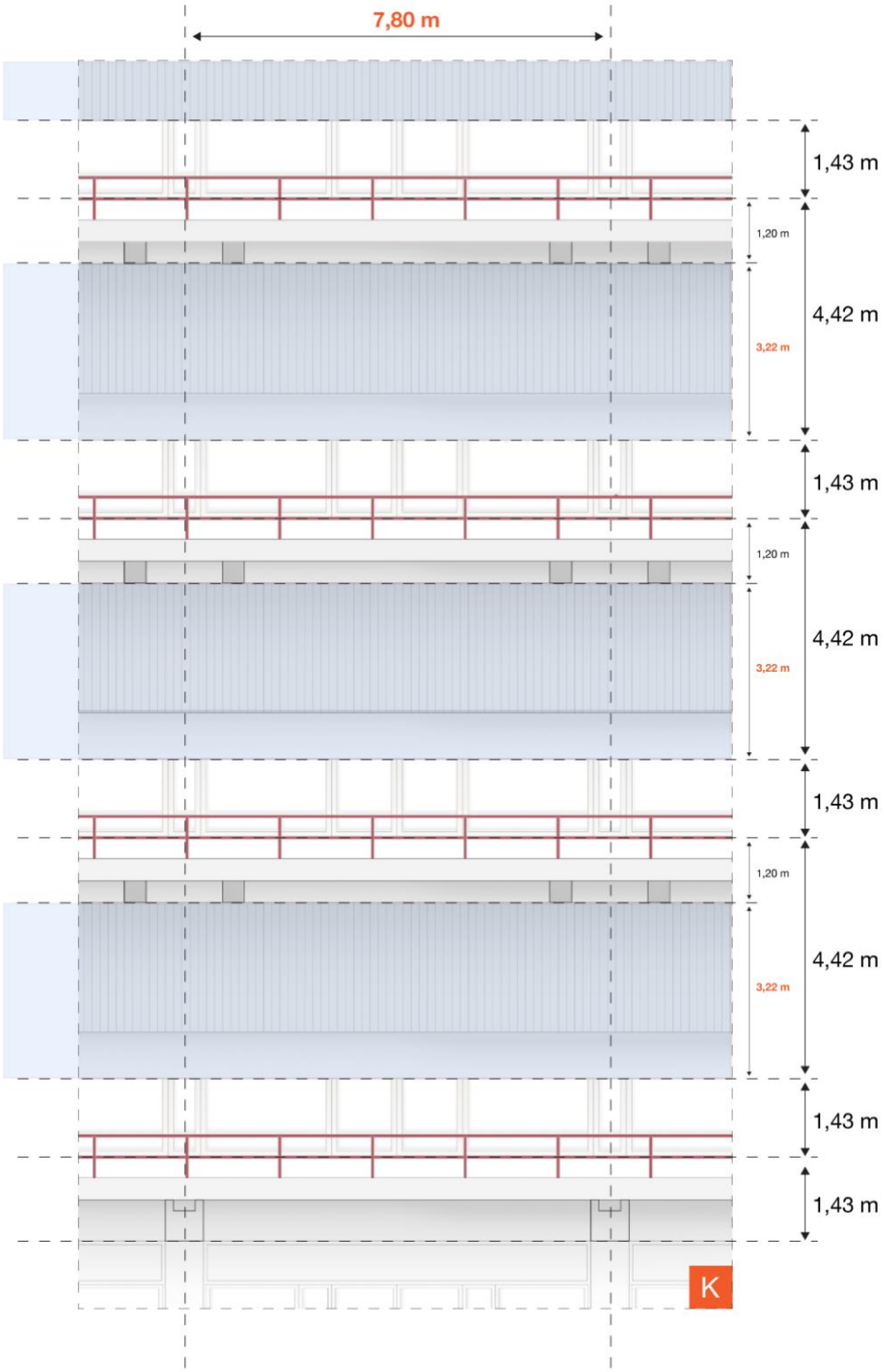

Figure 51: Partial elevation of the block K with its dimensions.

4.2.2. Pre-allocating panels

It is not possible to fill the entire façade with single-sized panels. There are articulations that prevent regular panelling Therefore, the panels fitting the 71,5 cm x 78 cm grid were placed on the façade manually. First, the façade geometry was created in Sketchup with a total surface area of 31.673,41 m2. The alignment was first made on the horizontal plane, considering the façade and the balconies. The horizontal alignment of the panels in the whole building can be observed in Figure 52.

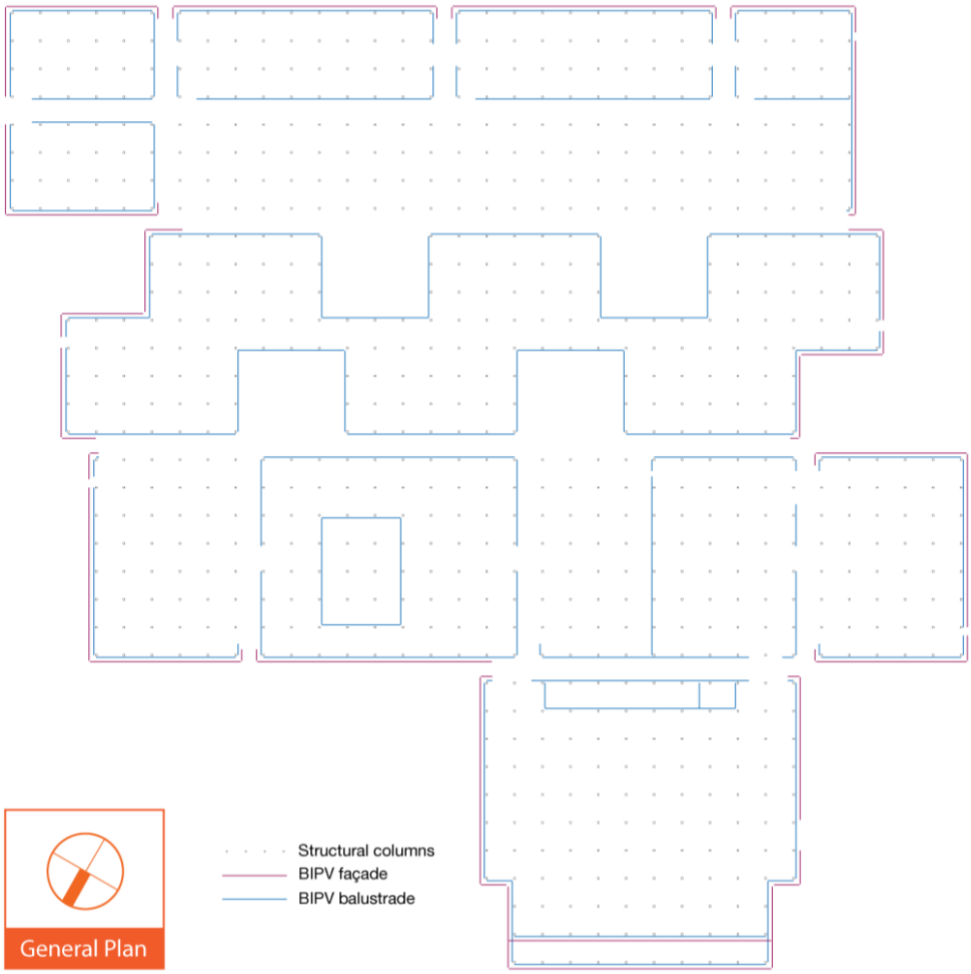

Figure 52:The horizontal alignment of the standardised panels on the façade and the balustrades all around the building.

48.105 of the standardised panels were placed on the façade, which constitutes 85,1 per cent of the whole opaque façade area. Additionally, 4.320 panels were placed over the balustrades of the balconies. The panel distribution as the result of pre-allocation can be observed in Figure 53.

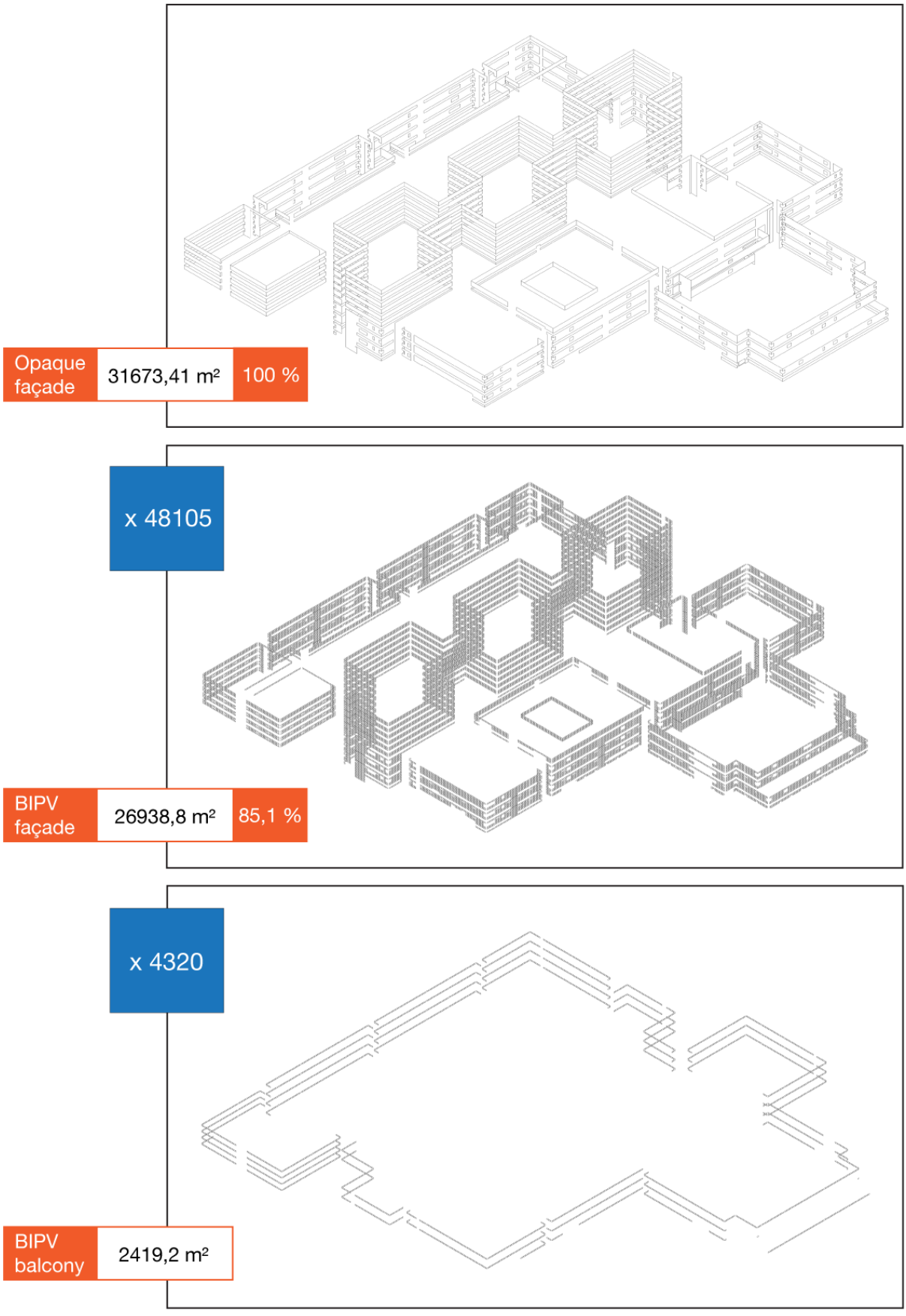

Figure 53: Panel distribution as a result of pre-allocation.

4.2.3. Cell arrangement

The façade was divided into 780 mm by 715 mm grid. The module dimensions were determined considering expansion joints, also required for installation. With 10 mm gaps, the module size was calculated as 770 mm by 705 mm. 16 Square c-Si cells of 15,6 mm by 15,6 mm were placed in the module. Façade and PV-module layouts can be seen in Figure 54. If half-cut cells are used, up to 36 cells can be placed in the module, as can be seen in Figure 55.

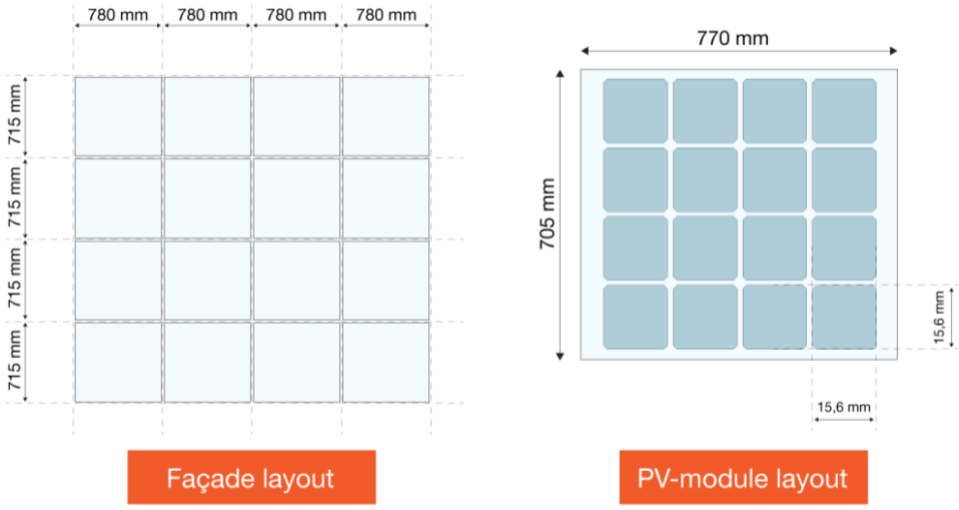

Figure 54: Façade and PV-module layouts.

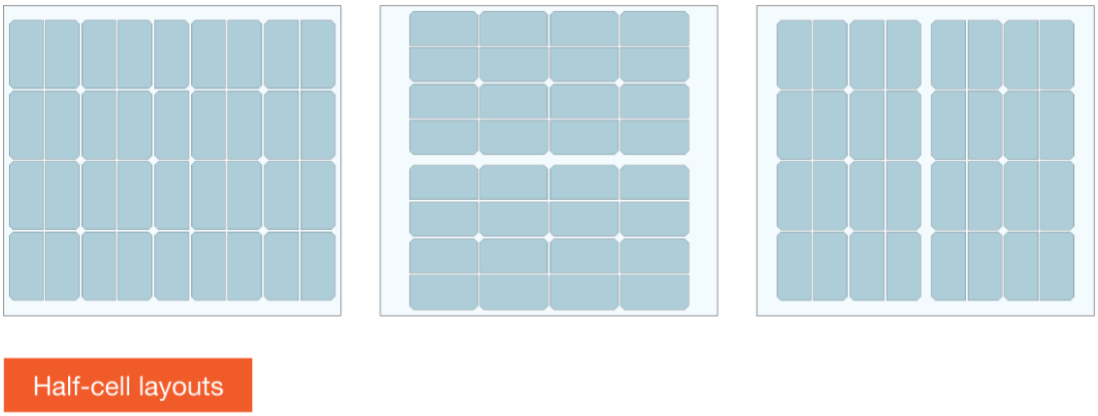

Figure 55: Module layouts with half-cut cells

The electronic connection of the cells and the alignments of the strings in the module can be made to minimise the negative effect of shading, as can be seen in Figure 56. This detailed research is falling out of the scope of the study.

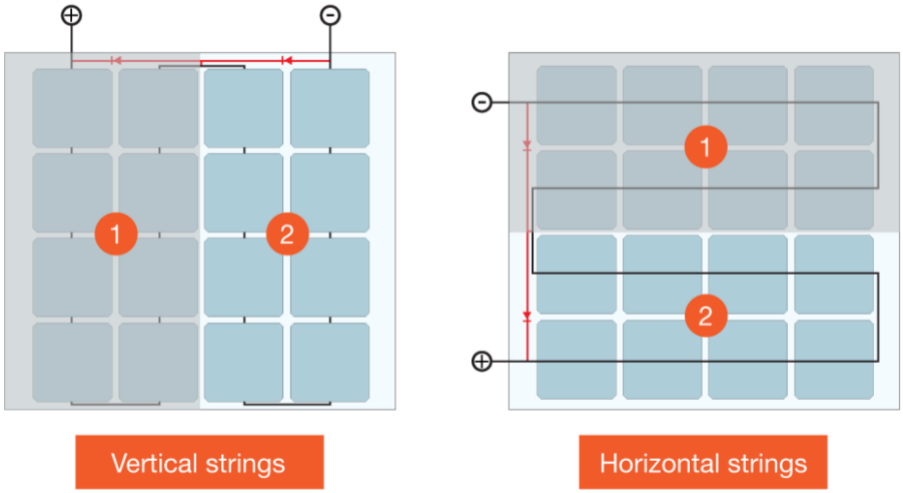

Figure 56: The string directions in the modules can be determined to minimise the effect of shading.

4.2.4. Tilting

The declination style of the panels was to be selected from several options. The PV-module on the panel is identical, and only the declination and orientation of the panels change. These options with their codes, descriptions, surfaces areas and panel height are defined in Table 7, and their images can be seen in Figure 57.

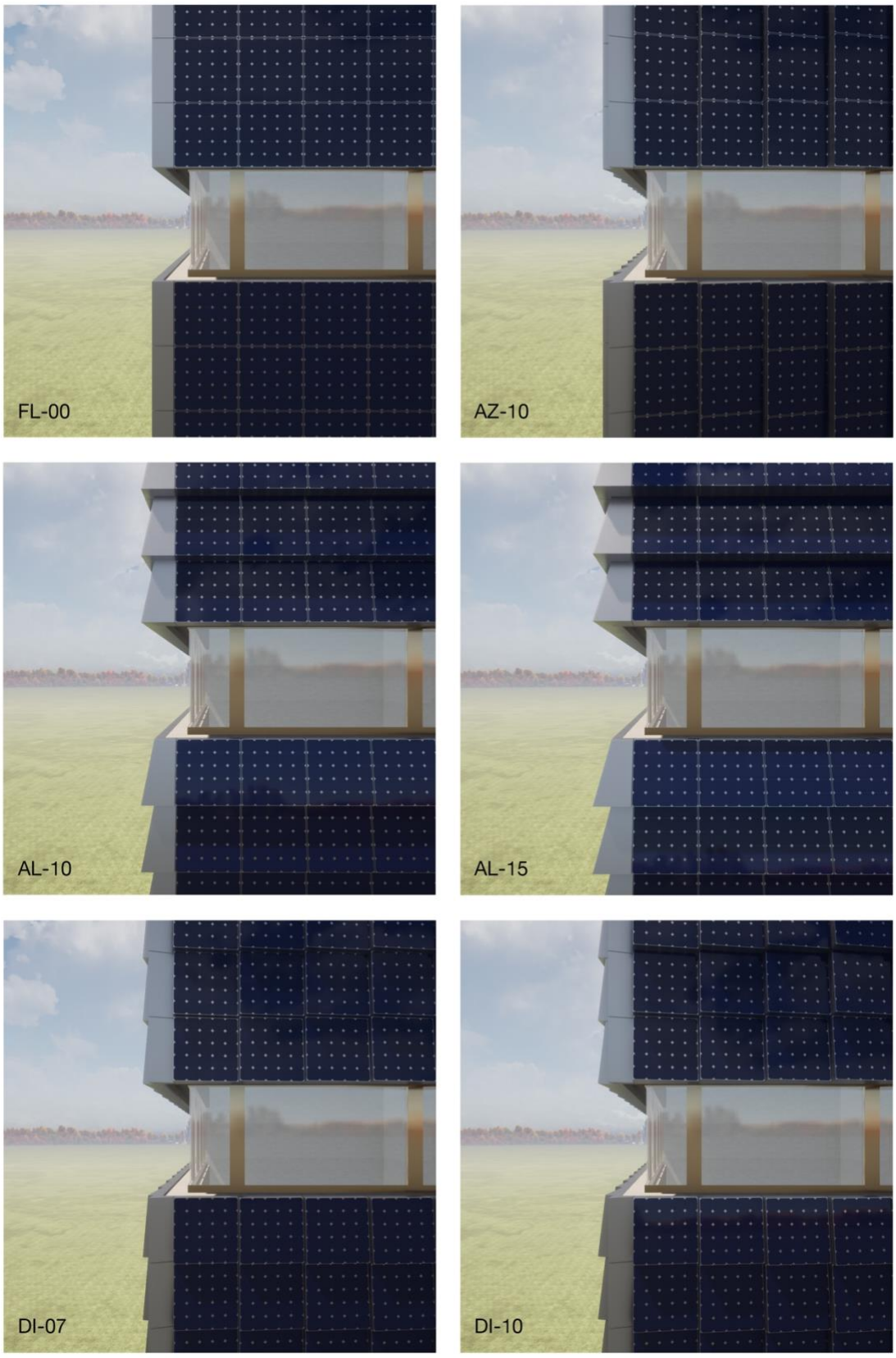

Figure 57: Façade impressions of the panel specimens.

The annual radiation amount falling on the panels is calculated using the Ladybug plugin for Grasshopper on the faces where the PV modules can be attached. The analyses were

made per specimen. Amsterdam 062400 (IWEC) weather data is used. The building façades and the floors were used as context with the other faces of the panels.

The total radiation values of façades totally covered with different specimens and the highest and lowest radiation values of modules are given in Table 7 with the surface area of the panel types and their ratings obtained by dividing the highest radiation amount multiplied by 100, into the surface area.

Table 7: Initial cost-benefit analysis for tilted panels

Code	Description	Surface area of the sides (cm^2)	Highest radiation on panel (kWh)	Rating (Highest radiation / Surface area)
Fl-00	Flat panels parallel to the façade	-	370,6	-
Az-10	10° tilted panels, oriented southwards	2000	377,5	0,19
Di-07	7° diagonally tilted panels, oriented south- and skywards	1900	410,3	0,22
Di-10	10° diagonally tilted panels, oriented south- and skywards	2700	425,3	0,16
Al-10	10° tilted panels oriented skywards	1800	433,8	0,24
Al-15	15° tilted panels oriented skywards	2700	461,4	0,17

Presumably, the tilted panels cast a shadow on each other, and the radiation amount shows a significant change from panel to panel around the building. This analysis showed that the flat panels and the panels tilted towards the sky are the most efficient, comparing the radiation amount and the surface area. So, the optimisation problem is decided to be conducted with flat and skyward-tilted modules. Shading is a significant factor affecting power output. This effect needs careful analysis, which falls out of the scope of this study. However, as shown in Figure 58, cells can be shifted downwards in tilted modules to avoid the negative consequences partially.

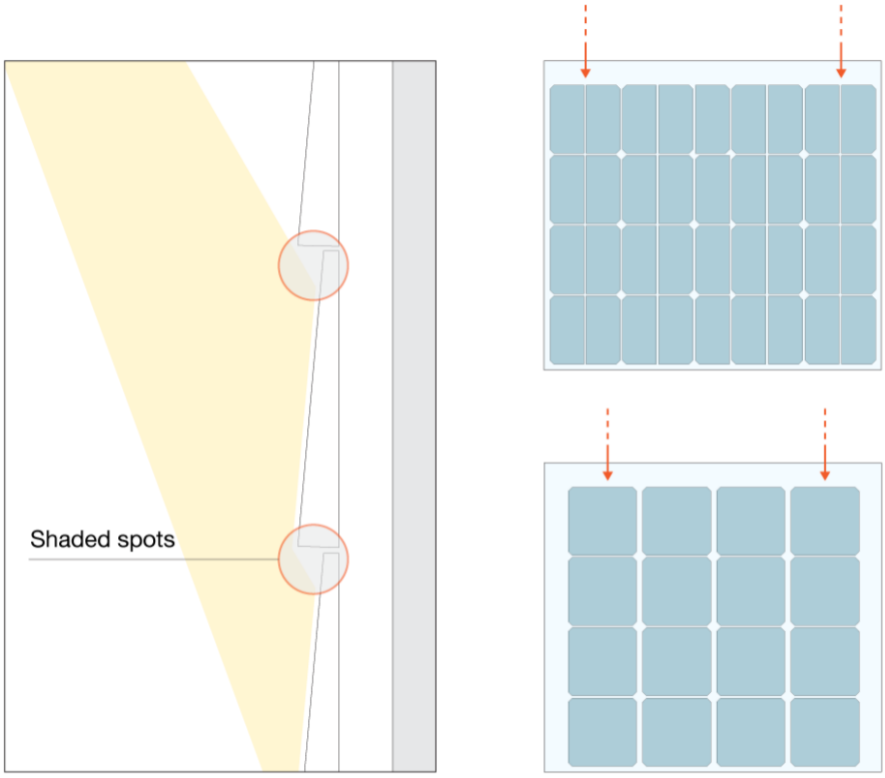

Figure 58: In the tilted modules, the cells can be shifted downwards to avoid the shading caused by the module above.

4.2.5. Mounting

We gave importance to replaceability when designing the module itself and also determining the mounting system. Most of the visible and concealed anchoring systems require ordered installation, which means that a consecutive panel must be placed after one is mounted and fixed. In this case, for a revision in the façade or just for the replacement of a broken module, many other PV- or non-PV panels would have to be picked off. The click system, on the other hand, is a patented mass-customised product consisting of semi-fixed distances between panels which currently do not match the required dimension in the project. So, we decided upon a mounting technology which is currently used in a thin-film BIPV cladding system (Avancis, 2019a). The illustration of how the system works with flat and tilted panels are shown in Figure 59.

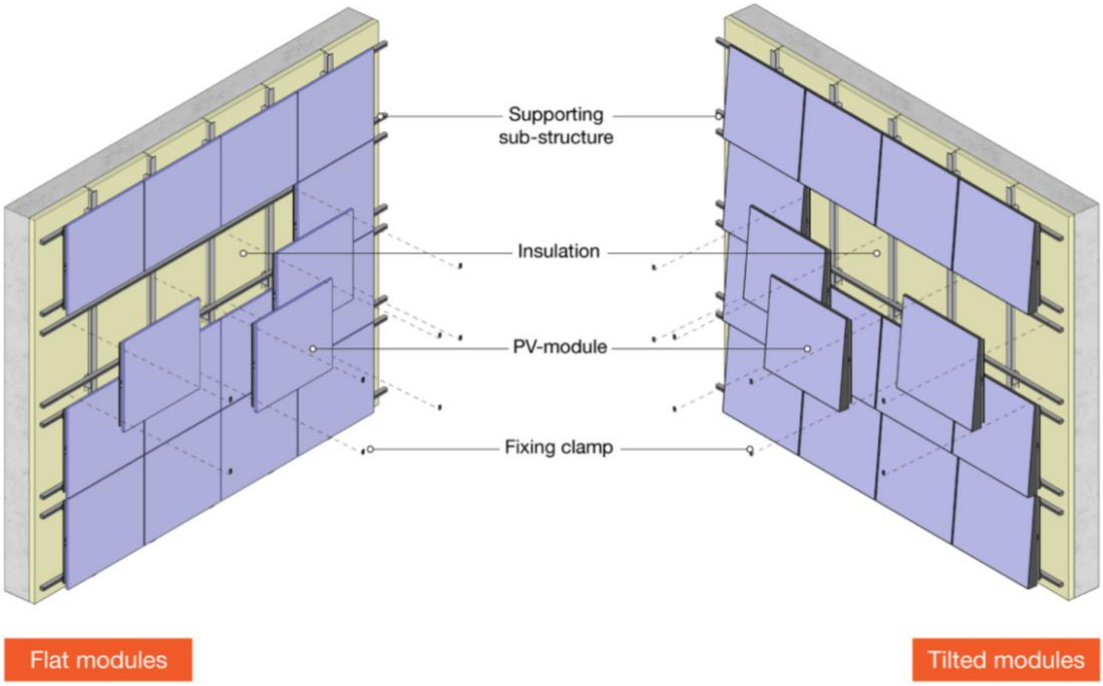

Figure 59: The façade system with flat and tilted panels.

The modules can be simple glass-to-back sheet PV-modules with junction boxes placed directly behind. The flat modules are frameless, and the hanger profiles are glued directly to the backseat. In the tilted panels, the module is placed in metal frames which give the modules an inclination. These frames are mostly open in the back, allowing ventilation of the module. The hanger profiles are fixed to the frame. In both cases, the hanger profiles are empty in the middle, allowing the cables to pass through and be connected horizontally. The illustrations of these modules with their front and back views and also components can be seen in Figure 60.

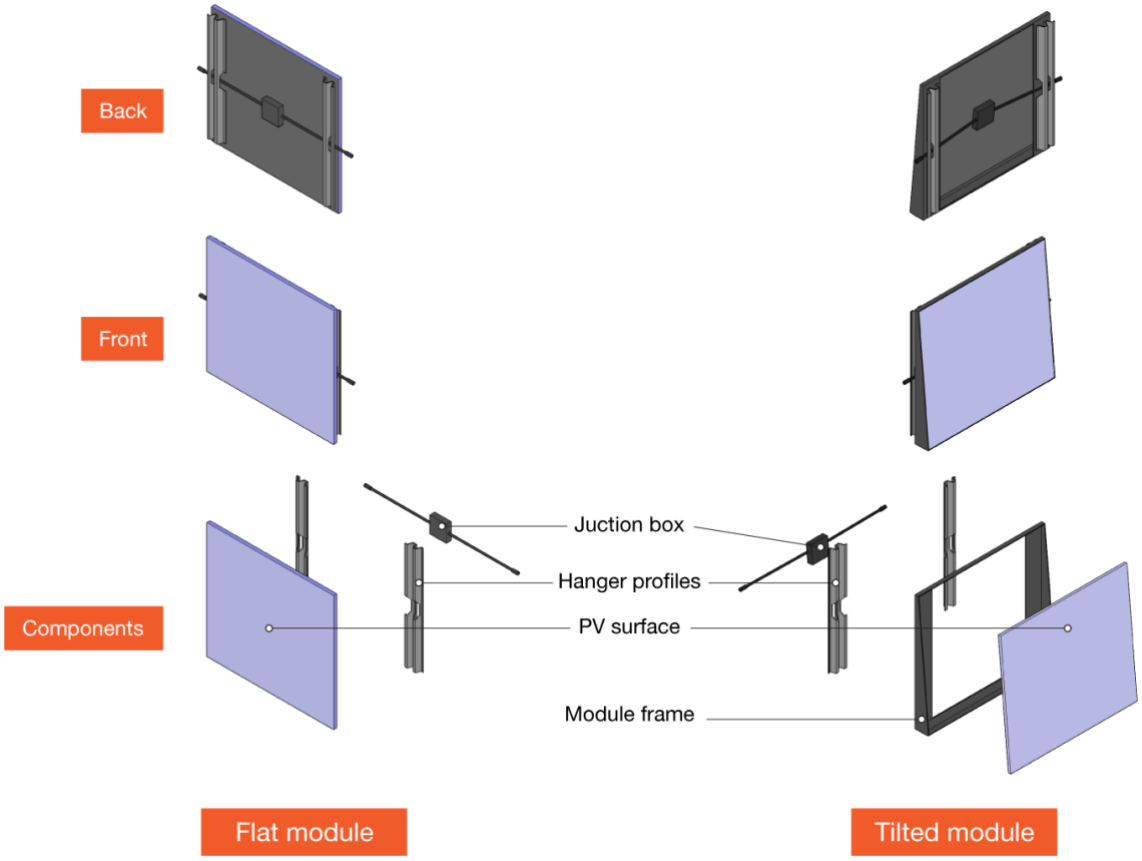

Figure 60: The front and back view of the modules, with their components.

4.3. Balconies

Balconies are other potential areas for BIPV-modules and other green architectural solutions, like planters. In Figure 61, the initial state of the balconies is given as a partial cross-section of the exterior. A 79 cm high part of the balustrades is exposed. This area can be used for placing the same BIPV-modules.

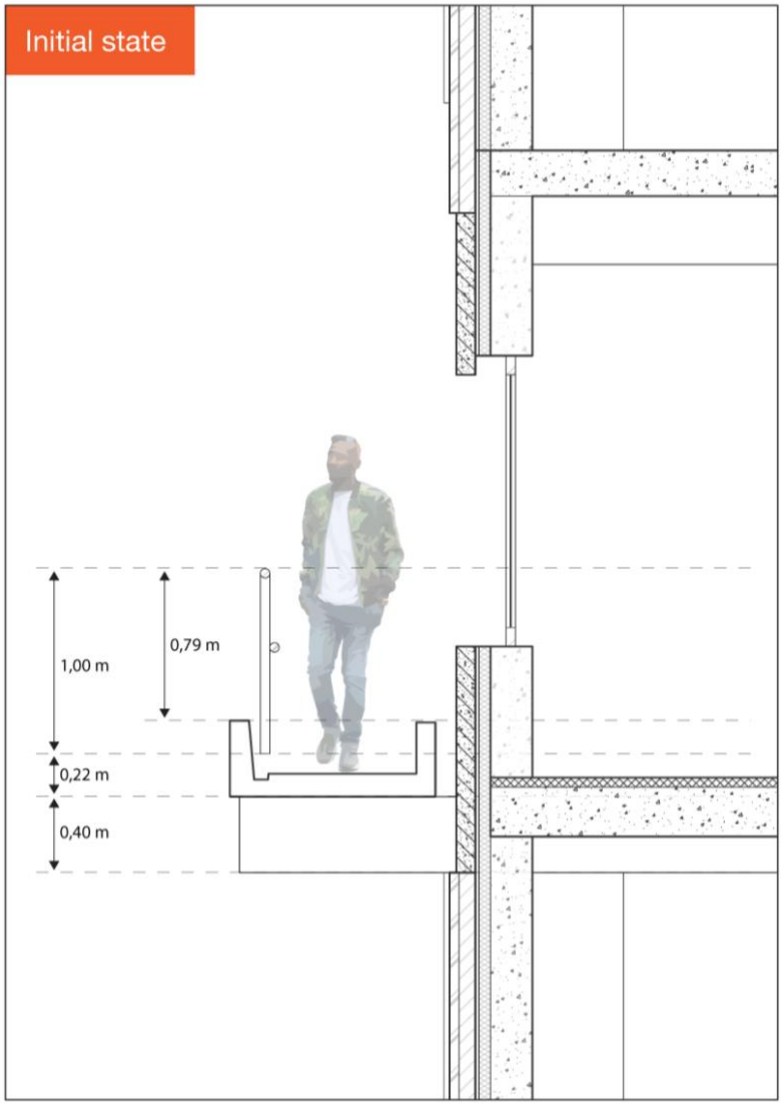

Figure 61: Initial state of the balconies.

Several solutions were considered to use the balconies as energy generation surfaces as can be observed in Figure 62. These solutions are 1 or 2 rows of BIPV-modules, either with a planter box or without. The 2-row BIPV options require additional substructure, as the bottom row would be hanging down from the prefabricated balcony slab over the projecting beams. Therefore, options with a single row of modules were adopted as a lower limit. Planter boxes would not only constitute a pleasant view from the inside but also can be part of a greater greening strategy of the building.

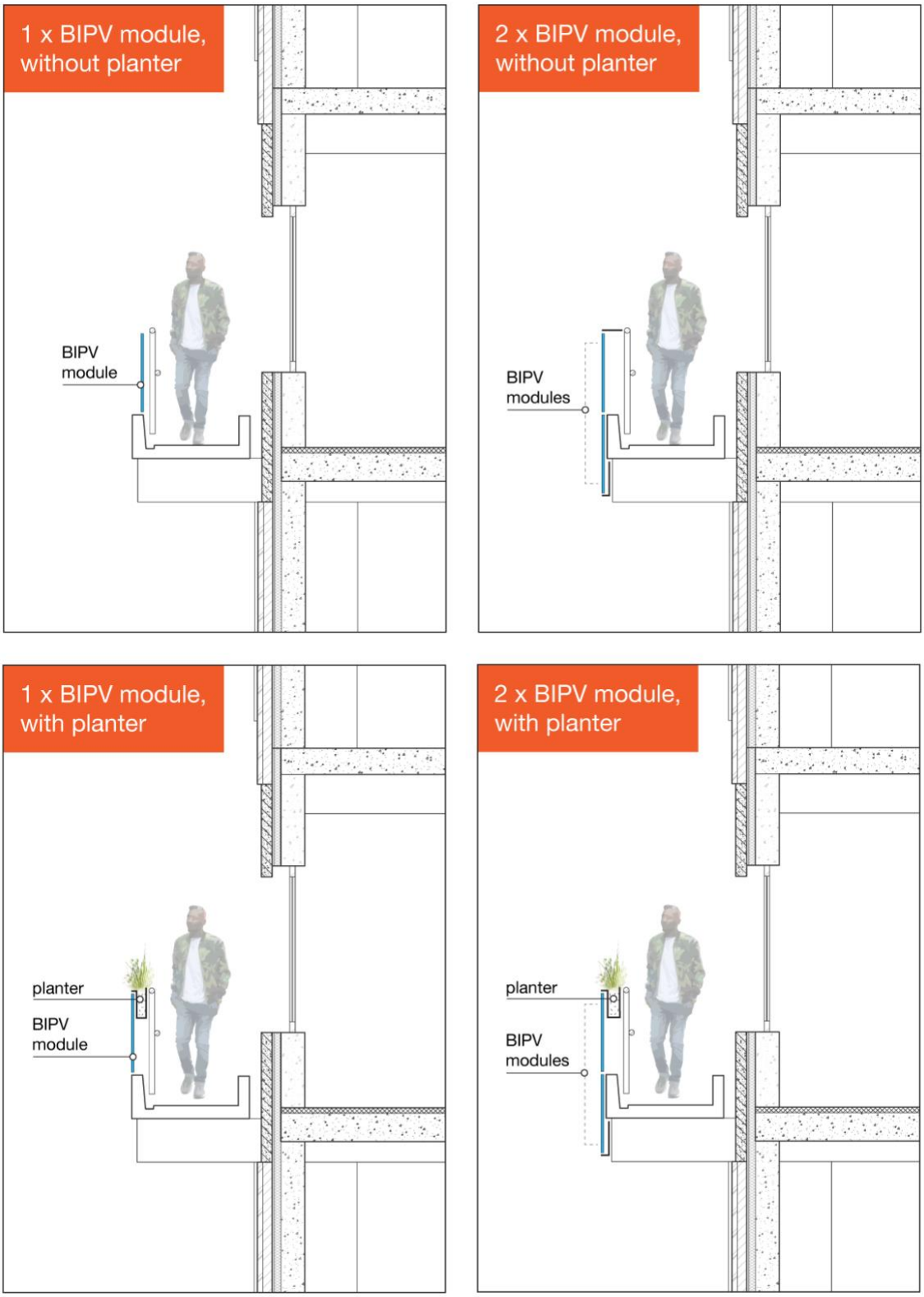

Figure 62: Different options for using the balustrades as BIPV surfaces.

5. Computational Design and Optimisation

5.1. Proposed methodology for optimisation

The main aim of this methodology is constituting a base for comparing design options in term of their cost-effectivity. The steps are firstly to panel the building with as many of the identical panels as possible, then to properly allocate a given budget to BIPV and LWS panels, ensuring that the system pays off within the project window. As the work was set in Rhinoceros 3D, existing workflows were used, namely radiation and sunlight hours analysis with Ladybug Tools. Together with these, a quick panelling process and workflows for finding cash flows and optimisation for budget allocating between different panel types were introduced. The flowchart of the proposed method can be seen in Figure 63.

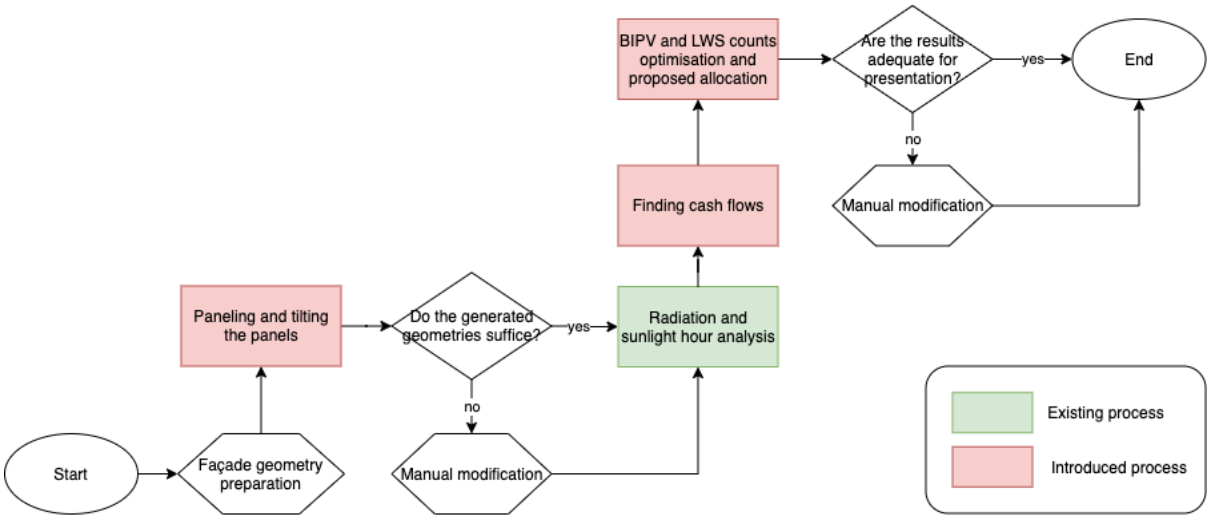

Figure 63: Flowchart of the proposed methodology for computational design and optimisation.

5.2. Mathematical base for optimisation

5.2.1. Engineering economics calculations

For more realistic calculations, the time value of money (TVM) was considered. The net present value (NPV) analyses the feasibility of a planned investment or project regarding the TVM. It should be noted that the accuracy and precision of the monetary projections made for the calculation directly affects the results. The main formulas used are given in Table 8.

Table 8: Main formulas for engineering economics calculations.

Symbol	Explanation	Equation
NPV	Net present value — difference between the present value of cash in-and outflows over a period of time.	$\sum_{t=1}^{n} \frac{R_t}{(1+i)^t}$

R	Net cash flow	$R_i - R_o$
R_i	Cash inflow	$E \times SP$
R_o	Cash outflow	$C_{BIPV} + C_{LWS}$
E	Energy output	$A \times r \times H \times PR$
SP	Energy selling price	$EP + S$

When expanding the NPV formula considering the initial investment cost for the first year and annual costs such as cleaning and maintenance costs to start from the second year on, the equation below is procured. The symbols and units with their explanation and the values used in the calculations are given in Table 9

$$NPV = \frac{A \times \left[(r_t \times H \times PR) \times (EP_1 + S_1) - \left(c_{i;BIPV} + c_{i;LWS}\right)\right]}{1+i} + \sum_{t=2}^{n} \frac{A \times \left[(r_t \times H \times PR) \times (EP_t + S_t) - \left(c_{a;BIPV} + c_{a;LWS}\right)\right]}{(1+i)^t}$$

Table 9: Symbols and values used in engineering economics calculations.

Symbols and units	Explanation	Value	Comment
$A(m^2)$	Total PV module area	—	—
$r_t(\%)$	PV module efficiency in year t	25	Decreasing 0,5 annually
$H(kWh/m^2)$	Annual irradiance of PV modules	—	Calculated with Grasshopper Ladybug
PR	Performance ratio	0,84	(Reich et al., 2012)
$EP_t(€/kWh)$	Energy price in year t	0,23	—
$S_t(€/kWh)$	Subsidy amount in year t	0,051	Only for the first 15 years (RVO, 2020)
$c_{i;BIPV}(€/m^2)$	Unit initial investment cost of BIPV panels	100	BIPV and standard façade price difference
$c_{i;LWS}(€/m^2)$	Unit initial investment cost of LWS panels	150	LWS and standard façade price difference

$c_{a;BIPV}(€/m^2)$	Unit annual cost of BIPV panels	5	(Van Winden, 2016)
$c_{a;LWS}(€/m^2)$	Unit annual cost of LWS panels	25	(Perini & Rosasco, 2013)
i	Interest rate determined by the investor	0,05	—

5.2.2. Optimisation problem

An optimisation problem was formulated to be computationally solved. The building is cladded with panels with their position i . With a given budget B and the least payback amount required P, find the maximum amount of LWS panels are to be purchased.

Decision variables:

$x_i = 1 \rightarrow buy\ LWS\ panel$
$x_i = 0 \rightarrow do\ not\ buy\ LWS\ panel$
$y_i = 1 \rightarrow buy\ BIPV\ panel$
$y_i = 0 \rightarrow do\ not\ buy\ BIPV\ panel$
Parametres:

$C_{i;LWS}$: $Initial\ cost\ of\ LWS\ panel$
$C_{i;BIPV}$: $Initial\ cost\ of\ BIPV\ panel$
$npv_{i;BIPV}$: $NPV\ of\ a\ BIPV\ panel\ at\ position\ i$
npv_{LWS}: $NPV\ of\ an\ LWS\ panel$
B: $budget$
P: $payback\ amount$
Objective:

$$max \sum_{i=i}^{N} x_i$$

Subject to:

$$C_{i;LWS}\left(\sum xi\right) + C_{i;BIPV}\left(\sum y_i\right) \leq B$$
$$\sum_{i=N} npv_{i;BIPV} y_i - npv_{LWS}\left(\sum x_i\right) \geq P$$
$$x_i, y_i \in \{0,1\}$$

5.2.3. Cost calculation for the tilted panels

There is an additional expense when manufacturing the tilted panels, which is the metal frame encasing the flat module. The cost of a tilted panel is given with the formula below:

$$c_{BIPV;t} = c_{BIPV} + c_{BIPV;f}$$

Where;

$c_{BIPV;t}$ Unit cost of the tilted BIPV-modules (EUR/m2)

c_{BIPV} Unit cost of BIPV modules (EUR/m2)

$c_{BIPV;f}$ Framing unit cost for tilting modules (EUR/m2)

The following equations were composed for the current design, as an estimate. The design and the dimensions of the panel design is given in Figure 64. However, the cost of tilted panels is highly likely to be different than this calculation in a real project.

$$c_{BIPV;f} = c_m\left(\frac{2A_1 + A_2 + 2A_3}{A_{module}}\right)$$

$$A_1 = \frac{1}{2}h^2 sin\alpha$$

$$A_2 = ah.2sin\frac{\alpha}{2}$$

$$A_3 = a'h$$

$$c_{BIPV;f} = c_m\left(\frac{h^2.\sin\alpha + ah.2sin\frac{\alpha}{2} + 2a'h}{ah}\right)$$

Where;

$c_{BIPV;f}$ Framing unit cost (EUR/m2)

c_m Unit cost of the metal sheet (EUR/m2)

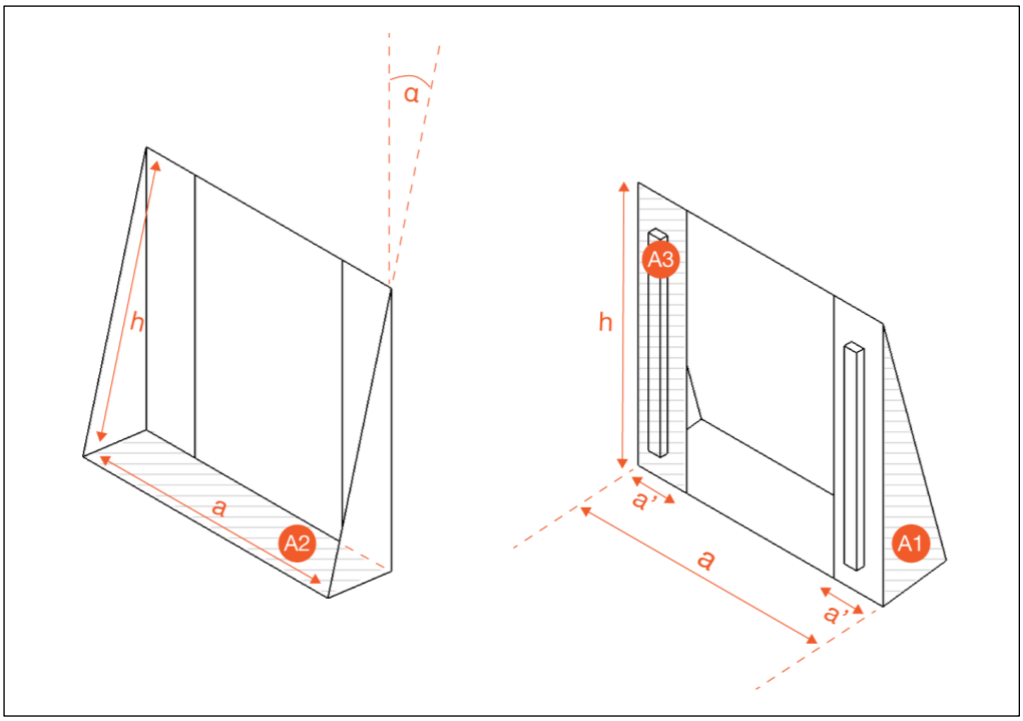

Figure 64: The geometry of the panels for cost calculation.

5.2.4. Monetary values for calculations

The literature sets out PV costs per Watt Peak (W_p) so that systems with different rated power can be compared. For 2018, the kWh to W_p ratio is 0,98 (SolarCare, n.d.). An

analysis of the solar panel market in the Netherlands is present, regarding 879 PV modules and more than 700 inverters, with an overview of the installation costs (W. van Sark et al., 2014). The findings of the research are given in Table 10 in terms of €/W_p. It is also indicated that the installation costs drop with larger solar panel systems.

Table 10: Dutch PV-system cost analysis (van Sark et. al., 2014).

Component	**Cost** (€/W_p)
PV modules	1,09
Inverter	0,10 - 0,90
Installation	0,20 – 0,80

Since we make the calculations per m2 and for a less optimal situation than the conventional installations, the price of the BIPV system had to be chosen from a wider range, depending on the manufacturer and the application. For a rainscreen façade technology, the price usually varies between 100 and 500 euros per m2 with insulation, anchorage and installation (Passera et al., 2018). As an estimate, we chose EUR 200/m2 module price and EUR 50/m2 for other costs such as inverters and other erratic expenses, which make EUR 250/m2 in total. However, since these modules would replace façade panels in which would be invested, subtracting an approximate façade replacement price of EUR 150/m2, we used EUR 100/m2 in our calculations. For the frames of the tilted panels were considered a price of EUR 80/m2 for material and labour expenditures. The annual maintenance costs of BIPV-modules include washing, and inspections for the system components (Van Winden, 2016). We considered a EUR 5/m2 annual maintenance cost.

Regarding the efficiency of the modules, 25 per cent efficient PV-cells were considered. A module contains 16 cells with a 0,025 m2 surface area each, and an upper cover glass with a solar direct transmittance of 0,91 (Wang, 2018). These result in approximately 16 per cent efficient modules. PV-cell decay rate was taken 0,5 per cent per year. Energy selling price was taken EUR 0,23/kWh. Within SDE+, depending on the system size, at least EUR 0,05/kWh subsidy is available for PV self-use for the systems above 15 kW_p is available for 15 years (RVO, 2020). EUR 0,28/kWh for the first 15 years and EUR 0,23 for the remaining 10 years were taken for a system life of 25 years, which is a typical warranty window. The discount rate was taken 5 per cent.

Living wall system costs were taken as EUR 300/m2 initial investment cost. With the same replacement principle as BIPV panels, we took EUR 150/m2 in our calculations. EUR 25/m2 annual maintenance costs (Perini & Rosasco, 2013).

5.3. Radiation and sunlight hours analysis

Ladybug radiation analysis and sunlight hours component were used for the calculation of irradiance values in Grasshopper. The test geometry was the pre-allocated façade panels and the context geometry is the 3D-geometry obtained from the BIM-model. Amsterdam

062400 (IWEC) weather file was used. The geometry had no geographic angle, the North value was adjusted to 150°. As can be seen in Figure 65, the outputs used were values and meshes. The meshes were exploded to be used with the corresponding numerical values as keys in the later stages.

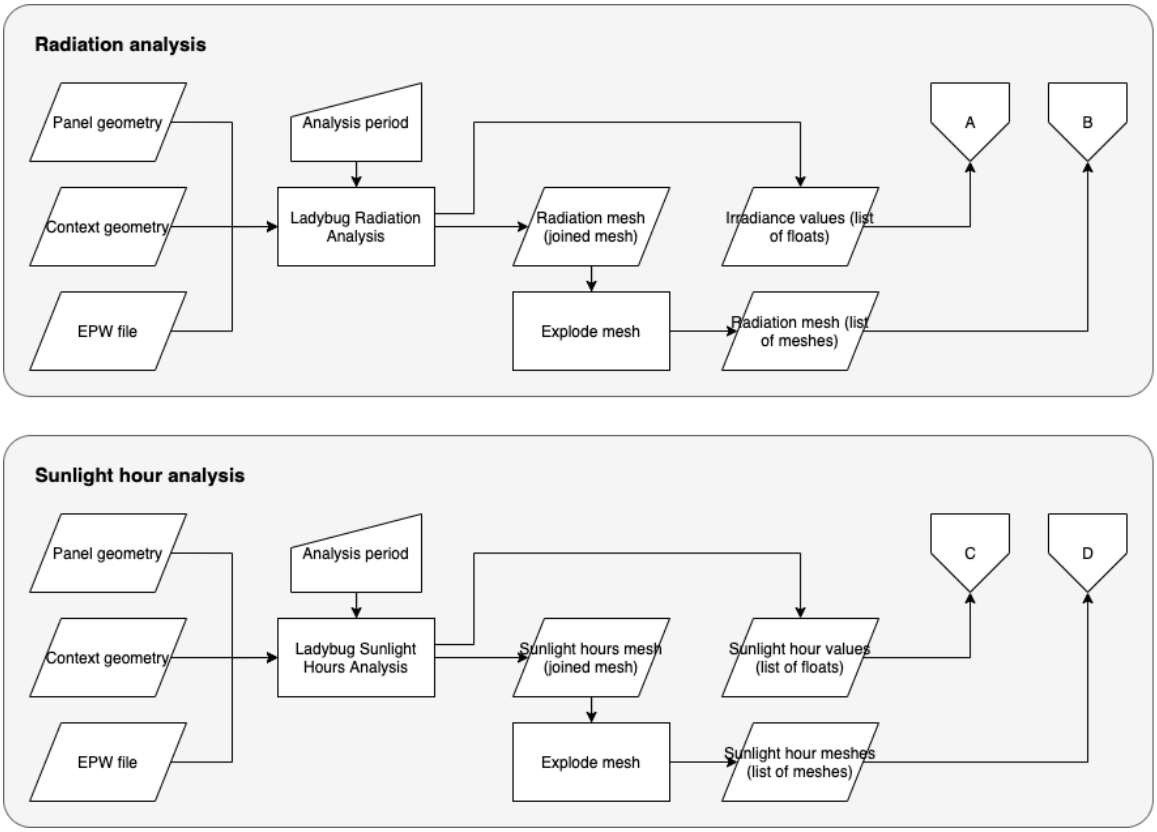

Figure 65: Inputs and outputs of the radiation and sunlight hours analysis.

5.4. The toolkit developed for design and optimisation

5.4.1. Creating the panel geometry with the toolkit

The first part of the toolkit which can be used for obtaining the panel geometry for solar analyses comprises the façade panelling and the panel tilting tools. The façade panelling tool fills the given geometry with as many rectangular panels with given width and height as possible with a tolerance input. The panel tilting tool can then be used for tilting the panels skywards by rotating them around their top edges, by the given angle. An example grasshopper definition for this partial workflow can be seen in Figure 66.

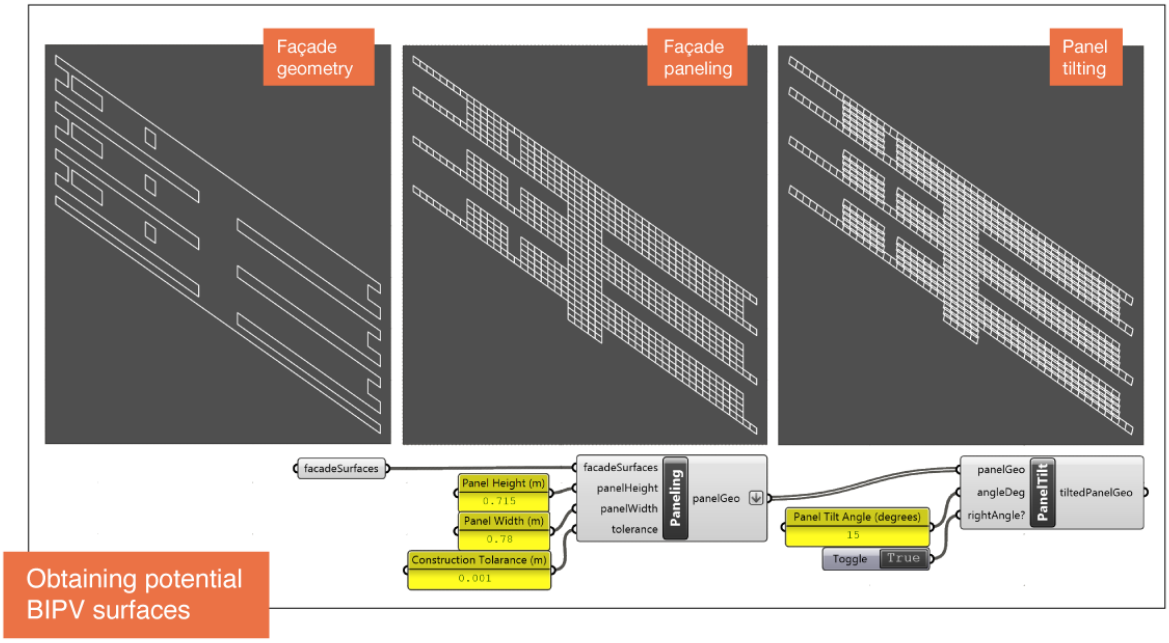

Figure 66: Example grasshopper definition for creating the panel geometries for solar analyses.

These tools are clusters benefiting from the standard components of Grasshopper and partially from the Pufferfish plugin with its "Bounding Rectangle" component in the panelling tool. The panelling tool finds the bounding rectangles of each façade surface, creates a rectangular grid slightly larger than the bounding rectangle and culls the cells completely outside the façade geometry or partially outside and exceeding the threshold of tolerance (This tool is mostly an interpretation of the work of (Abaide, 2015) posted in an online forum). The content of the tool cluster is given in Figure 67 (Visualisation credit (Dmitriev, 2016).

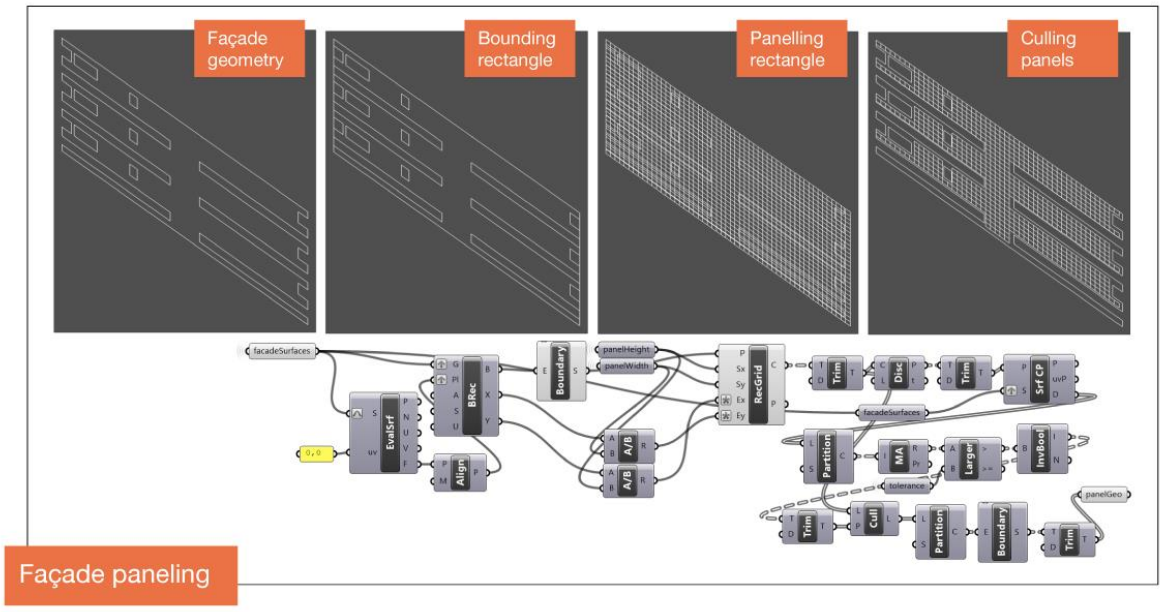

Figure 67: Content of the panelling tool.

A notice when using this tool is that the surfaces of the façade should be aligned correctly. In other words, the front face of the surface should be the face exposed to the sun. Non-aligned façade surfaces of the AMC and their aligned form are shown in Figure 68: The faces of the façade geometry should be aligned and oriented correctly before being put to process.. The geometry was prepared in SketchUp.

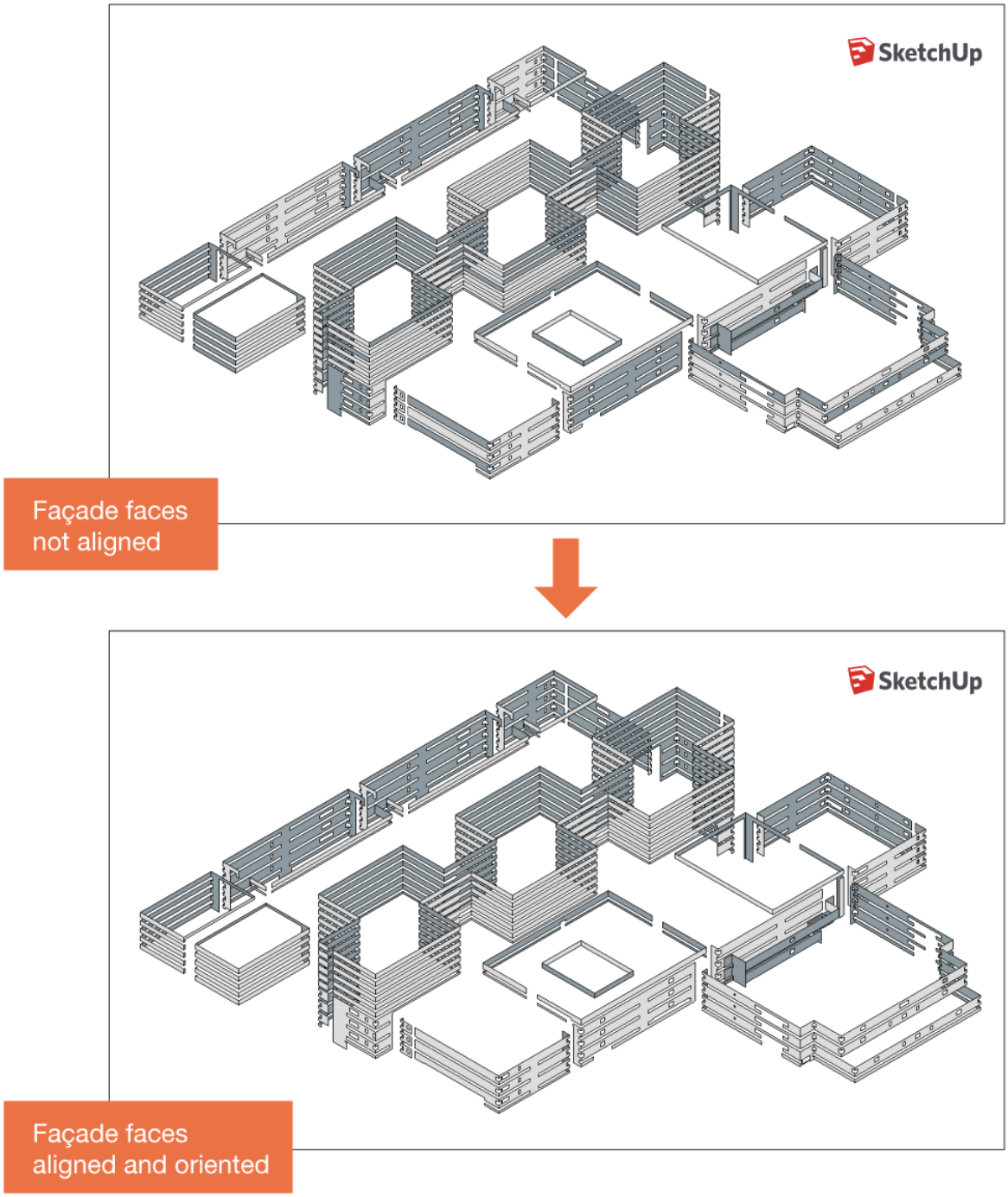

Figure 68: The faces of the façade geometry should be aligned and oriented correctly before being put to process.

It can also be seen in Figure 67, that a toggle is placed into the panel tilting tool, asking if the tilting is made correctly. This is because the tools employ a set of aligning components and in some cases, the geometry is aligned with the right face normal, but

reversed U and V directions as shown in Figure 69. UVN directions can be found by the right-hand rule (Robert McNeel & Associates, 2015). If the tilting is done to the wrong direction initially, this button negates the tilt angle.

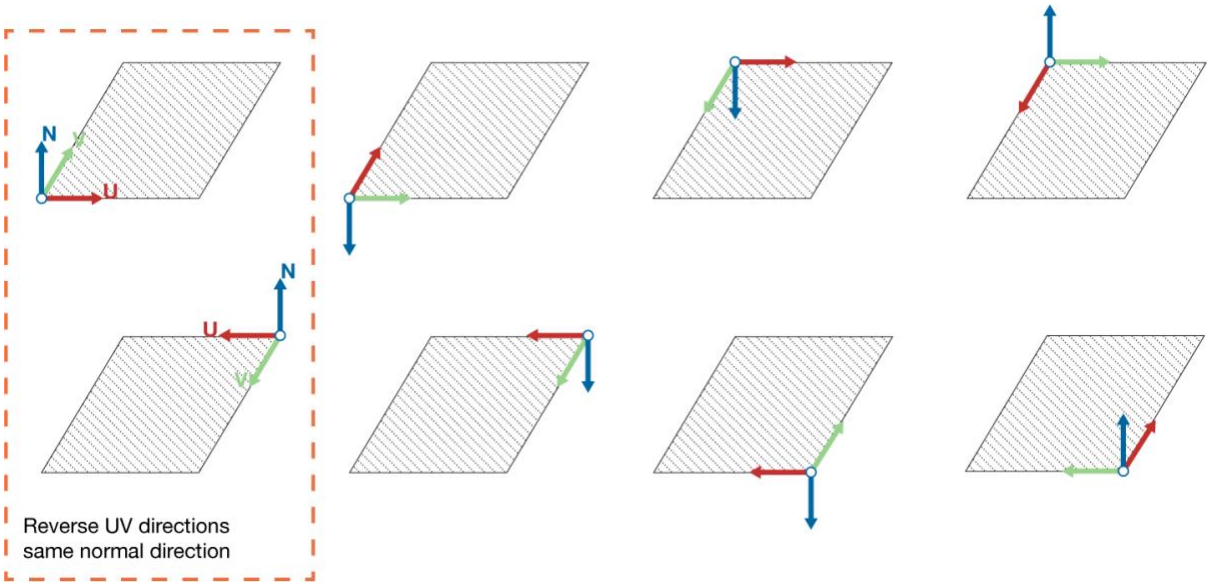

Figure 69: Faces may have reversed U and V direction even when facing the same direction.

The panelling of the AMC was initially done manually by investigating the building dimensions which has relatively regular blocks and finding a sensible panel dimension. Eventually, 85 per cent of the whole façade was cladded within a 78 cm wide and 71,5 cm high grid. As a part of the toolkit, this step was automated and the result gathered by using the panelling tool was compared with the results obtained by manually placing the panels, on a single façade surface. By using the panelling tool, around 76 per cent of the single façade, while this ratio reaches 83 per cent by adding spaces manually when necessary. The geometries for comparison can be seen in Figure 70.

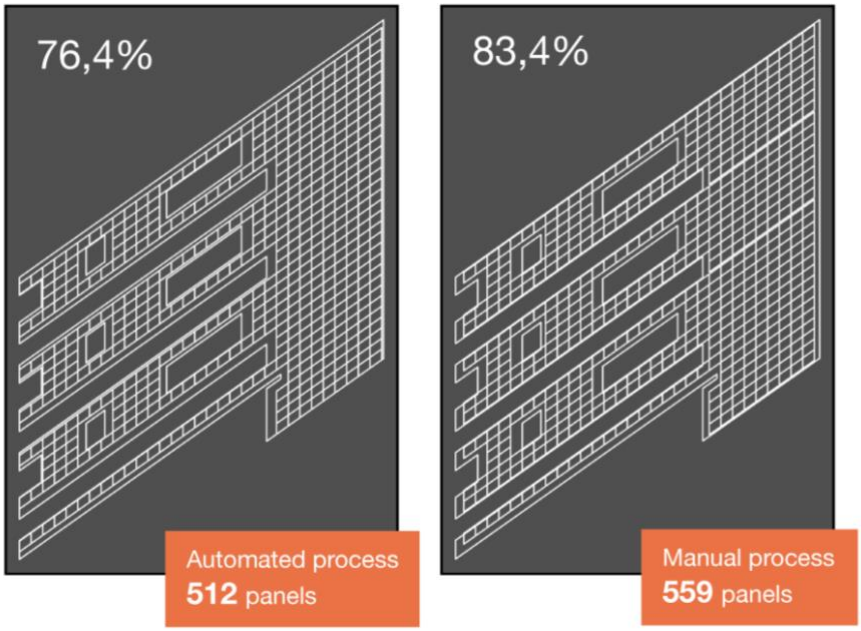

Figure 70: Comparison of the manual and the automated panelling.

5.4.2. Optimising designs using the toolkit

The second part of the toolkit consists of a series of components written in GhPython, which is the Python interpreter component for Grasshopper. These components can be used for calculations such as the cash flows in a project, the payback time, NPV and LCoE. Some complementary components to calculate the PV-module efficiency, annual energy calculation and yearly energy selling price were made as well. In this chapter these components are introduced. The written codes of the components can be found in Appendix 1: GHPython codes of the components. In Figure 71 an overall impression of how these components come together is given.

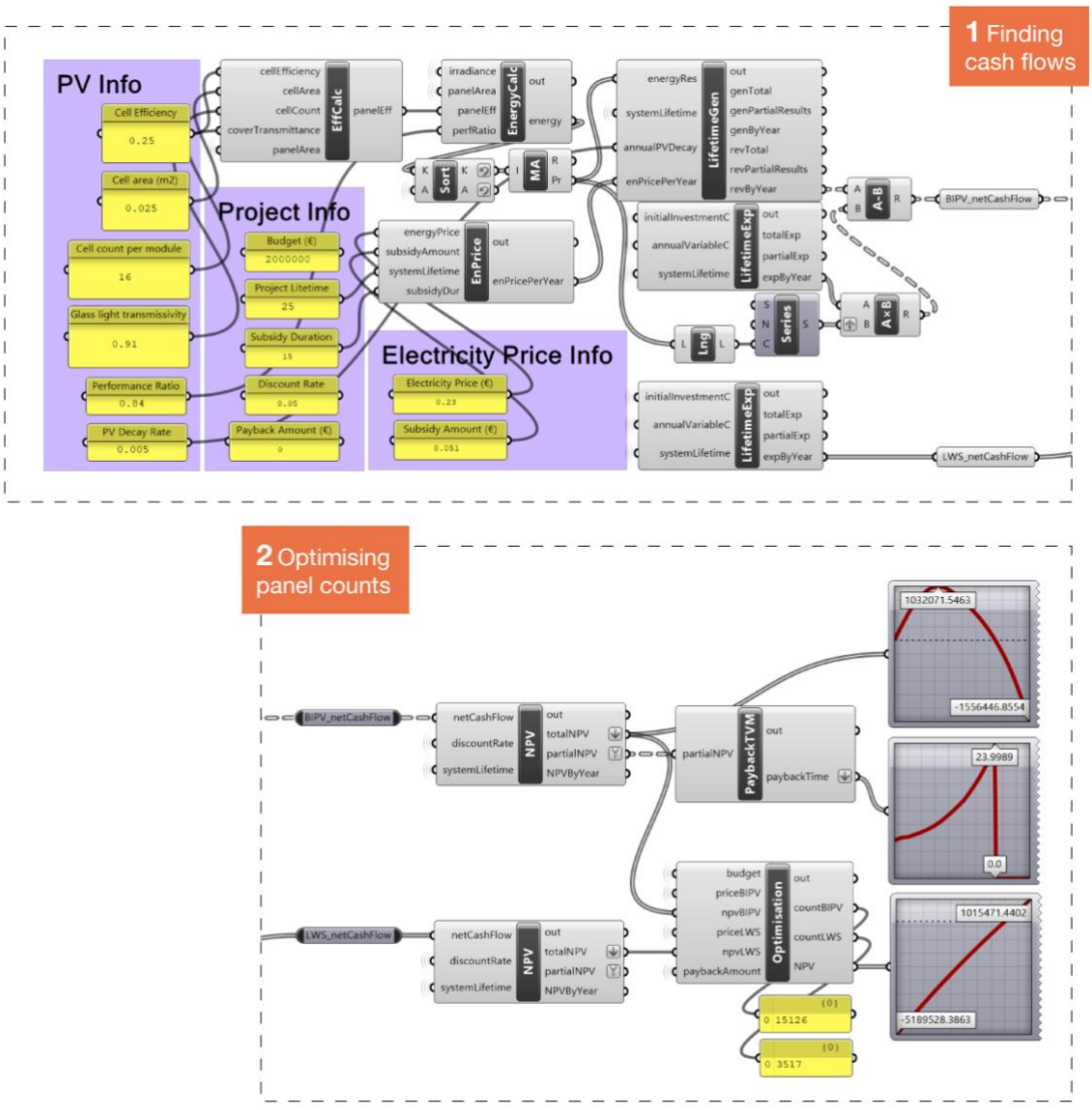

Figure 71: An overall impression of how some of the toolkit components come together in an optimisation setting.

5.4.2.1. Cash flow calculating tools

This fragment of the components focuses on the cash flow calculations. The tilted BIPV price calculator uses the calculation explained Chapter 5.2.3. I should be noted that this calculation is design-specific and would largely vary depending on the panel producer.

The efficiency calculator can be used for calculating the light-to-electricity conversion efficiency of the BIPV panels, considering cell efficiency, cell-to-panel area ratio and the solar direct transmissivity of the upper cover. Annual energy generation calculator takes the irradiance values were calculated by Ladybug for Grasshopper (Chapter 5.3), panel area, panel efficiency and PR values as inputs to calculate the energy produced in the first year. As the efficiency will drop in time because of the degradation of the PV-cells, the energy generated decreases yearly. This calculation can be made using the lifetime energy generation and revenues calculator. Here, the subsidies supplied for the project also play a role. The yearly energy selling price list was prepared using the yearly energy selling price calculator. These together constitute the positive cash flows of the project. The negative cash flows were found by using the lifetime expenditures calculator with the inputs of initial investment cost, annual costs and the project lifetime. The images of the Grasshopper components with their inputs and outputs are given in Figure 72.

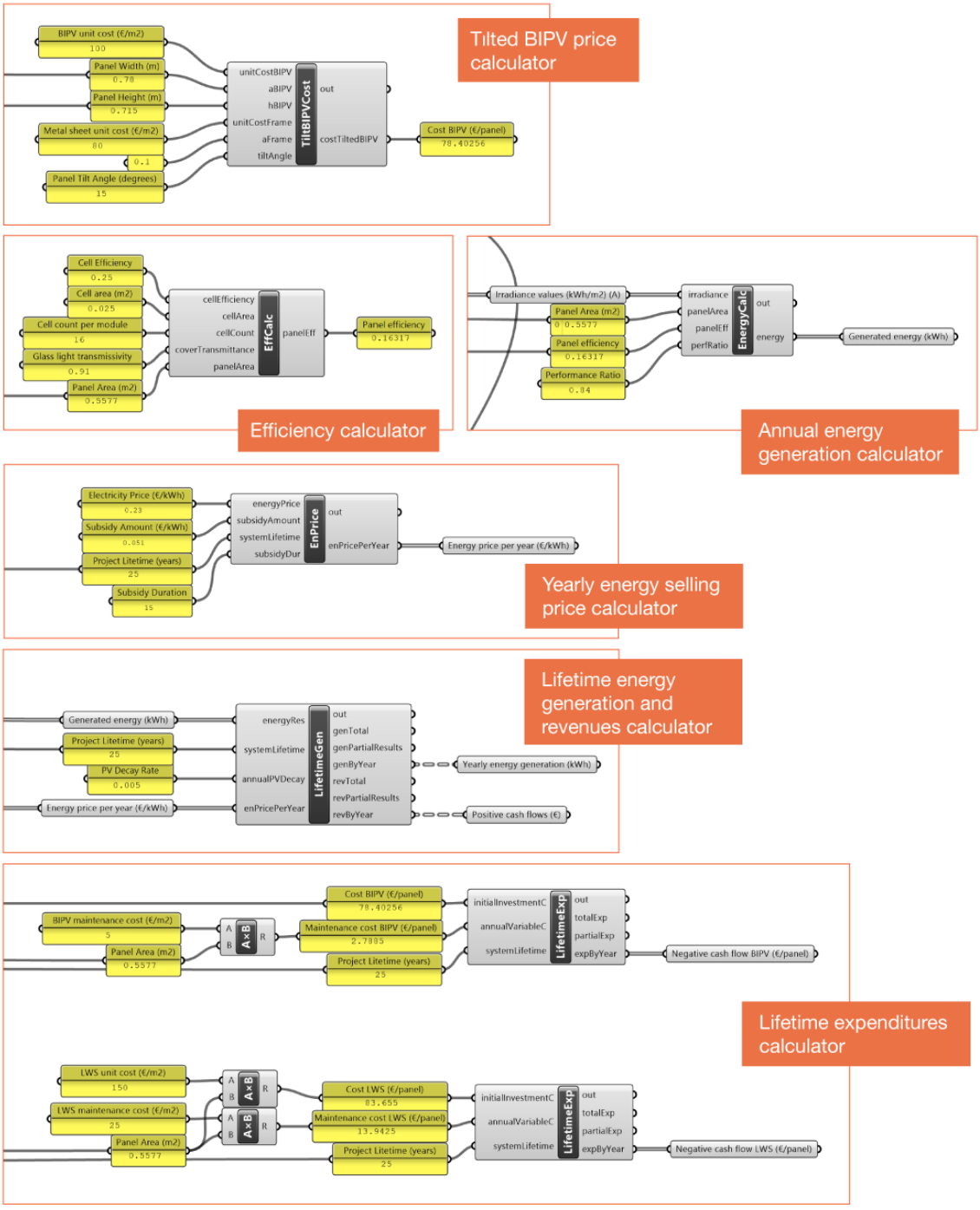

Figure 72: The tools used for calculating the cash flows.

5.4.2.2. Assessment and optimisation tools

Assessment components in the toolkit comprise calculators prepared using the engineering economics concepts. The comparable values of different façade options in different project durations were found by using the NPV calculator. The discount rate can be calculated using the Fisher effect calculator or any discount rate seized by the investor can be used. The LCoE calculator can be used for comparing the price of the electricity generated by the power plant with the grid electricity aiming to reach a parity. The

payback time calculator finds the time period that the projects pays off, regarding the TVM.

To calculate the optimum BIPV and LWS panel counts with a given budget and payback amount desired in the project lifetime, an iterative optimisation component was made. This component first buys one BIPV panel and allocates the rest to the living wall panels. It continues increasing the number of purchased BIPV panels and allocating the rest of the budget to the LWS panels until the point that there are no LWS panels purchased. The NPV in the given year with all the options are simultaneously recorded. In the second part of the code, the recorded values are compared with the payback amount that has been set and gives the count of BIPV and the green wall panels when their NPV reaches the payback amount. The images of the Grasshopper components with their inputs and outputs are given in Figure 73.

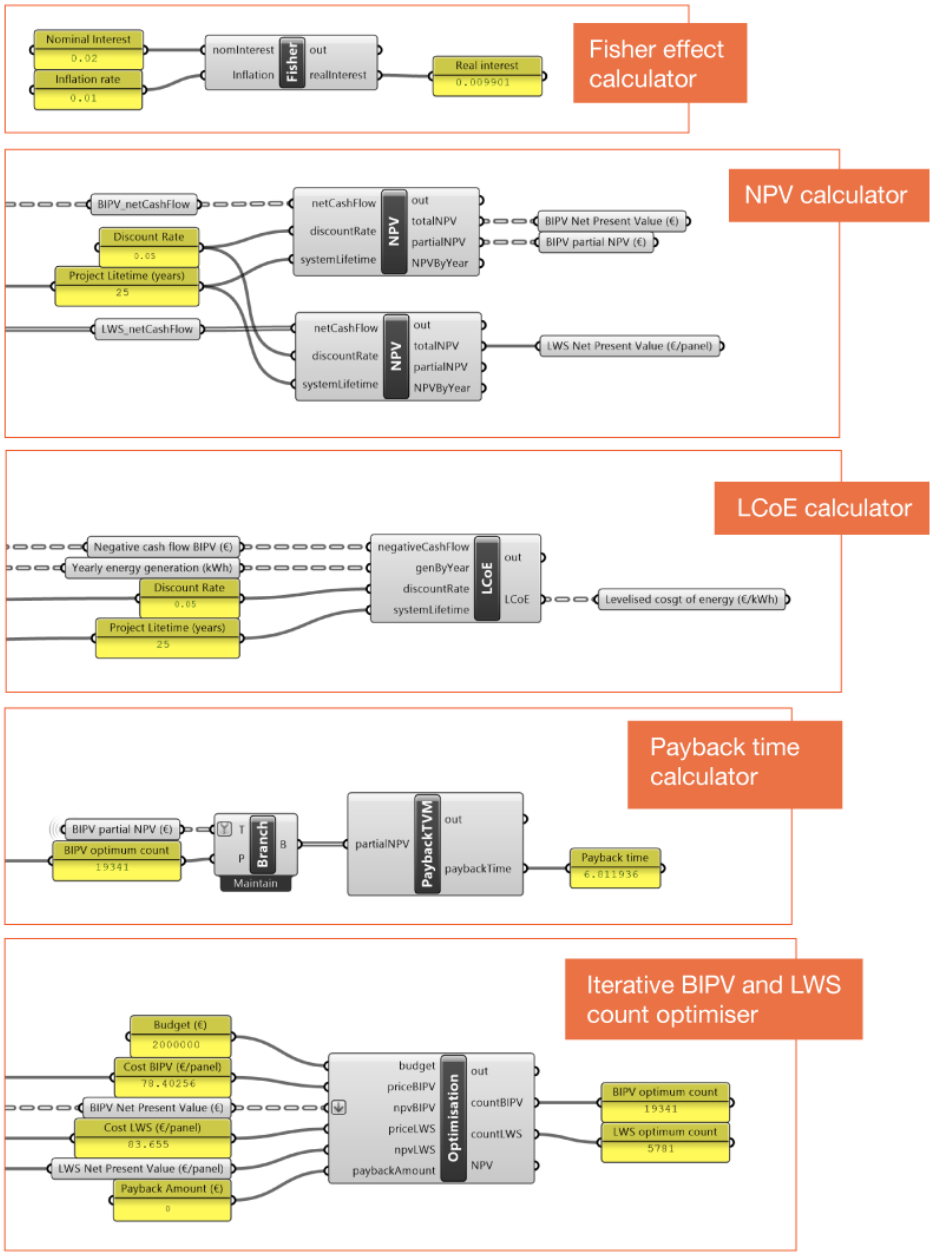

Figure 73: The tools used for asssessment and optimisation.

5.5. Learning from scenarios

Different scenarios starting with an irradiance analysis were tested. Each scenario is run with flat panels and panels tilted by 5°, 10° and 15°. In the Scenario-0, maximum NPV and minimum LCoE values, which can be achieved without any budget restrictions, were investigated. With the best possible options, Scenario-1 was conducted. In this scenario, the payback times of the best options were calculated. In the Scenario-2, the possibility for the PV revenues to finance living wall systems was investigated. In the Scenario-3, a limited budget was considered for the initial investment and the living wall panel count was tried to be maximised, where all of their expenditures are covered by the BIPV generation over a given amount of time. A diagram showing the relation between the

scenarios can be seen in Figure 74. The complete flowchart as a result of this chapter can be observed in Appendix 2: Optimisation flowchart.

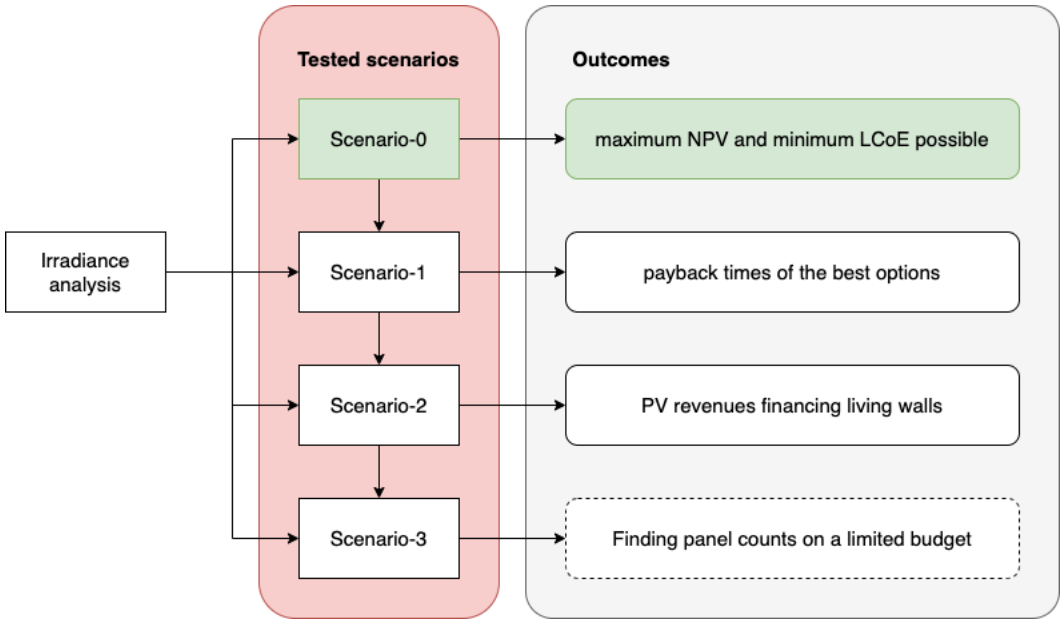

Figure 74: The relation between the scenarios.

5.5.1. Scenario-0

The aim of the Scenario-0 was to find the maximum NPV and the minimum LCoE possible in a system with a 25-year lifetime, without any budget limitations. The third research question, "What may be the energy yield benefit compared to the added costs of custom-made BIPV-panels?" was addressed at this stage, by comparing the NPV and LCoE values for flat panels, 5°, 10° and 15° tilted panels. As can be seen in Figure 75, the workflow consists of the main sections, which are annual energy generation with NPV and LCoE at the end of the 25th year. The annual energy generation constitutes the base for calculating the positive cash flows for the other calculations.

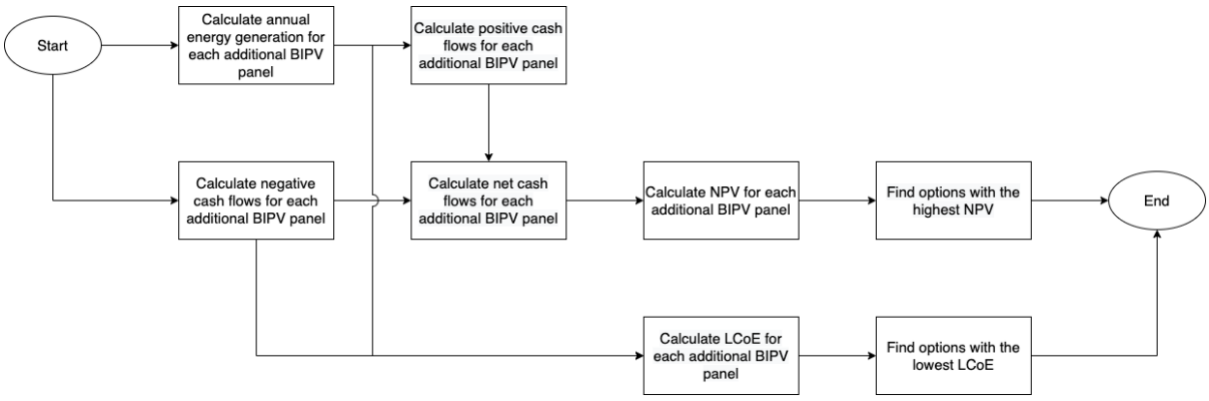

Figure 75: Flowchart of the Scenario-0 model.

NPV and LCoE are including the time factor, considering the future value of the money. At the same time, PV systems lose their efficiency gradually and the electricity generation can lower down to 80 per cent of their initial state at the end of 25 years. These factors were also considered in these calculations.

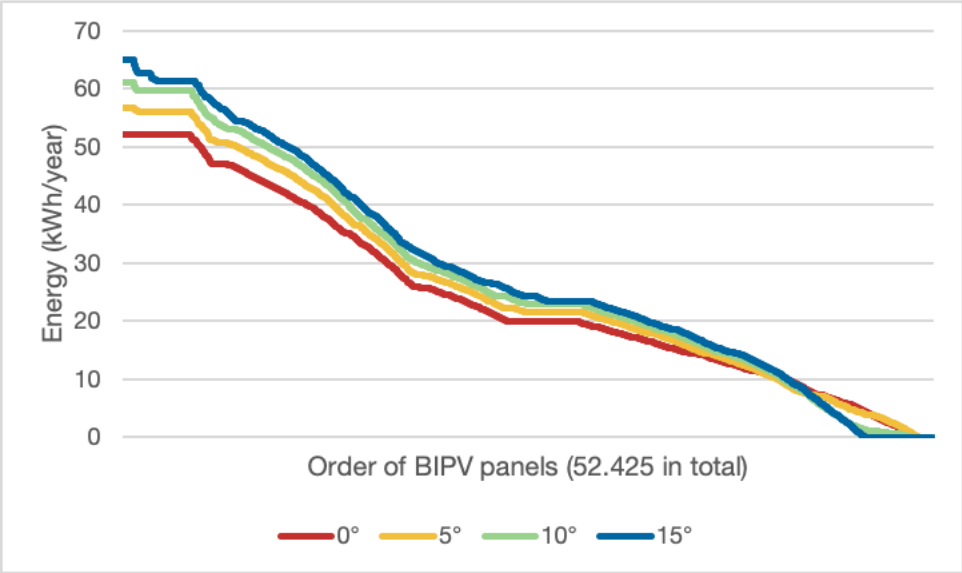

Figure 76: Scenario-0, energy generation of each BIPV-module, descending sort.

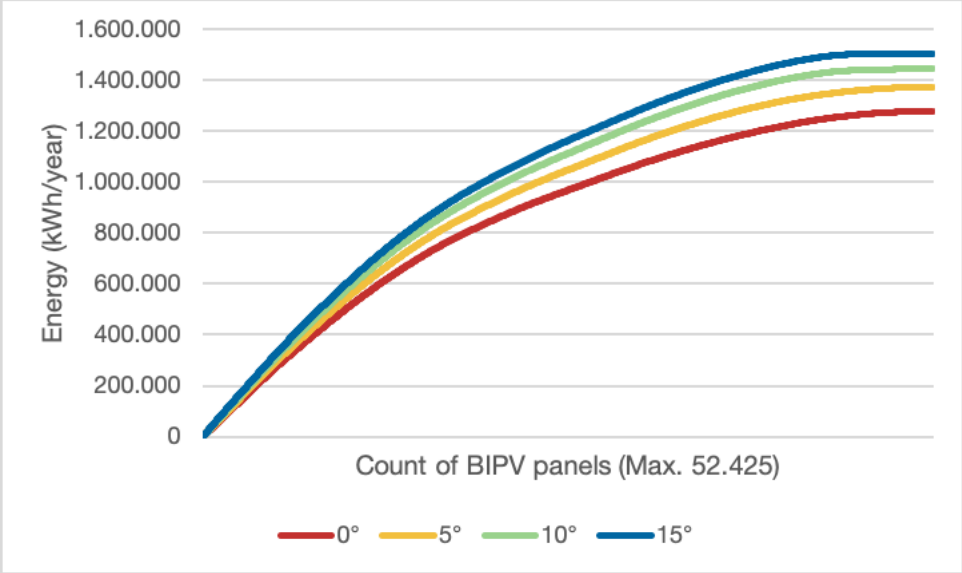

Figure 77: Scenario-0, energy generation with each additional BIPV-module.

The annual energy generation of each panel sorted is given in Figure 68 and the increase with each additional panel is shown in Figure 69. It can be seen that it becomes unfavourable to purchase BIPV-modules after a point as the graph is decreasingly growing. So, the number of panels leading to the maximum NPV and the lowest LCoE at the end of the project lifetime was investigated. The maximum NPV and the minimum LCoE are given in Table 11 with the number of panels, their total price and the tilting amount. The results show that tilting the panels may have a benefit. However, as can be seen at 5° tilting situation, the benefit does not compensate the customization costs. The solar PV LCoE for the Netherlands is EUR 0,12/kWh (Statista, 2016), and it can be seen that the LCoE of this façade system cannot compare with the utility-scale applications in any case.

Table 11: Maximum NPV, minimum LCoE values and the required panel counts.

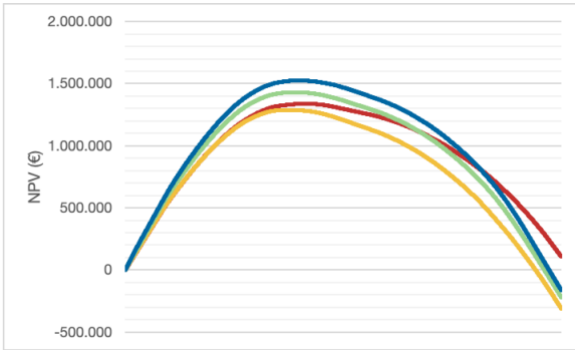

	0°	5°	10°	15°
Count of panels	21.764	19.519	20.620	20.800
Total price (EUR)	1,21M	1,39M	1,54M	1,63M
Max. NPV25 (EUR)	1,34M	1,29M	1.43M	1,53M

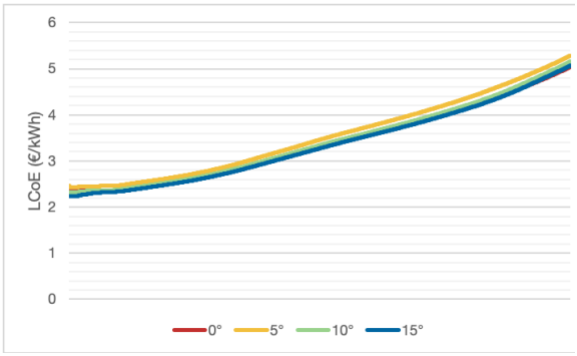

	0°	5°	10°	15°
Count of panels	3627	675	143	75
Total price (EUR)	201K	48K	10K	6K
Min. LCoE25 (EUR/kWh)	2,35	2,43	2,32	2,24

5.5.2. Scenario-1

In the Scenario-1, we purchase BIPV-panels as many as would make the highest revenue at the end of 25 years. The flowchart looks similar to the NPV section of the Scenario-0. The difference is that we find the most profitable options with an unlimited budget and investigate their payback time regarding the TVM, PV-decay rate and the variable subsidy amount. The flowchart of the model can be seen in Figure 78.

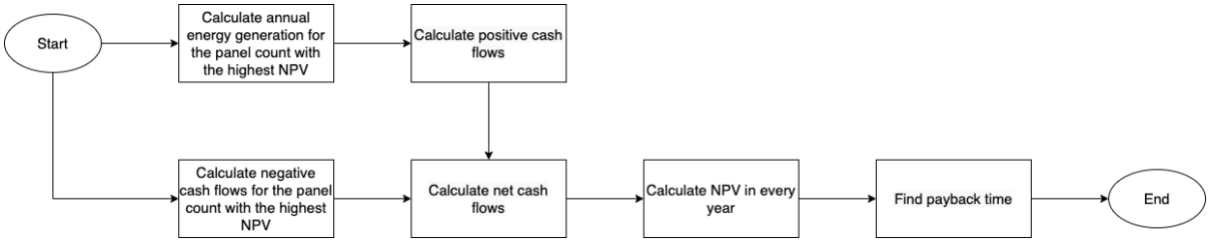

Figure 78: Flowchart of the Scenario-1 model.

We used the payback time calculator in this model, where we can have a float value of where the line cuts the time axis in the NPV-Time graph, as seen in Figure 79. This value was acknowledged as the payback time. The payback time of the flat panels is the lowest. However, in time, 15˚ tilted panels gain a higher revenue. Tilting the panels for 5˚ do not constitute any benefit.

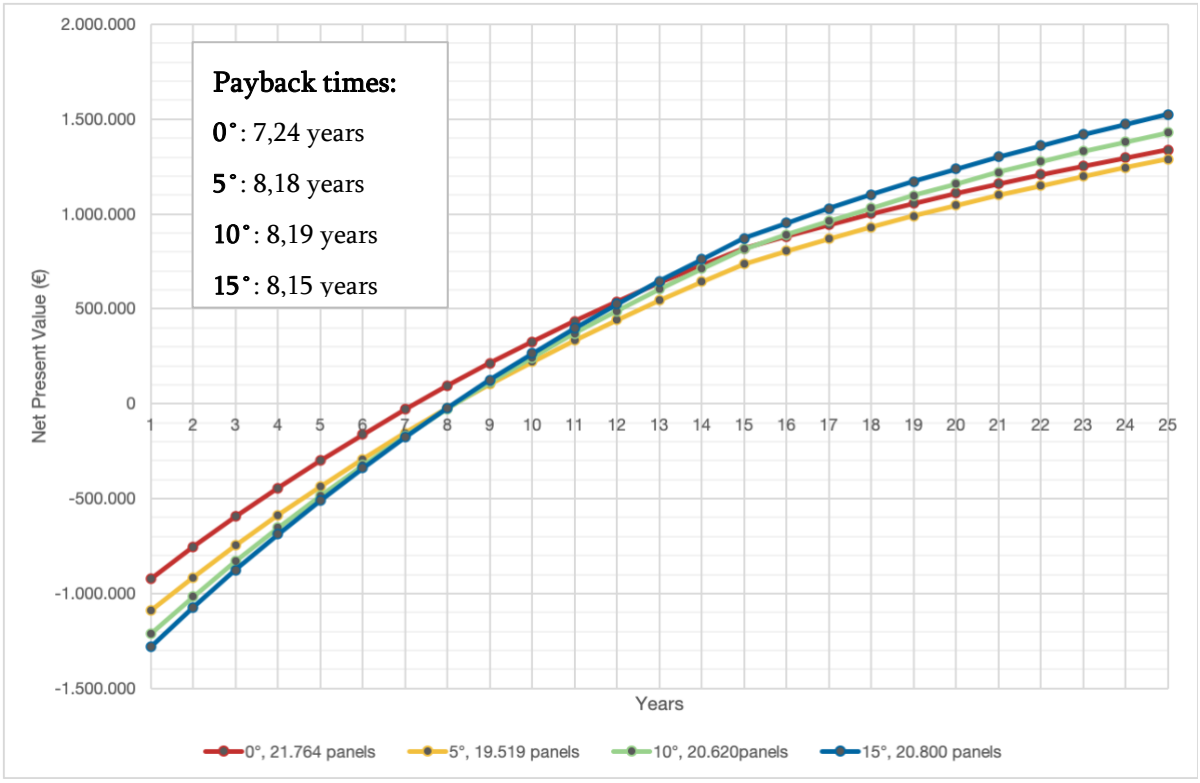

Figure 79: Scenario-1, NPV graphs of the best option from the Scenario-0.

5.5.3. Scenario-2

In the Scenario-2, the power of the BIPV system to finance the living wall systems was investigated. It was assumed that the budget is not limited. This is important b because even though the system would pay off short after the payback times in Figure 79, the investor would have to invest more in the beginning. The LWS panel count that can be financed can be calculated by dividing the NPV of the BIPV system into the negative NPV of a single LWS panel at each year. The flowchart can be seen in Figure 80 and the results can be seen in Figure 81.

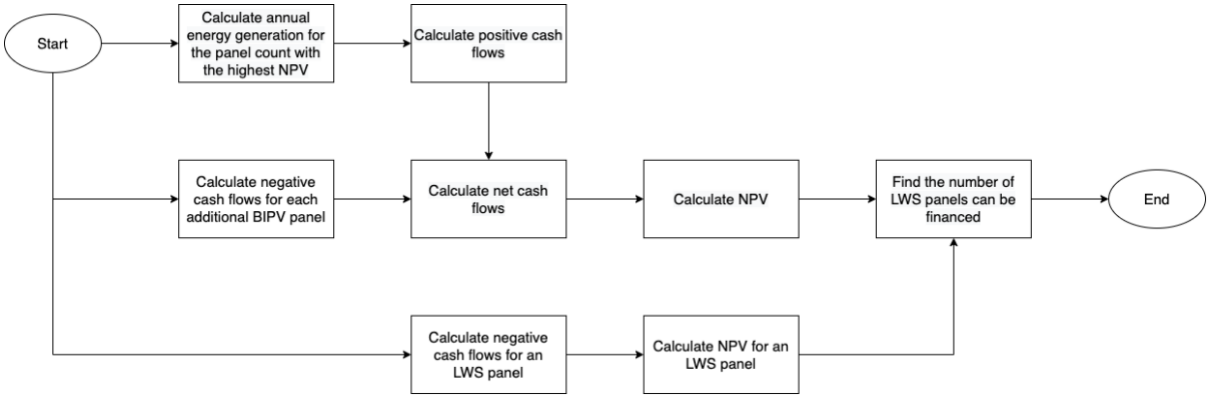

Figure 80: Flowchart of the Scenario-2 model.

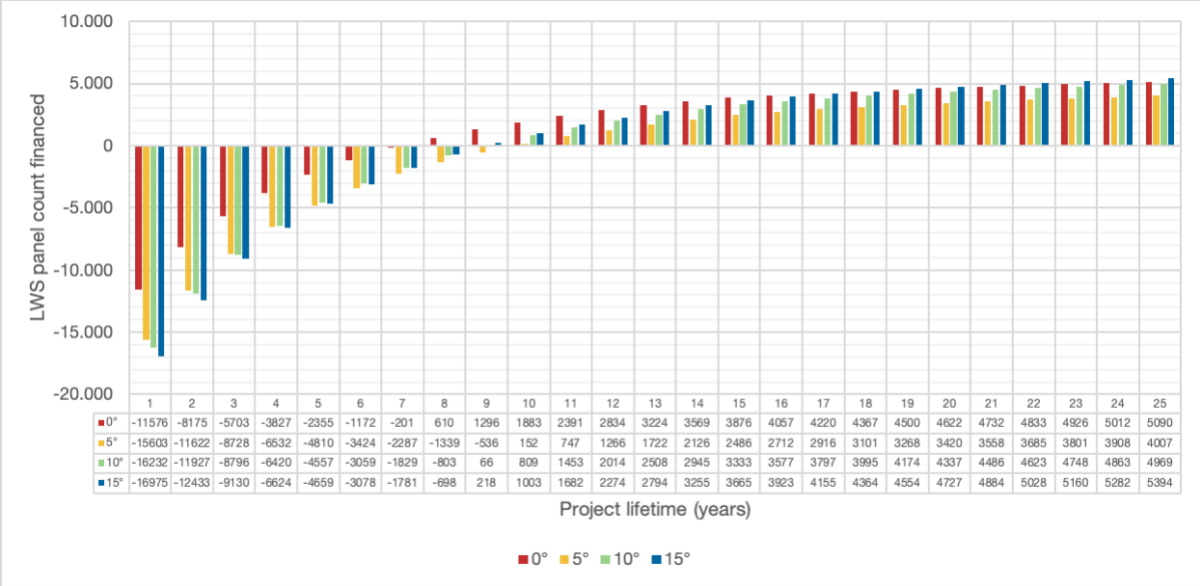

	1	2	3	4	5	6	7	8	9	10	11	12	13	14	15	16	17	18	19	20	21	22	23	24	25
0°	-11576	-8175	-5703	-3827	-2355	-1172	-201	610	1296	1883	2391	2834	3224	3569	3876	4057	4220	4367	4500	4622	4732	4833	4926	5012	5090
5°	-15603	-11622	-8728	-6532	-4810	-3424	-2287	-1339	-536	152	747	1266	1722	2126	2486	2712	2916	3101	3268	3420	3558	3685	3801	3908	4007
10°	-16232	-11927	-8796	-6420	-4557	-3059	-1829	-803	66	809	1453	2014	2508	2945	3333	3577	3797	3995	4174	4337	4486	4623	4748	4863	4969
15°	-16975	-12433	-9130	-6624	-4659	-3078	-1781	-698	218	1003	1682	2274	2794	3255	3665	3923	4155	4364	4554	4727	4884	5028	5160	5282	5394

Figure 81: The count of living wall panels over the project's lifetime that can be financed by the BIPV panels of the best options of the Scenario-1.

5.5.4. Scenario-3: Proposing computationally optimised designs for the AMC

In the Scenario-3, a situation where a limited budget was spared for the special panels. This budget is allocated to BIPV and living wall panels in the beginning of the project. The BIPV walls are constantly generating energy and earns money and the living walls only consume energy over their lifetime apart from their other environmental benefits. The project lifetime and the payback amount were set in the beginning besides the budget. This amount can be 0 or the future value of the budget, for instance. The aim is to buy maximum living wall panels in the beginning while still having an NPV above the set payback amount at the end of the project lifetime. The flowchart of the model can be seen in Figure 82.

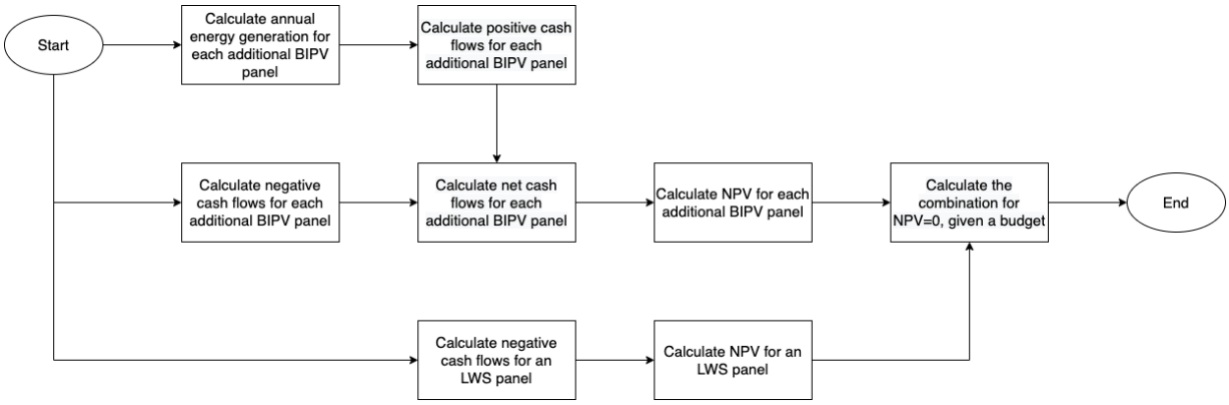

Figure 82: Flowchart of the Scenario-3.

5.5.4.1. Panel counts

Designs were created with the proposed method, considering different budget and panel tilting angle options. 250K, 500K, 1M and 2M Euro budgets and tilting angles of 0°, 5°, 10° and 15° were tested. The optimum BIPV and LWS panel counts for a 25-year project are given in Figure 83. As can be observed, tilting the BIPV panels start to increase the

amount of financed LWS panels after a certain amount of budget. However, it can also be seen that the LWS panel counts do not increase proportionally to the budget.

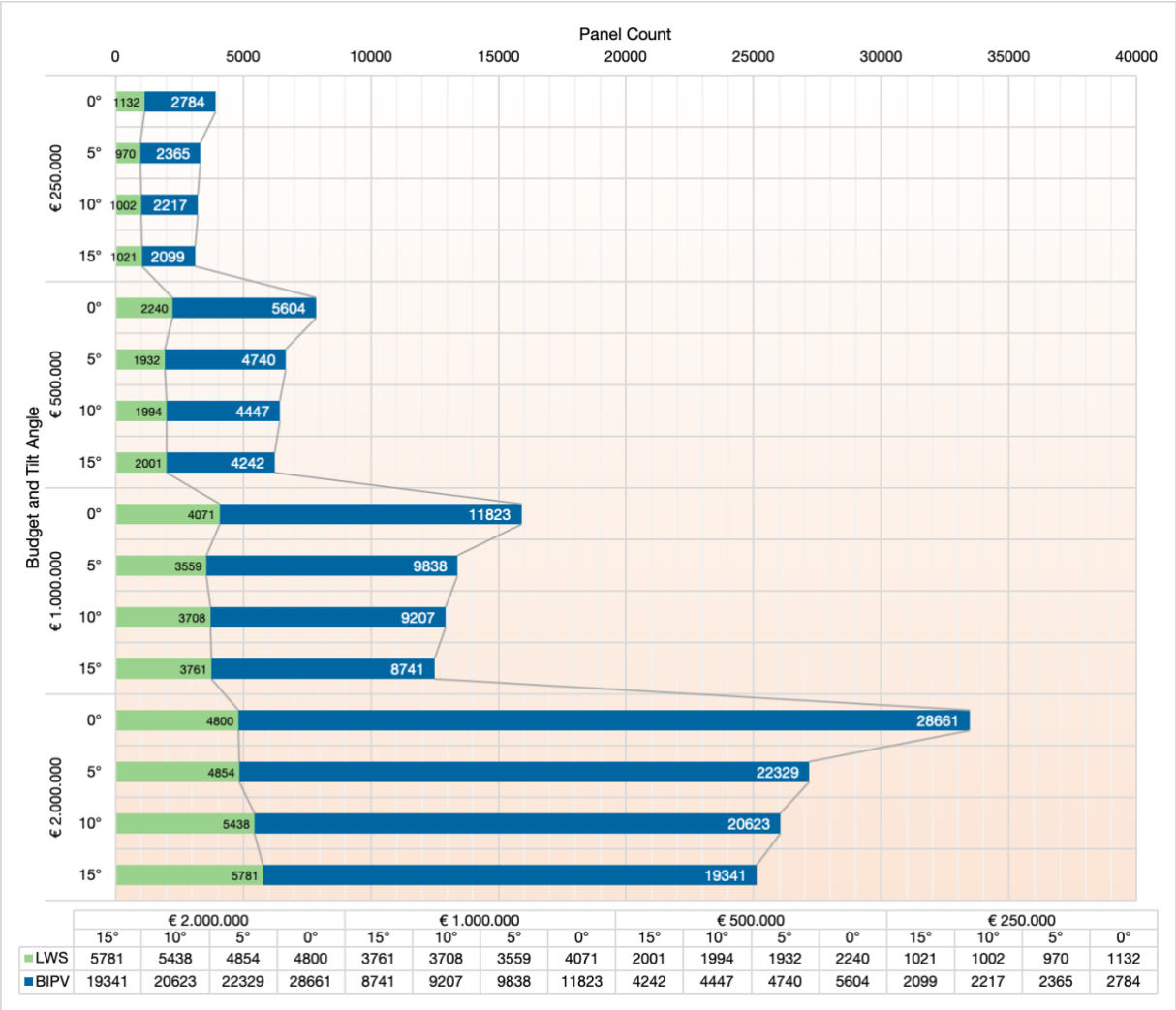

	€ 2.000.000				€ 1.000.000				€ 500.000				€ 250.000			
	15°	10°	5°	0°	15°	10°	5°	0°	15°	10°	5°	0°	15°	10°	5°	0°
LWS	5781	5438	4854	4800	3761	3708	3559	4071	2001	1994	1932	2240	1021	1002	970	1132
BIPV	19341	20623	22329	28661	8741	9207	9838	11823	4242	4447	4740	5604	2099	2217	2365	2784

Figure 83: The optimum panel counts to pay off the investment costs with most LWS panels with different budgets and tilt angles.

5.5.4.2. Panel allocation

The allocation of the panels was done by the following steps:

1. Sorting the panels by their radiation values.
2. Reserving the best places for BIPV to maximise energy generation.
3. Sorting remaining panels by their sunlight hour values.
4. Reserving the places for LWS.

After following these steps, the process can be started over for a project revision in the future. Visualisation of the process, which is also a complementary tool in the toolkit is made in Figure 84.

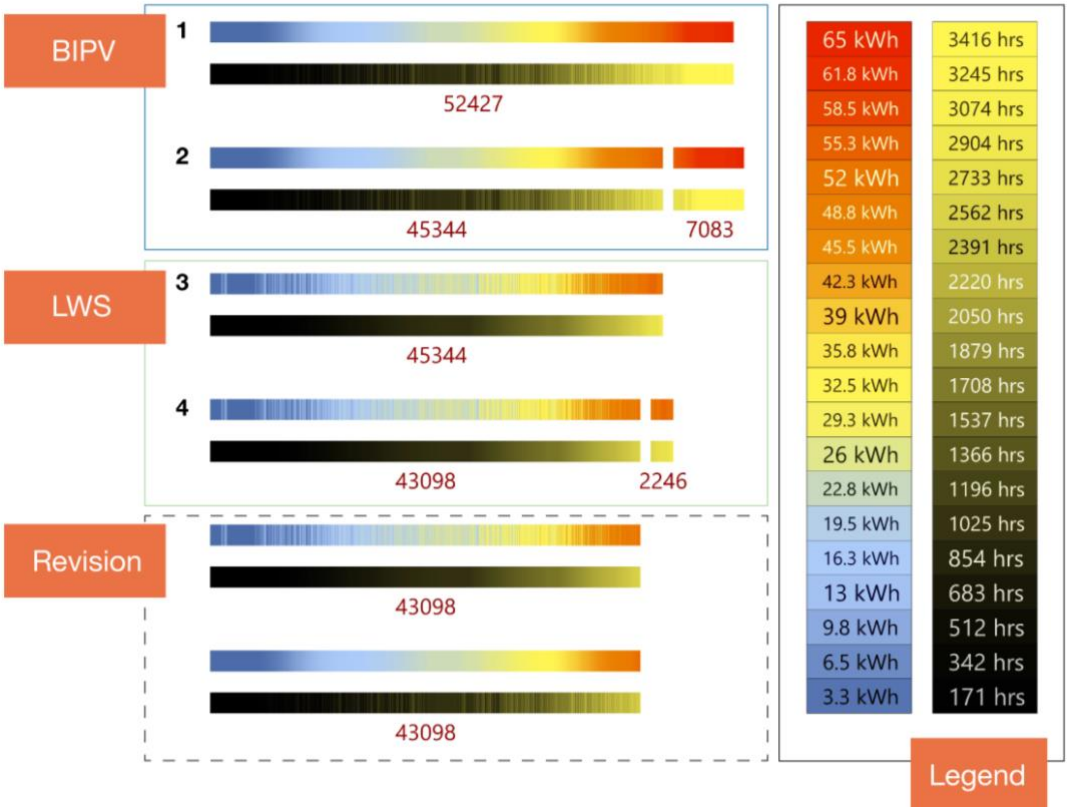

Figure 84: Visualisation of the panel allocation process.

The plant species used in the LWS panels affect their potential allocation. Some types of LWS plants may require less sunlight daily or annually or some might need more. In this case, the LWS allocator tool can be used with the inputs of sorted sunlight hour list of the remaining panels, minimum sunlight hour required and the LWS panel count. How the tool can be used is shown in Figure 85.

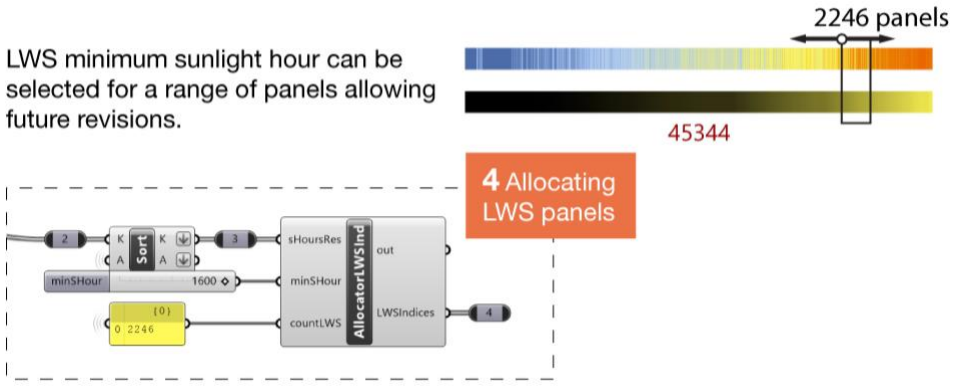

Figure 85: Allocating the LWS panels according to their minimum sunlight hour requirement.

While irradiance and sunlight hour values show similarity in their order, they do not match exactly, since the radiation analysis counts diffused radiation in a day with overcast sky, which decreases the direct sunlight exposure of the panel. However, by selecting LWS panels which would require shorter sunlight exposure, a buffer zone for

reserving the next best positions for BIPV panels for a future project revision. How the minimum annual sunlight hours affect the allocation of the LWS panels is shown in Figure 86, for a budget of 2M Euros, project lifetime of 25 years and 15° tilted panels.

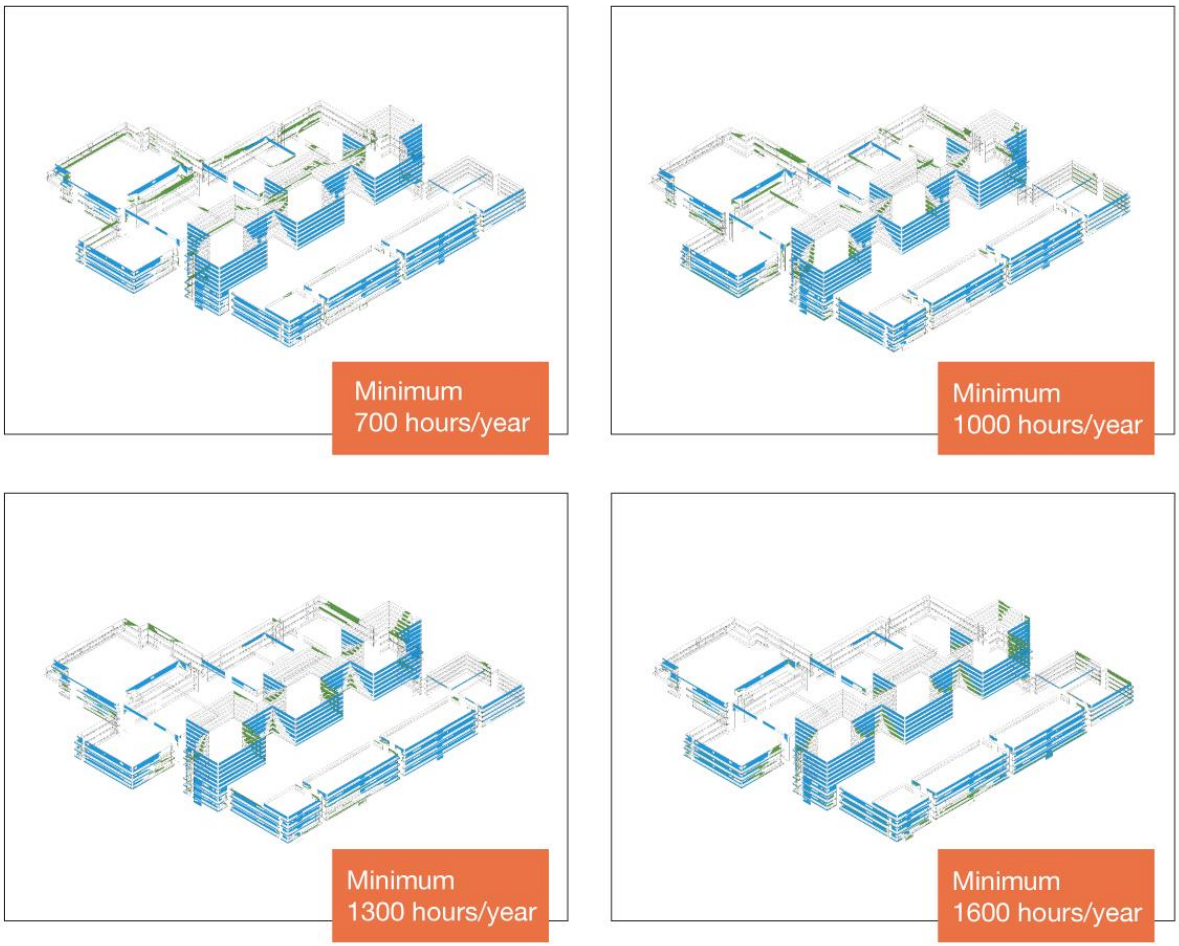

Figure 86: Computationally allocated BIPV and LWS panels with different minimum sunlight hours, affecting the positioning of the LWS panels.

5.6. Analysis of an architectural design

In the real world, an architectural design does not always adopt computationally optimal solutions. According to Vitruvius' belief, an architectural design should carry the three elements: firmitas (strength), utilitas (functionality) and venustas (beauty) (Granger, 1925). The beauty and the functionality of a building certainly needs the insight of the architects and their decisions may conflict with the computationally optimal, for other benefits.

In such a case, the toolkit can be used for creating a more financially realistic vision for the architects to help with their design. Then, the architects can initially only determine the energy-generating surfaces. The toolkit can then be used for panelling these surfaces with standardised panels which cover most of the surfaces. With financial components of the toolkit, the architects can know how much wall area can be covered with living wall systems which would be financed by the generated energy. An example design decision which is also shown in Figure 87, can be concentrating the BIPV panels on the upper

levels for less obstructed energy generation and putting the living wall systems closer to the ground floor level or even inside the building. Then, the computational workflow can be altered to what can be observed in Appendix 3: Analysis flowchart. The architect can try to find the optimum panel dimensions within a given range, to cover most of the surface area, using a standard solver such as Galapagos evolutionary solver. In our calculations, the optimum dimensions for the panels was found as 64 cm by 57 cm, which would cover around 93 per cent of the whole surface.

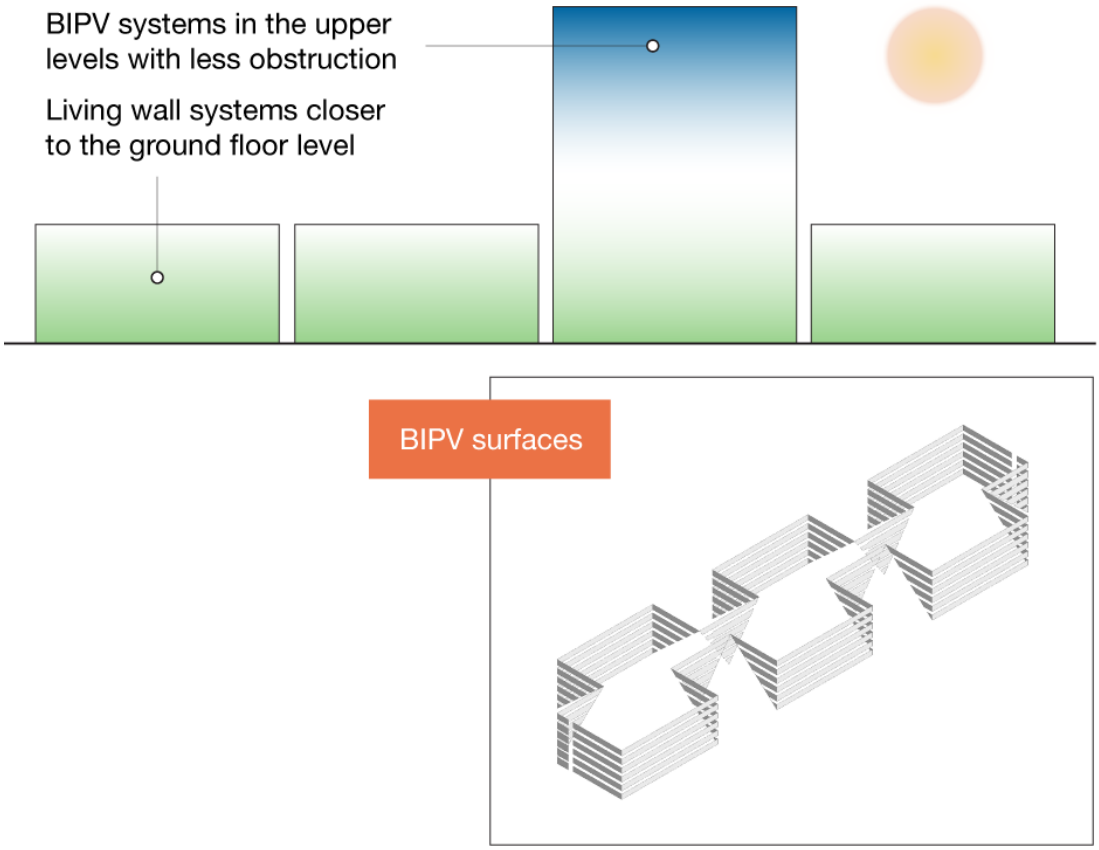

Figure 87: An example façade design decision and the façade surface to be covered with BIPV panels.

In the next step, the PV cell technology can be selected comparing how the c-Si and thin-film cells can be fit into the panels and how would they perform. In this phase, it should be noted that the PR value can lower and the uncertainties may be higher for thin-film PV cells (Müller et al., 2016). Possible BIPV panel designs to compare are shown in Figure 88.

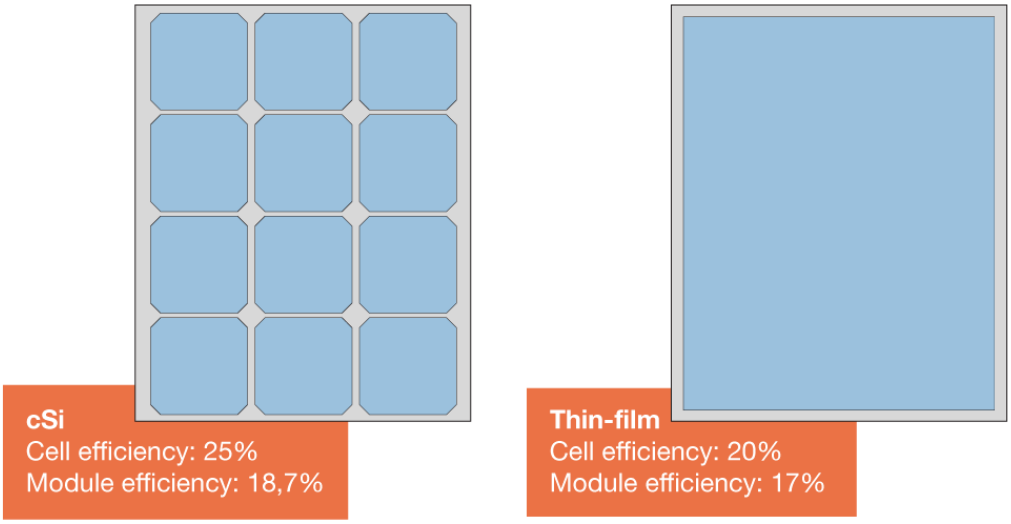

Figure 88: Possible PV technologies for the BIPV panels.

The next step involves the investigation of cash flows during the project time window. For this calculation we used 15° tilted c-Si modules with dimensions of 64 cm by 57 cm. The cash flow diagram can be observed in Figure 89. A version with corresponding values can be found in the Appendix 4: Cash flow graphs. The NPV of the project is 746.347 Euros and the payback time is 14,3 years. This project itself is already feasible. Additionally, it can finance LWS panels to be integrated into the project.

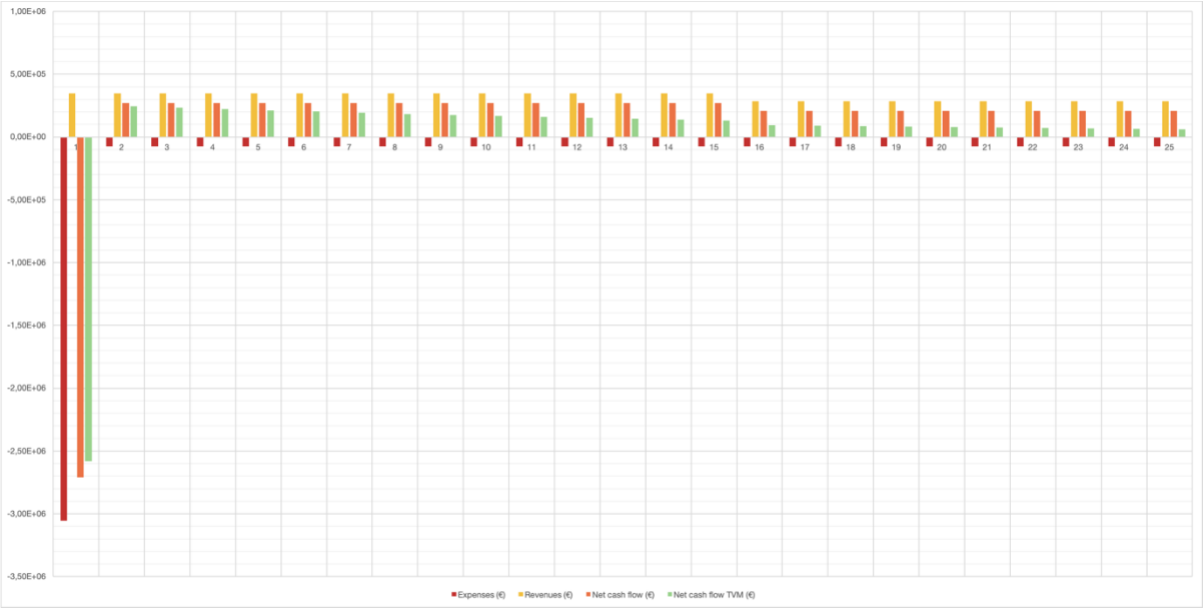

Figure 89: Cash flows of the analysed architectural design for a 25-year project lifetime.

LWS is calculated to cost 800 Euros per square metre to the hospital, including the initial investment and annual costs. However, this amount is dispersed to a 25-year project. So, the decision of whether to put 1 square metre of LWS or not costs as much as the net present value of 800 Euros. The NPV of 1m2 of LWS panel was calculated as 519 Euros. This means that the hospital can install 1.438 square metres of LWS in the beginning and

the whole system would have amortised itself in 25 years. The cash flow considering the LWS panels can be seen in Figure 90 and a version with individual values can be observed in the Appendix 4: Cash flow graphs.

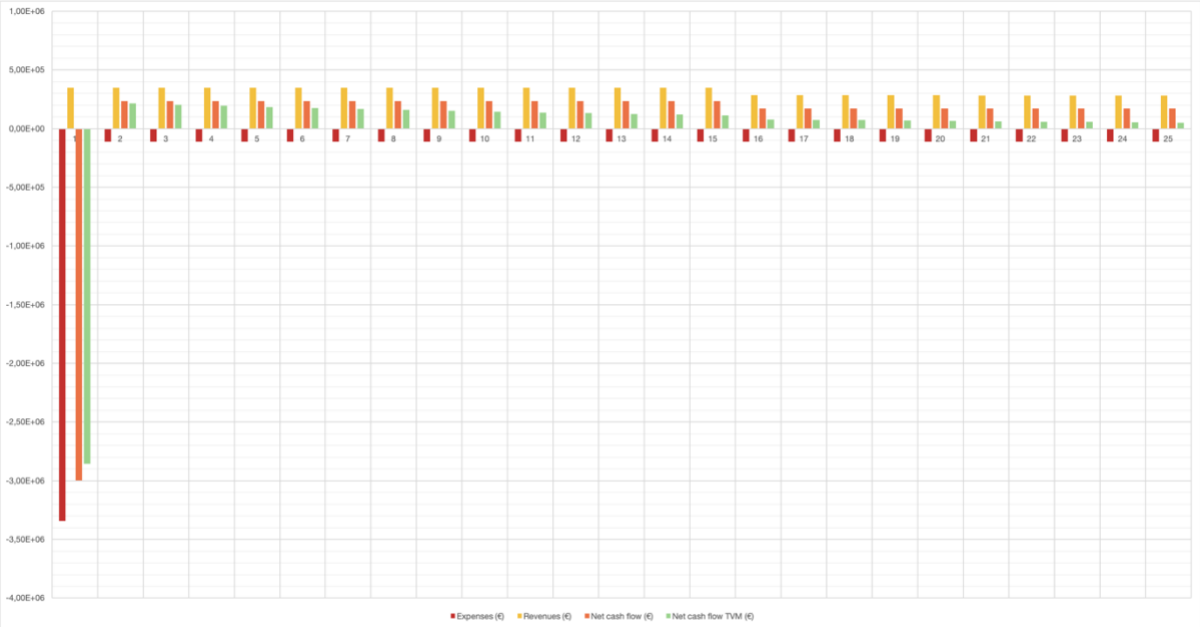

Figure 90: Cash flows of the analysed architectural design for a 25-year project lifetime, 1.438 m2 LWS added.

6. Conclusions

6.1. Summary of the results

6.1.1. Chapter 1

Many buildings in the Netherlands are being refurbished to improve insulation properties for energy-efficiency (Konstantinou, 2014). A step further is making the buildings generating their own energy to make the former "consumer" owners, "prosumers" (Smets et al., 2016). A concept to employ BIPV to the existing buildings is to replace the façade cladding with BIPV panels whenever possible. BIPV usage in urban settlements cannot always be as efficient as dedicated solar power plants, since the optimal orientation — which is 37° tilted to the south in the Netherlands— cannot be achieved in every context. Furthermore, parameters such as colour, finishing, transparency and size are of primary importance for BIPV implementations in contrast with utility-scale applications (Palm et al., 2018).

Many projects are being developed to promote renewable energy usage in urban settlements, but few of them can be realised due to cost-related challenges. The motivation of this study is to contribute to finding cost-effective BIPV solutions to apply in areas where renewable energy generation is less prevalent. Amsterdam's near-future climatic ambitions are being CO2- and energy-neutral, fossil-free and circular in all terms of materials. AMC Amsterdam is a large building with large opaque façades where BIPV solutions can be investigated with other façade materials like living walls, which can also contribute to improve air quality, to mitigate the urban heat island effect (Cheng et al., 2010), to reduce noise pollution, to improve water sensitive urban design and to increase

urban biodiversity. So, the research question was formulated as, “How can a cost-effective and applicable BIPV retrofit be designed and computationally optimised for a concrete façade in combination with different cladding materials?”

6.1.2. Chapter 2

In this chapter, we founded the informational basis of the research. We discussed how the AMC can be a subject of performance approach and how the case can be contextualised for a transition in its energy systems. We reflected on the relevant engineering economics concepts to form the criteria of the computational assessment and optimisation. We also showed our finding in existing PV technologies, BIPV systems in particular, façade systems with vegetation, and generic façade systems that can constitute a base for hosting different cladding materials.

6.1.3. Chapter 3

Since the research test the proposed methodology on AMC Amsterdam, which is a hospital building built in the 70s, the building itself was analysed to find focus points to lead the computational design. In terms of Performance Based Design, the starting point of the project is the aim of making the AMC more environmentally friendly and add architectural quality to it. Affordable, flexible and innovative solutions are needed to improve the properties of the external walls and contribute to the building’s energy generation. Currently, the building relies on its CHP plant run on gas, in terms of electricity and buys a small proportion from the grid. As a result of the solar potential analysis, it was seen that PV systems installed on the building itself cannot meet the demand but contribute to it or be chosen to finance other façade cladding options, such as LWS.

There are many façade cladding types used in the building, such as concrete, steel sheets and sandwich panels. These façade types were investigated, and their components were tried to be revealed to determine the retrofitting options. The thermal properties of the façades do not meet the standards anymore, due to decaying and its outdated technology. So, we assumed that the façade of the low-rise and high-rise buildings with concrete wall core would be completely replaced.

6.1.4. Chapter 4

In this chapter, we stated a comprehensive design vision, incorporating a façade system with interchangeable panels of BIPV, LWS and other claddings. The aim is to make the system flexible for the designer’s insight and affordable for the investor. By using interchangeable panels, the design can be revised to keep up with the changing demand trends.

By investigating the dimensioning of this relatively regular building, we decided upon a grid, with which around 85 per cent of the building can be cladded with the same size of panels. The layout of PV-cells on these panels and the effect of tilting angle were also elaborated. A conceptual panel mounting system, inspired by the existing technologies, was introduced.

6.1.5. Chapter 5

In this chapter, we introduced an early-stage computational design method to compare different variations of designs in terms of their cost effectivity. The workflow was supported with a toolkit made for this research. This toolkit involves parts for quick panelling a façade geometry, finding cash flows with given financial inputs and optimising design solutions. Another use of the same toolkit constitutes the financial analysis of a given design by its finding cash flows and monitoring its payback time and total financial value. The toolkit was tested over scenarios and the proceedings were recorded. We generated optimum early-stage design proposals computationally and reflected on how these proposed designs can give clues for final designs.

6.2. Response to the research questions

This is the subchapter in which we retrospectively look at to which degree we could answer the research questions in the beginning of the study. The main research question and the research sub-questions drove this research are restated followingly.

How can the cost-effectivity of an early-stage BIPV design be assessed and optimised computationally within the frame of the AMC case?

To answer the main question, we developed a computational toolkit can be used for the financial assessment of a given design and generate optimum early-design solutions integrating BIPV and LWS technologies. The toolkit adopts engineering economics concepts and methods for assessment.

- Which measures can be taken to improve the energy performance of the AMC Amsterdam's external walls and what is the solar electricity potential of the building?

The answer of this question was partially enlightened by a readymade thermal analysis of the AMC façades and the building code. It was seen that the insulation of the walls should be replaced to meet the building standards. The windows can be renewed or repositioned, but the benefit of this particular solution is questionable. There is trade-off between insulating the building from the outside and inside.

The solar energy generating potential of the building was found by a computational analysis. The results showed that even though the building is entirely covered with PV panels, it would not be able to cover its energy demand. However, this type of energy transition can contribute cutting down natural gas use.

- Which façade systems can be used for BIPV retrofit to the AMC's concrete external walls, in combination with other cladding options?

To answer this question, a design vision was made, encompassing interchangeable panels allowing flexible design and future revisions of the project. This necessitated adopting a façade system permitting individual replacement of the cladding panels. Ventilated façade systems with specially designed fixing elements can be a suitable option for such a design.

- What may be the energy yield benefit compared to the added costs of custom-made BIPV-panels?

A generic panel design was made to answer this question, regarding the added material costs when increasing the panel tilting angle. This angle was integrated into the workflow as a design variable. It was concluded that the tilting of the panels may increase the benefits of the system by compensating the added material and labour costs, generating more energy. However, the eventual answer of this question is design-specific and lies within the panel cost bidden by the supplier.

- What is the financial aspect of BIPV usage in combination with other façade materials, such as façades with vegetation?

The visible financial effect of BIPV is generating energy and thus revenue after its payback time. On the other hand, LWS is a type of investment which comes with high maintenance cost and no direct revenues. However, façades with vegetation has other environmental and architectural benefits, resulting in a better user experience and so, a higher chance of indirect revenues. It was concluded that although the BIPV installed in the AMC would not cover its electricity demand but can constitute an incentive for the investor to embrace different environmentally friendly façade options by financing the LWS.

- To what extent can the proposed methodology maximise the profits on a limited budget?

The proposed methodology aims to find the best possible options by finding how many of each panel type to buy and their proper allocation. However, the computational workflow proposed does not constitute a final decision tool, as architectural design is a much more complex process. It should also be noted that these calculations would be based on multiple assumptions and would only be an estimate as explained in Subchapter 2.4. This method used for optimisation can become an early-stage design exploration tool, and the optimised design proposals can enlighten the designer to reach good-quality and cost-effective final designs.

6.3. Limitations

The methodology was proposed for early-stage design development and has its limitations. Firstly, we see no harm in repeating the fact that architectural design is a very complex process in terms of the effect of the built environment on user experience and a design computationally optimised would not necessarily be considered as a good design. This methodology would only help the communication between the designer and the investor by setting a common language.

One other limitation to consider is that the calculations are based on existing solar analysis tools which not only have their own degree of uncertainty, but also are based on averaged weather data. The real-life behaviour of the PV systems would depend on many external and intrinsic factors which may or may not be foreseen. Furthermore, solar calculations on large buildings take a long time. Thus, optimisation of the design variables such as tilting angle is computationally affordable only with much fast computers or strict restrictions.

6.4. Recommendations

This study was endeavoured to be positioned in between many fields, which all have their own research directions. It is pleaded that the proposed methodology brings these disciplines together to a certain degree. Firstly, the conceptually proposed façade system has its challenges to integrate different cladding types which have different infrastructures. Developing a modular system to improve the compatibility of these different façade types would certainly help the design flexibility, which was taken granted for our design vision.

Furthermore, the integration of this early-stage design and assessment methodology with other methodologies which lean over the spatial quality, building envelopes, energy systems and many others would enhance the comprehensiveness and give a clearer insight in pursue of good and realisable designs.

7. References

Abaide, D. G. (2015). *Circle Packing but w/ Squares? Help? - Grasshopper*. https://www.grasshopper3d.com/forum/topics/circle-packing-but-w-squares-help

Agarwal, P. (2019). *The Fisher Effect*. Intelligent Economist. https://www.intelligenteconomist.com/fisher-effect/

Agea-Blanco, B., Meyer, C., Müller, R., & Günster, J. (2018). Sand erosion of solar glass: Specific energy uptake, total transmittance, and module efficiency. *International Journal of Energy Research*, *42*(3), 1298–1307. https://doi.org/10.1002/er.3930

Al-Mohamad, A. (2004). Efficiency improvements of photo-voltaic panels using a Sun-tracking system. *Applied Energy*, *79*(3), 345–354. https://doi.org/10.1016/j.apenergy.2003.12.004

Alternative Energy Tutorials. (2018). *Bypass Diode for Solar Panel Protection*. http://www.alternative-energy-tutorials.com/energy-articles/bypass-diode.html

Architizer Editors. (n.d.). *An Architect's Guide To: Metal Cladding*. https://architizer.com/blog/product-guides/product-guide/eantka-metal-cladding/

Avancis. (2019a). *Avancis Skala Photovoltaic Modules Safety, Installation and Operation Manual*. www.avancis.de

Avancis. (2019b). *The Avantgarde of Solar Façades*. https://www.avancis.de/wp-content/uploads/2019/05/AVANCIS_SKALA_SF_2019_05-01_EN.pdf

Bellini, E. (2019). *Netherlands to maintain current net-metering conditions until 2023*. Pv Magazine. https://www.pv-magazine.com/2019/04/26/netherlands-to-maintain-current-net-metering-conditions-until-2023/

Bellini, E. (2020). *Power-to-heat-to-power storage for rooftop PV*. Pv Magazine International. https://www.pv-magazine.com/2020/05/07/power-to-heat-to-power-storage-for-rooftop-pv/

Bläsi, B., Kroyer, T., Höhn, O., Wiese, M., Ferrara, C., Eitner, U., & Kuhn, T. E. (2017). Morpho Butterfly Inspired Coloured BIPV Modules. *33rd EUPVSEC*, *September*, 2–6. https://www.ise.fraunhofer.de/content/dam/ise/de/documents/publications/conference-paper/33-eupvsec-2017/Blaesi_6BV370.pdf

Brakels, R. (2018). *Half Cut Solar Panels Give Higher Efficiency & Better Shade Tolerance*. SolarQuotes Blog. https://www.solarquotes.com.au/blog/half-cut-solar-cells-panels/

Britannica. (2005). *Economy of scale*. Economics. https://www.britannica.com/topic/economy-of-scale

Business.gov.nl. (n.d.). *Building regulations*. Retrieved July 2, 2020, from https://business.gov.nl/regulation/building-regulations/

CBS. (2020). *StatLine - Hernieuwbare elektriciteit; productie en vermogen*.

https://opendata.cbs.nl/statline/#/CBS/nl/dataset/82610NED/table?ts=1587936164756

Chairunnisa, I., & Susanto, D. (2018). *Toward Mechanical Performance on Pre-Vegetated Concrete*. 1266–1275.

Cheng, C. Y., Cheung, K. K. S., & Chu, L. M. (2010). Thermal performance of a vegetated cladding system on facade walls. *Building and Environment*, *45*(8), 1779–1787. https://doi.org/10.1016/j.buildenv.2010.02.005

da Silva, W. (2016). *Milestone in solar cell efficiency by UNSW engineers*. UNSW Newsroom. https://newsroom.unsw.edu.au/news/science-tech/milestone-solar-cell-efficiency-unsw-engineers

De Isolatieshop. (n.d.). *Wat is het beste isolatiemateriaal voor mijn klus?* Retrieved February 28, 2020, from https://www.isolatiemateriaal.nl/kenniscentrum/wat-is-het-beste-isolatiemateriaal/

DGMR Bouw. (2016). *Academisch Medisch Centrum Amsterdam gevelrenovatie fase 2 – scenario's*.

Dmitriev, S. (2016). *Viewport with Sketch - Grasshopper*. https://www.grasshopper3d.com/profiles/blogs/viewport-with-sketch

Edgerton, E., Ritchie, L., & McKechnie, J. (2010). Objective and subjective evaluation of a redesigned corridor environment in a psychiatric hospital. *Issues in Mental Health Nursing*, *31*(5), 306–314. https://doi.org/10.3109/01612840903383976

Eicker, U. (2005). Solar Technologies for Buildings. In *Solar Technologies for Buildings*. https://doi.org/10.1002/0470868341

EnergySage. (2019). *How Does Net Metering Work With Solar? | EnergySage*. https://www.energysage.com/solar/101/net-metering-for-home-solar-panels/

EnergySage. (2020). *Types of Solar Panels: What Are Your Options?* https://www.energysage.com/solar/101/types-solar-panels/

Engineering ToolBox. (2009). *Perpetuities*. https://www.engineeringtoolbox.com/perpetuity-d_1497.html

European Comission. (2014). *2030 climate & energy framework*. https://ec.europa.eu/clima/policies/strategies/2030_en

European Comission. (2018). *2050 long-term strategy*. https://ec.europa.eu/clima/policies/strategies/2050_en

Fan, X., Liu, B., Liu, J., Ding, J., Han, X., Deng, Y., Lv, X., Xie, Y., Chen, B., Hu, W., & Zhong, C. (2020). Battery Technologies for Grid-Level Large-Scale Electrical Energy Storage. *Transactions of Tianjin University*, *26*(2), 92–103. https://doi.org/10.1007/s12209-019-00231-w

Fedkin, M., & Dutton, J. A. (2018). *Types of PV technology and recent innovations*. EME 812: Utility Solar Power and Concentration. https://www.e-education.psu.edu/eme812/node/608

Florida Solar Energy Center. (2014). *Cells, Modules, & Arrays*. Solar Electricity Basics. http://www.fsec.ucf.edu/en/consumer/solar_electricity/basics/cells_modules_arrays.htm

Fraunhofer ISE. (2013). *World Record Solar Cell with 44.7% Efficiency*. Press Release #22. https://www.ise.fraunhofer.de/en/press-media/press-releases/2013/world-record-solar-cell-with-44-7-efficiency.html

Freitas, S., Serra, F., & Brito, M. C. (2015). Pv layout optimization: String tiling using a multi-objective genetic algorithm. *Solar Energy*, *118*, 562–574. https://doi.org/10.1016/j.solener.2015.06.018

Gallo, A. (2014). *A Refresher on Net Present Value*. Harvard Business Review. https://hbr.org/2014/11/a-refresher-on-net-present-value

Goodrich, A., James, T., & Woodhouse, M. (2012). Residential, commercial, and utilityscale photovoltaic (PV) System prices in the United States: Current drivers and cost-reduction opportunities. *Photovoltaic Costs in the U.S.: Analyses of Prices and Trends*, *February*, 1–58.

Government of the Netherlands. (2016). *A circular economy in the Netherlands by 2050*. 72. https://www.government.nl/binaries/government/documents/policy-notes/2016/09/14/a-circular-economy-in-the-netherlands-by-2050/17037+Circulaire+Economie_EN.PDF

Granger, F. (1925). Vitruvius' Definition of Architecture. *The Classical Review*, *39*(3/4), 67–69. http://www.jstor.org/stable/697676

Granta Design. (2019). *CES EduPack 2019* (19.2.0).

Green, M. A., Dunlop, E. D., Levi, D. H., Hohl-Ebinger, J., Yoshita, M., & Ho-Baillie, A. W. Y. (2019). Solar cell efficiency tables (version 54). *Progress in Photovoltaics: Research and Applications*, *27*(7), 565–575. https://doi.org/10.1002/pip.3171

GSES. (2013). *Metering 101: Understanding metering for rooftop PV systems - GSES India - Global Sustainable Energy Solutions India, Renewable Energy Innovation and Technology Education Training, Engineering, Consulting, Publications*. http://www.gses.in/about-us/news/198-metering-101

Henrie, J., Kellis, S., Schultz, S. M., & Hawkins, A. (2004). Electronic color charts for dielectric films on silicon. *Optics Express*, *12*(7), 1464. https://doi.org/10.1364/opex.12.001464

Hollands, J., & Korjenic, A. (2019). Ansätze zur ökonomischen Bewertung vertikaler Begrünungssysteme. *Bauphysik*, *41*(1), 38–54. https://doi.org/10.1002/bapi.201800033

Honsberg, C. B., & Bowden, S. G. (2019a). Anti-reflection coating color. In *www.pveducation.org*.

Honsberg, C. B., & Bowden, S. G. (2019b). Anti-reflection coatings. In *www.pveducation.org*. https://www.pveducation.org/pvcdrom/design-of-silicon-

cells/anti-reflection-coatings

Infinite Energy. (2019). *Solar Panel Efficiency Explained*. Commercial Solar. https://www.infiniteenergy.com.au/solar-panel-efficiency-explained/

IPEX. (2020). *Fastening methods*. I-Facade® - Facade Mounting Systems. https://www.ipex-group.com/b002?show_pcm=1

Kalzip. (2019). *Kalzip FC Fassadensystem*. https://www.kalzip.com/wp-content/uploads/2020/01/Kalzip-FC-Facade-System-1219_ENG.pdf

Kenton, W. (2020). *Feed-In Tariff (FIT) Definition*. https://www.investopedia.com/terms/f/feed-in-tariff.asp

Konstantinou, T. (2014). Facade Refurbishment Toolbox. In *Bk Books*.

Kutter, C., Bläsi, B., Wilson, H. R., Kroyer, T., Mittag, M., Höhn, O., & Heinrich, M. (2018). Decorated Building-Integrated Photovoltaic Modules: Power Loss, Color Appearance and Cost Analysis. *35th European Photovoltaic Solar Energy Conference and Exhibition*, *1*(September), 1488–1492. https://doi.org/10.4229/35thEUPVSEC20182018-6AO.8.6

Loh, S. (2008). Living walls - A way th green the built environment. *BEDP Environment Design Guide ACT*, *August*, 1–7. http://www.environmentdesignguide.com.au/media/TEC26.pdf

Lombardo, T. (2014). *What Is the Lifespan of a Solar Panel?* Archives. https://www.engineering.com/3DPrinting/3DPrintingArticles/ArticleID/7475/What-Is-the-Lifespan-of-a-Solar-Panel.aspx

Mao, K. (2006). *Engineering Economics Overview and Application in Process Engineering Industry*. 1–13. https://ocw.mit.edu/courses/chemical-engineering/10-490-integrated-chemical-engineering-i-fall-2006/projects/eng_econ_lecture.pdf

Marazzi Engineering. (2019). *Workbook: Soluzioni per l'Architettura-Architectural Solutions*. golinelli.it. www.marazzi.it

Marsh, J. (2018). *Half-cut Solar Cells: What You Need to Know | EnergySage*. Solar 101. https://news.energysage.com/half-cut-solar-cells-overview/

Masson, G., Briano, J. I., & Baez, M. J. (2016). *REVIEW AND ANALYSIS OF PV SELF-CONSUMPTION POLICIES*. https://iea-pvps.org/wp-content/uploads/2020/01/IEA-PVPS_-_Self-Consumption_Policies_-_2016_-_2.pdf

Matasci, S. (2018). *2020 Average Solar Panel Size and Weight*. EnergySage | Solar 101. https://news.energysage.com/average-solar-panel-size-weight/

McCarthy, J. J., Canziani, O. F., Leary, N. A., Dokken, D. J., & White, K. S. (2001). *Climate Change 2001: Impacts, Adaptation and Vulnerability*. Cambridge University Press. http://doi.wiley.com/10.1002/joc.775

MECASOLAR. (2017). *Products – MECASOLAR*. https://mecasolar.com/products/

Mertin, S., Hody-Le Caër, V., Joly, M., Scartezzini, J., & Schüler, A. (2011). Coloured

Coatings for Glazing of Active Solar Thermal Façades By Reactive Magnetron Sputtering. *Proceedings of CISBAT 2011 - CleanTech for Sustainable Buildings*, *1*, 31–36. https://infoscience.epfl.ch/record/174434/files/Mertin_et_al_CISBAT_2011_proceedings.pdf

Mills, A. (2015). *Shining More Light on Solar Panels*. Michigan Technological University News. https://www.mtu.edu/news/stories/2015/october/shining-more-light-solar-panels.html

Milne, G., & Reardon, C. (2013). *Embodied energy*. YourHome. https://www.yourhome.gov.au/materials/embodied-energy

Mittag, M., Kutter, C., Ebert, M., Wilson, H. R., & Eitner, U. (2017). Power loss through decorative elements in the front glazing of BIPV modules. *33rd European Photovoltaic Solar Energy Conference and Exhibition*, *September*, 24–29. https://doi.org/10.4229/EUPVSEC20172017-6BV.3.63

Müller, B., Hardt, L., Armbruster, A., Kiefer, K., & Reise, C. (2016). Yield predictions for photovoltaic power plants: empirical validation, recent advances and remaining uncertainties. *Progress in Photovoltaics: Research and Applications*, *24*(4), 570–583. https://doi.org/10.1002/pip.2616

NDT Resource Center. (2011). *Combined Standard Uncertainty and Propagation of Uncertainty*. General Resouces. https://www.nde-ed.org/GeneralResources/Uncertainty/Combined.htm

Newnan, D. G., Eschenbach, T. G., & Lavelle, J. P. (2004). *Engineering economic analysis* (9th ed.). Oxford University Press.

Nunez, C. (2017). *Deforestation facts and information*. Climate 101: Deforestation. https://www.nationalgeographic.com/environment/global-warming/deforestation/

Odersun. (2011). *Manual for BiPV Projects 1*. https://www.ntnu.no/wiki/download/attachments/40800075/Odersun-BiPV-Download.pdf

Onyx Solar. (n.d.). *Technical Specifications*. Retrieved May 6, 2020, from https://www.onyxsolar.com/product-services/technical-specifications

Palm, J., Tautenhahn, L., Weick, J., Kalio, R., Kullmann, J., Heiland, A., Grinsteid, S., Schmidt, N., Borowski, P., & Karg, F. (2018). BIPV Modules: Critical Requirements and Customization in Manufacturing. *2018 IEEE 7th World Conference on Photovoltaic Energy Conversion, WCPEC 2018 - A Joint Conference of 45th IEEE PVSC, 28th PVSEC and 34th EU PVSEC*, 2561–2566. https://doi.org/10.1109/PVSC.2018.8547306

Passera, A., Lollini, R., Avesani, S., Lovati, M., Maturi, L., & Moser, D. (2018). *BIPV Facades : Market Potential of Retrofit Application in the European Building Stock*. *May*. https://doi.org/10.13140/RG.2.2.24051.63528

Peng, C., Huang, Y., & Wu, Z. (2011). Building-integrated photovoltaics (BIPV) in architectural design in China. *Energy and Buildings*, *43*(12), 3592–3598. https://doi.org/10.1016/j.enbuild.2011.09.032

Pérez, G., Rincón, L., Vila, A., González, J. M., & Cabeza, L. F. (2011). Green vertical systems for buildings as passive systems for energy savings. *Applied Energy*, *88*(12), 4854–4859. https://doi.org/10.1016/j.apenergy.2011.06.032

Perini, K., & Rosasco, P. (2013). Cost-benefit analysis for green façades and living wall systems. *Building and Environment*, *70*, 110–121. https://doi.org/10.1016/j.buildenv.2013.08.012

Reich, N. H., Mueller, B., Armbruster, A., Van Sark, W. G. J. H. M., Kiefer, K., & Reise, C. (2012). Performance ratio revisited: Is PR > 90% realistic? *Progress in Photovoltaics: Research and Applications*, *20*(6), 717–726. https://doi.org/10.1002/pip.1219

Richardson, L. (2019a). *Thin Film Solar Panels: Do They Make Sense?* Buyer's Guide. https://news.energysage.com/thin-film-solar-panels-make-sense/

Richardson, L. (2019b). *Thin film solar panels: do they make sense for residential?* Buyer's Guide. https://news.energysage.com/thin-film-solar-panels-make-sense/

Richter, M., Kalisch, J., Schmidt, T., Lorenz, E., & De Brabandere, K. (2015). Best Practice Guide On Uncertainty in PV Modelling. *Public Report Performance Plus WP2 Deliverable 2.4*, *308991*, 1–37. http://www.perfplus.eu/frontend/files/userfiles/files/308991_PerfPlus_Deliverable_D2_4_20150205.pdf

Robert McNeel & Associates. (2015). *UnifyMeshNormals | Rhino 3-D modeling*. http://docs.mcneel.com/rhino/5/help/en-us/commands/unifymeshnormals.htm

RVO. (2020). *SDE+ Spring 2020. April*.

Sathyanarayana, P., Ballal, R., Lakshmi-Sagar, P. S., & Kumar, G. (2015). *Effect of Shading on the Performance of Solar PV Panel*. *5*(1A), 1–4. https://doi.org/10.5923/c.ep.201501.01

Saur News Bureau. (2016). *Here is how you can calculate the annual solar energy output of a photovoltaic system*. https://www.saurenergy.com/solar-energy-blog/here-is-how-you-can-calculate-the-annual-solar-energy-output-of-a-photovoltaic-system

Schulze, S. H., Pander, M., Ehrich, C., & Ebert, M. (2009). Influence of Vacuum Lamination Process on Laminate Properties – Simulation and Test Results. *Pv-Sec*, *September*, 3367–3372.

Schulze, S. H., Pander, M., Naumenko, K., & Altenbach, H. (2012). Analysis of laminated glass beams for photovoltaic applications. *International Journal of Solids and Structures*, *49*(15–16), 2027–2036. https://doi.org/10.1016/j.ijsolstr.2012.03.028

Sinapis, K., & Donker, M. van den. (2013). BIPV REPORT 2013 State of the art in Building Integrated Photovoltaics. *The Solar Energy Application Centre (SEAC)*, 109. http://www.seac.cc/fileadmin/seac/user/doc/SEAC_BIPV_Report_2013.pdf

Skyrobot Inc. (n.d.). *SKYCOMBINATION®*. Retrieved May 11, 2020, from https://www.skyrobot.co.jp/en/skycombination.html

Smets, A. H. M., Jäger, K., Isabella, O., van Swaaij, R. A. C. M. M., & Zeman, M. (2016). *Solar energy : the physics and engineering of photovoltaic conversion technologies and systems*. UIT.

SolarCare. (n.d.). *Zon PV opbrengst in Nederland in topjaar 2018 : 0,98 kWh/Wp*. Retrieved July 2, 2020, from https://www.solarcare.eu/nl/nieuws/12-gemiddelde-zon-pv-opbrengst-nederland.html

SolarLab. (n.d.). *Energy producing façades*. www.solarlab.dk

Solaxess. (n.d.). *Innovation by color*. Technology. Retrieved May 4, 2020, from https://www.solaxess.ch/en/photovoltaic-panels-pv/innovation-by-color/

Statista. (2016). *LCOE generation costs in the Netherlands 2015-2035*. https://www.statista.com/statistics/974195/estimated-levelized-cost-of-electricity-generation-netherlands/

Statista. (2019). *Prices of electricity for industry in the Netherlands from 2008 to 2018*. Energy & Environmental Services.

SwissINSO. (n.d.). *Kromatix™ Adding Colour to the Solar Industry*. Technology. Retrieved May 5, 2020, from https://www.swissinso.com/technology

Szigeti, F. (2005). The PeBBuCo Study : Compendium of Performance Based (PB) Statements of Requirements (SoR). *Combining Forces - Advancing Facilities Management & Construction through Innovation Series*, 94–107. http://www.irbnet.de/daten/iconda/CIB6737.pdf

Thevenard, D., & Pelland, S. (2013). Estimating the uncertainty in long-term photovoltaic yield predictions. *Solar Energy*, *91*, 432–445. https://doi.org/10.1016/j.solener.2011.05.006

TU Delft. (2018). *Anatomy of the AMC*.

U.S. Department of Energy. (n.d.). *Crystalline Silicon Photovoltaics Research*. Retrieved July 2, 2020, from https://www.energy.gov/eere/solar/crystalline-silicon-photovoltaics-research

Ulrich, R. S. (1984). View through a window may influence recovery from surgery. *Science (New York, N.Y.)*, *224*(4647), 420–421. https://doi.org/10.1126/science.6143402

van der Linden, A. C. (2013). *Building Physics*. ThiemeMeulenhoff. https://books.google.nl/books?id=yWGsmwEACAAJ

Van Sark, W. G. J. H. M., Reich, N. H., Müller, B., Armbruster, A., Kiefer, K., & Reise, C. (2012). Review of PV performance ratio development. *World Renewable Energy Forum, WREF 2012, Including World Renewable Energy Congress XII and Colorado Renewable Energy Society (CRES) Annual Conferen*, *6*(6), 4795–4800.

https://doi.org/10.13140/2.1.2138.7204

van Sark, W., Rutten, G., & Cace, J. (2014). *Inventarisatie PV market Nederland-Status april 2014*. http://www.zonnestroomnl.nl/wp-content/uploads/2014/08/markt-apr2014def.pdf

Van Winden, J. J. N. (2016). *Value and cost assessment of an Integrated Facade as a Product Service System*. https://repository.tudelft.nl/islandora/object/uuid:27dc58f2-3029-4da6-b6b0-753026d0fb03?collection=education

Victron Energy. (2020). *Which solar charge controller: PWM or MPPT?* https://www.victronenergy.com/upload/documents/White-paper-Which-solar-charge-controller-PWM-or-MPPT.pdf

Wagemans, M. (2016). *Modularity of living wall systems*. 200.

Wang, G. (2018). *Technology, manufacturing and grid connection of photovoltaic solar cells*. John Wiley & Sons China Electric Power Press.

Weinmaster, M. (2009). Are Green Walls as "Green" as They Look? An Introduction to the Various Technologies and Ecological Benefits of Green Walls. *Journal of Green Building*, *4*(4), 3–18. https://doi.org/10.3992/jgb.4.4.3

Appendices

Appendix 1: GHPython codes of the components

Tilted BIPV cost calculator (TiltBIPVCost)

Inputs	Outputs
unitCostBIPV: Cost of BIPV per m2 aBIPV: Width of the module in m hBIPV: Height of the module in m unitCostFrame: Cost of the frame material per m2 aFrame: Back rail width tiltAngle: Tilting angle of the panel in degrees	costTiltedBIPV: Cost of 1 tilted BIPV module

Code

```
import math as math

def sin(t):
    return math.sin(math.radians(t))

a = float(aBIPV)
h = float(hBIPV)
a2 = float(aFrame)
c = float(tiltAngle)

if c == 0:
    costTiltedBIPV = a * h * float(unitCostBIPV)

else:
    A1 = h ** 2 * sin(c) / 2
    A2 = 2 * a * h * sin(a / 2)
    A3 = a2 * h

    costTiltedBIPV = ((2 * A1) + A2 + (2 * A3)) * float(unitCostFrame) + a * h *
float(unitCostBIPV)
```

Fisher effect calculator (Fisher)

Inputs	Outputs
nomInterest: Nomimal interest rate Inflation: Inflation rate	real Interest: Real interest rate

Code

```
a = float(nomInterest)
b = float(Inflation)

def fisher():
    c = (1 + a) / (1 + b) - 1
    return c

c = fisher()


realInterest = c
```

Module (panel) efficiency calculator (EffCalc)

Inputs	Outputs
cellEfficiency: Efficiency value for the cells used in the panel. cellArea: Area of the cells, in m2. cellCount: Cell count per panel. coverTransmittance: The fraction of incident solar radiation that is directly transmitted by the upper cover. panelArea: Area of the panel, in m2.	panelEff: Efficiency value for the panel.

Code

```
x = float(cellEfficiency)
y = float(cellArea)
z = float(cellCount)
u = float(coverTransmittance)
v = float(panelArea)

panelEff = x * y * z * u / v
```

Energy yield calculator (EnergyCalc)

Inputs	Outputs
irradiance: Irradiance value, in kWh/m2 panelArea: Surface area of the panels, in m2 panelEff: Efficiency value of the panels, calculated with EffCalc perfRatio: Performance ratio value of the system	energy: The calculated energy yield, in kWh

Code

```
x = float(irradiance)
y = float(panelArea)
z = float(panelEff)
u = float(perfRatio)

energy =  x*y*z*u
```

Energy selling price calculator (EnPrice)

Inputs	Outputs
energyPrice: Energy price, in Euros. subsidyAmount: Subsidy amount, in Euros. systemLifetime: Project lifetime, in years. subsidyDur: Possible subsidy duration, in years.	enPricePerYear: The energy selling price value for each year, in Euros

Code

```
x = float(energyPrice)
y = float(subsidyAmount)
z = int(systemLifetime)
u = int(subsidyDur)

a = []

if z <= u:
    for v in range(z):
        a.append(x+y)
else:
    for v in range(u):
        a.append(x+y)
    for v in range(z-u):
        a.append(x)

enPricePerYear = a
```

Lifetime energy generation and revenue calculator (LifetimeGen)

Inputs	Outputs
energyRes: A year's revenue of the system, in kWh. systemLifetime: Expected lifetime of the system, in years. annualPVDecay: Degradation rate of the PV-cells used in the module, in percentage, value or list of values. enPricePerYear : Energy price, value or list of values.	totalGen: Total enery yield by the end of lifetime, in kWh. genPartialResults: Partial energy yield by the year t, in kWh. genByYear: Energy generatation for each year, in kWh. totalRev: Total revenue from electricity, in Euros. revPartialResults: Partial revenue by the year t, in Euros. revByYear: Revenue for each year, in Euros

Code

```
x = energyRes
y = systemLifetime
z = annualPVDecay
u = enPricePerYear

a = 0
b = []
c = []

b.append(int(x))
c.append(int(x))

d = int(x) * float(u[0])
e = []
```

```
f = []
e.append(d)
f.append(d)

ui = 1
zi = 0

def gent():
    return c[-1] * (1 - (float(z[zi]) / 100))

if len(z) == 1:
    for v in range(int(y)-1):
        a += gent()
        b.append(a)
        c.append(gent())
        d += gent() * float(u[ui])
        e.append(d)
        f.append(gent() * float(u[ui]))
        ui = ui + 1
elif len(z) == int(y):
    for v in range(int(y)-1):
        a += gent()
        b.append(a)
        c.append(gent())
        d += gent() * float(u[ui])
        e.append(d)
        f.append(gent() * float(u[ui]))
        ui = ui + 1
        zi += 1
elif len(z) < int(y) and len(z) > 1 or len(z) == 0:
    print("annualPVDecay list too short.")

genTotal = a
genPartialResults = b
genByYear = c
revTotal = d
revPartialResults = e
revByYear = fenPricePerYear = a
```

Lifetime expenditures calculator (LifetimeExp)

Inputs	Outputs
initialInvestmentC: System's initial investment cost, in EUR. annualVariableC: Annual expenditures, in EUR, value or list of values systemLifetime: Expected lifetime of the system, in years.	totalExp: Total expenses at the end of system's lifetime, in EUR. partialExp: Expenses by the year t, in EUR expByYear: Expense in the year t

Code

```
x = initialInvestmentC
y = annualVariableC
z = systemLifetime

a = 0
b = []
c = []

t = range(int(z))

yi = 0
def yt():
    yt = float(y[yi])
    return float(yt)

if len(y) == 1:
    a = float(x)
    b.append(a)
    c.append(a)
    def vet():
        vext = float(yt())
        return vext
    for v in t[1:int(z)]:
        a += vet()
        b.append(a)
        c.append(yt())


elif len(y) == int(z):
    a = float(x)
    c.append(a)
    for v in t[1:int(z)+1]:
        yi = yi + 1
        a += yt()
        b.append(a)
        c.append(yt())


totalExp = a
partialExp = b
expByYear = c
```

Net present value calculator (NPV)

Inputs	Outputs
netCashFlow: Net cash flow at the year t, in Euros. discountRate: Discount or interest rate. systemLifetime: System lifetime, in years.	totalNPV: Net present value, in Euros. partialNPV: Partial sums of NPVs, in Euros. NPVByYear: Isolated NPV of the year t, in Euros.

Code

```
x = netCashFlow
y = float(discountRate)
z = int(systemLifetime)

a = 0
b = []
c = []

xi = 0
zt = 1

for v in range(z):
    d = float(x[xi]) / ((1 + y) ** zt)
    c.append(d)
    a += d
    b.append(a)
    xi += 1
    zt += 1

totalNPV = a
partialNPV = b
NPVByYear = c
```

Levelised cost of electricity calculator (LCoE)

Inputs	Outputs
negativeCashFlow: List of expenditure until year t genByYear: Annual energy generation list until year t. discountRate: Discount or interest rate systemLifetime: year t	LCoE: Levelised cost of energy at the year t

Code

```
x = negativeCashFlow
y = genByYear
z = float(discountRate)
u = int(systemLifetime)

a = 0

xi = 0
yi = 0
ut = 1

def xt():
    return float(x[xi])
def yt():
    return float(y[yi])
for v in range(u):
    a += (xt() / ((1 + z) ** ut)) / (yt() / ((1 + z) ** ut))
    xi = xi + 1
    yi = yi + 1
    ut = ut + 1

LCoE = a
```

Payback time calculator regarding TVM (PaybackTVM)

Inputs	Outputs
partialNPV: The partial NPV value tree from the NPVByYear component.	paybackTime: The payback time regarding the TVM

Code

```
x = partialNPV
xi = 0

def t():
    m = (float(x[xi]) - float(x[xi-1]))
    return xi - float(x[xi]) / m
for v in x:
    if float(x[xi]) >= 0:
        result = t()
    elif xi == len(x) - 1:
        result = 0
    else:
        xi += 1
paybackTime = result
```

Iterative optimiser (Optimisation)

Inputs	Outputs
budget: Budget of the project, in Euros. priceBIPV: Price of a single BIPV panel, in Euros. npvBIPV: Net present value partial summation list of BIPV panels, in Euros (ascending sort). priceLWS: Price of a single LWS panel, in Euros. npvLWS: Net present value of a single LWS panel, in Euros. paybackAmount: Required payback at the end of the project lifetime, in Euros.	countBIPV: Optimum number of BIPV panels. countLWS: Optimum number of LWS panels. NPV: Net present value of the project iterations, in Euros.

Code

```
B = float(budget)
pb = float(priceBIPV)
pg = float(priceLWS)
mb = npvBIPV
mg = float(npvLWS)

nb = 1
n = []

def tpb():
    return pb * nb
def numg():
    return (B - tpb()) // pg
def tpg():
    return pg * numg()

def NPV():
    return float(mb[nb - 1]) - (numg() * mg)

while tpg() >= 0:
    n.append(NPV())
    nb += 1

nb = 1
y = float(paybackAmount)


while float(n[nb - 1]) < y and nb < len(n):
    nb += 1

countBIPV = nb
countLWS = numg()
NPV = n
```

Appendix 2: Optimisation flowchart

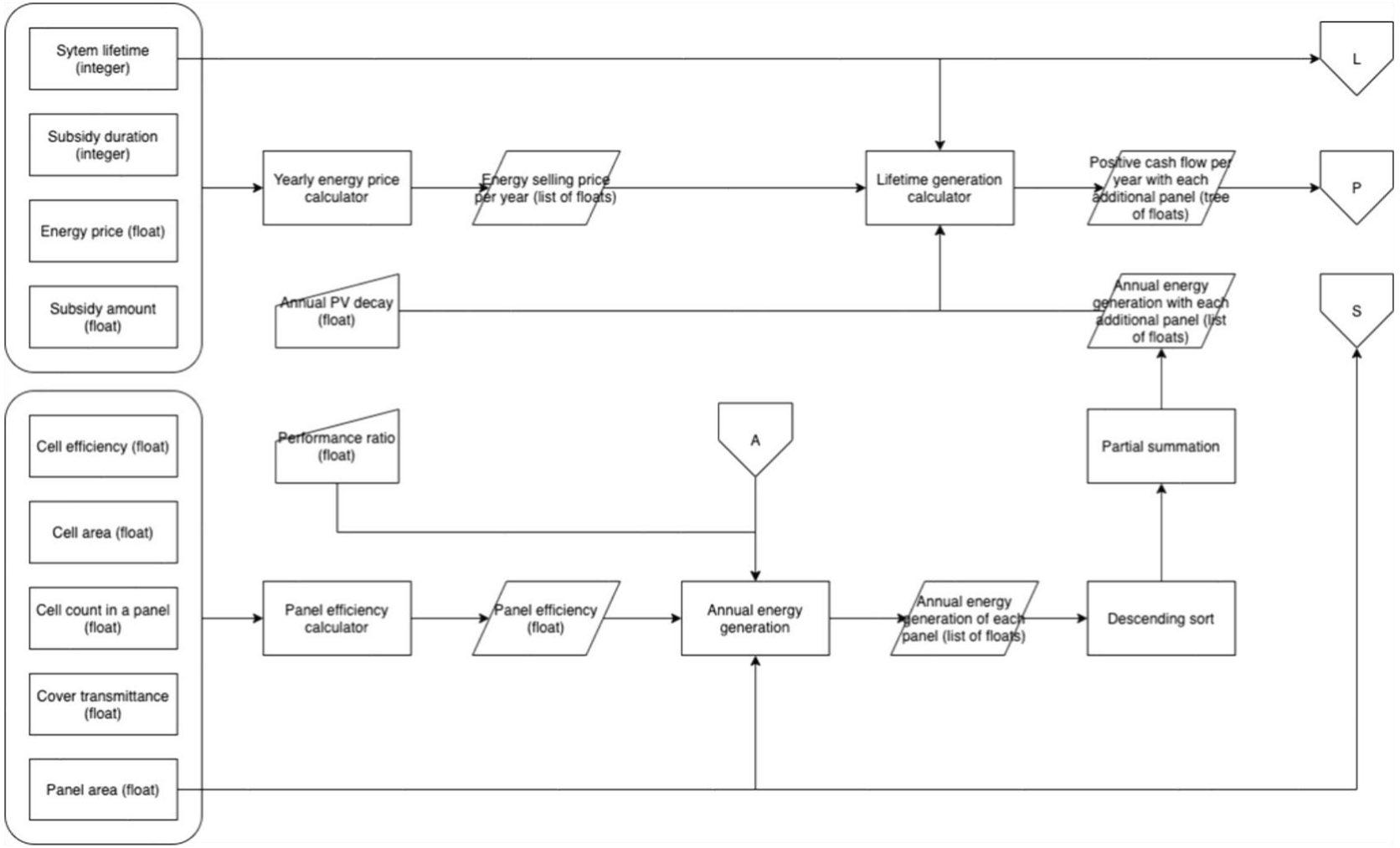

Figure 91: Optimisation flowchart, part 1 (positive cash flows).

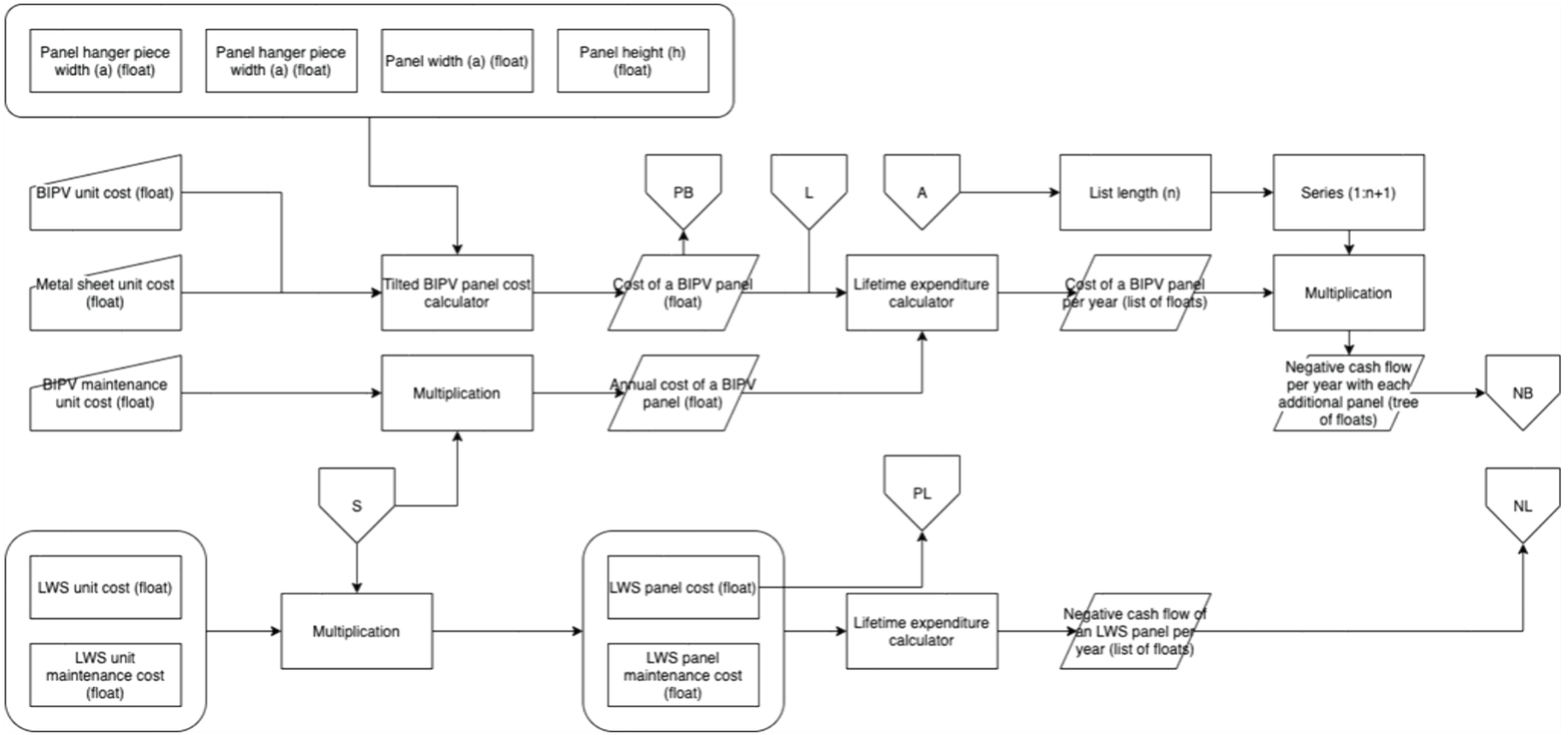

Figure 92: Optimisation flowchart, part 2 (negative cash flows).

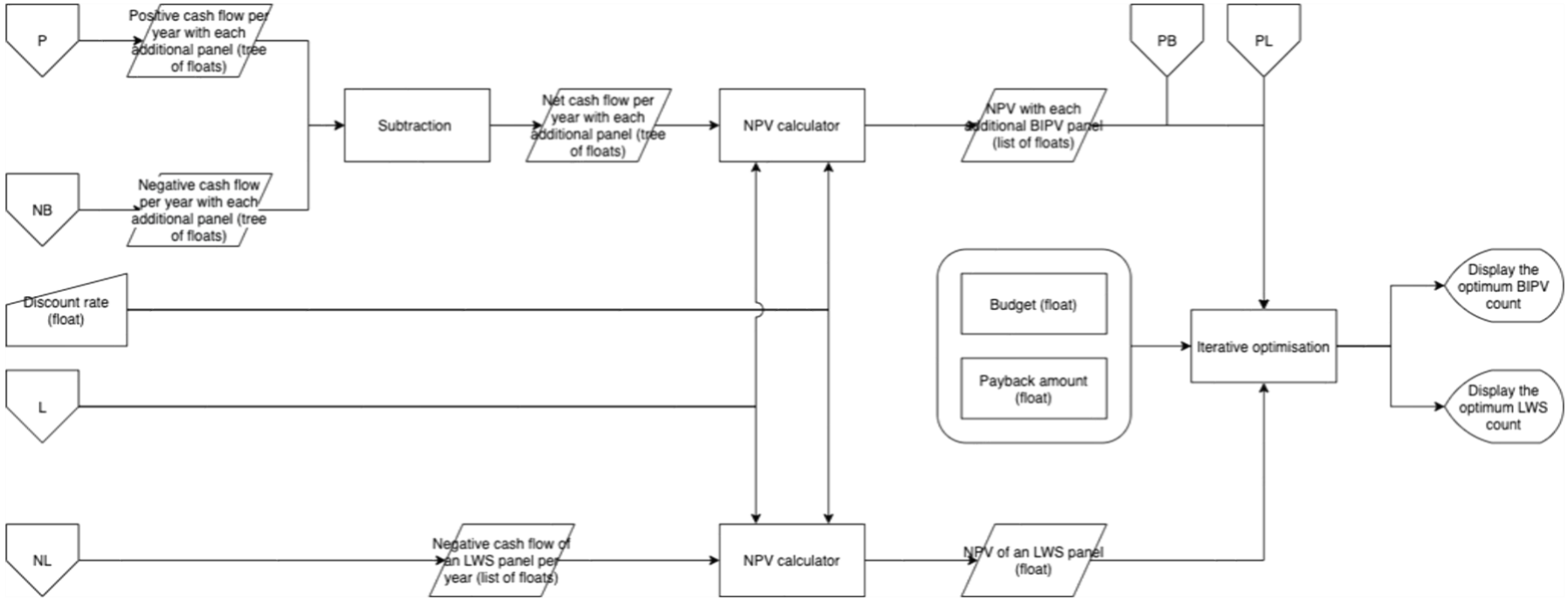

Figure 93: Optimisation flowchart, part 3 (optimising panel counts).

Appendix 3: Analysis flowchart

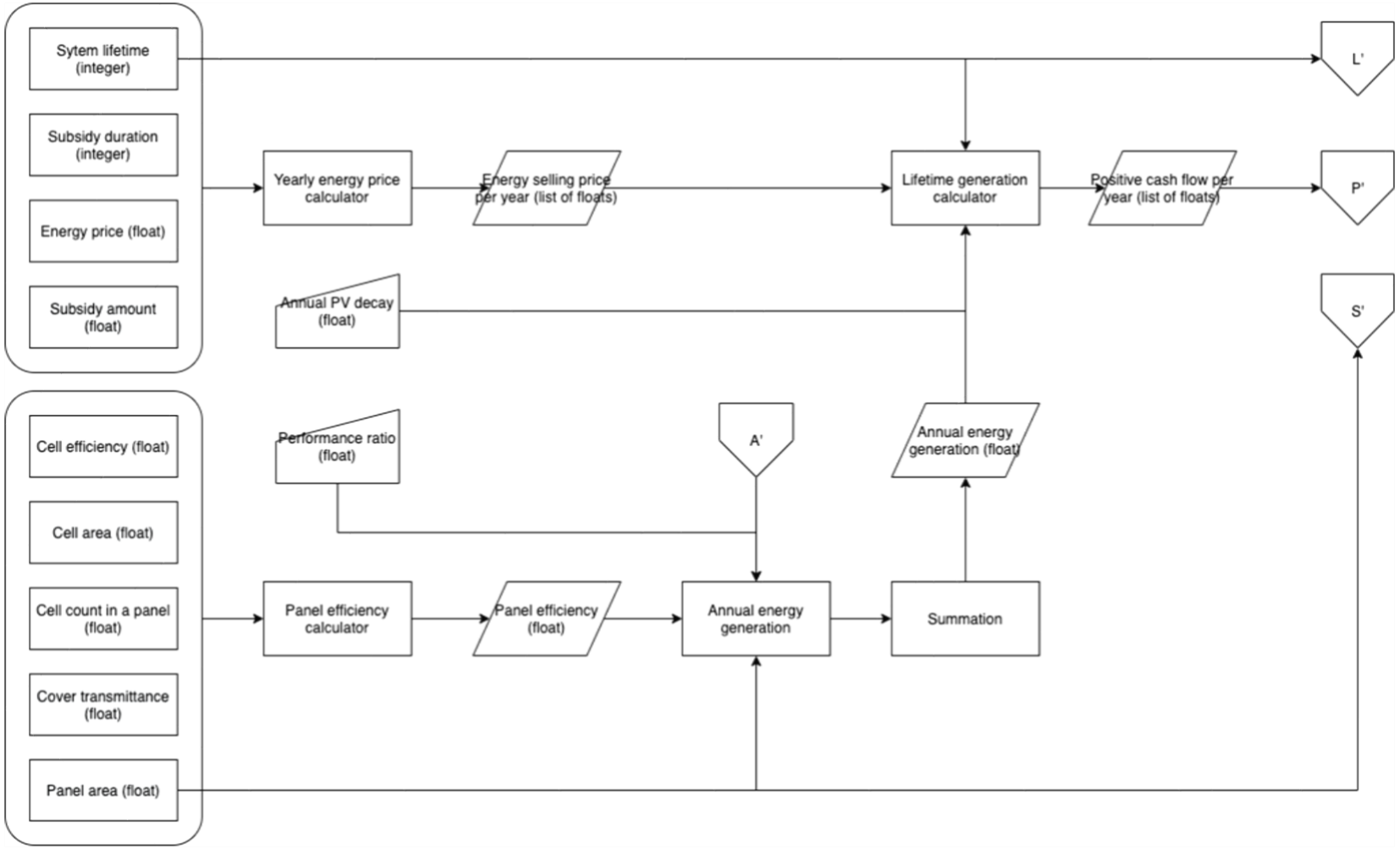

Figure 94: Analysis flowchart, part 1 (positive cash flows).

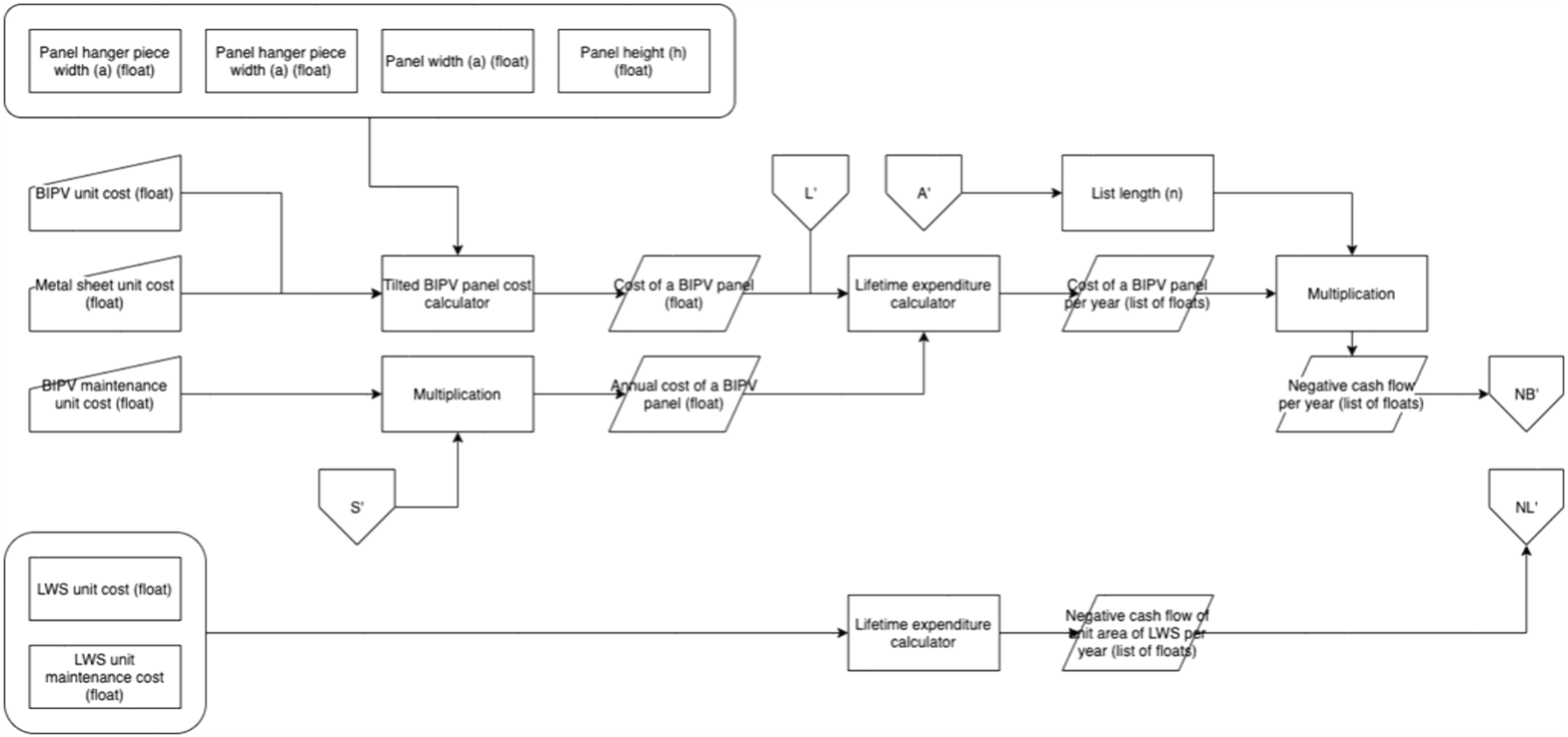

Figure 95: Analysis flowchart, part 2 (negative cash flows).

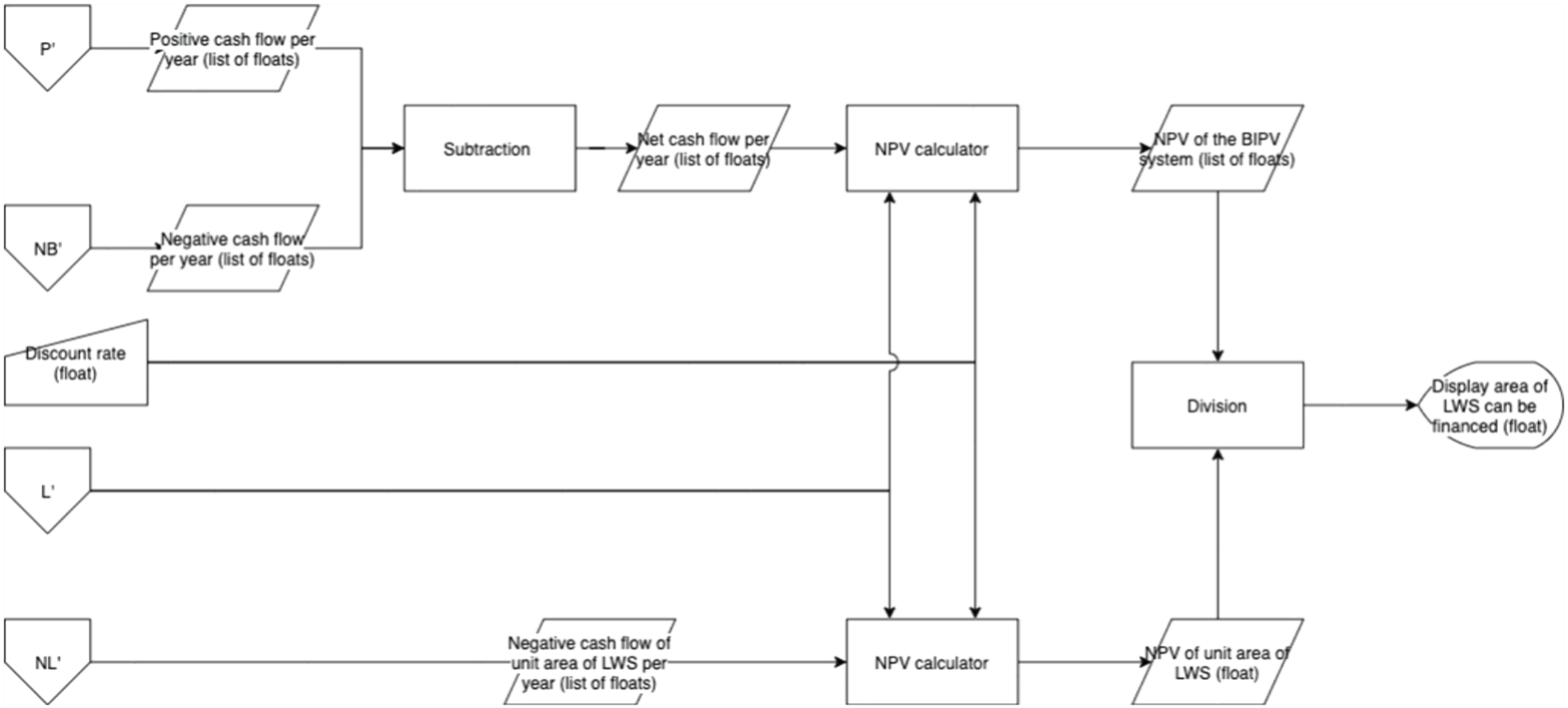

Figure 96: Analysis flowchart, part 3 (finding the area of LWS can be financed)

Appendix 4: Cash flow graphs

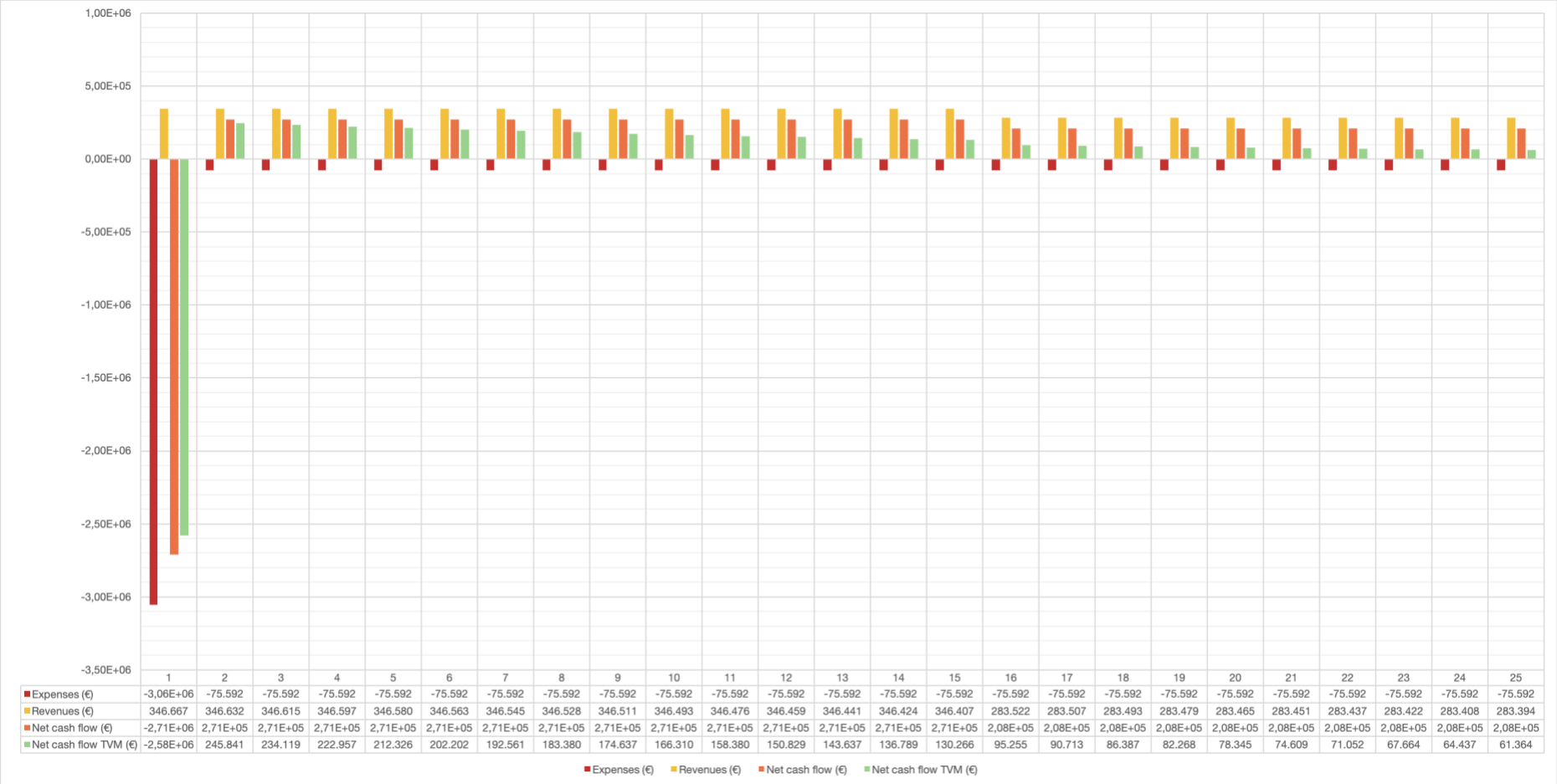

	1	2	3	4	5	6	7	8	9	10	11	12	13	14	15	16	17	18	19	20	21	22	23	24	25
Expenses (€)	-3,06E+06	-75.592	-75.592	-75.592	-75.592	-75.592	-75.592	-75.592	-75.592	-75.592	-75.592	-75.592	-75.592	-75.592	-75.592	-75.592	-75.592	-75.592	-75.592	-75.592	-75.592	-75.592	-75.592	-75.592	-75.592
Revenues (€)	346.667	346.632	346.615	346.597	346.580	346.563	346.545	346.528	346.511	346.493	346.476	346.459	346.441	346.424	346.407	283.522	283.507	283.493	283.479	283.465	283.451	283.437	283.422	283.408	283.394
Net cash flow (€)	-2,71E+06	2,71E+05	2,71E+05	2,71E+05	2,71E+05	2,71E+05	2,71E+05	2,71E+05	2,71E+05	2,71E+05	2,71E+05	2,71E+05	2,71E+05	2,71E+05	2,71E+05	2,08E+05	2,08E+05	2,08E+05	2,08E+05	2,08E+05	2,08E+05	2,08E+05	2,08E+05	2,08E+05	2,08E+05
Net cash flow TVM (€)	-2,58E+06	245.841	234.119	222.957	212.326	202.202	192.561	183.380	174.637	166.310	158.380	150.829	143.637	136.789	130.266	95.255	90.713	86.387	82.268	78.345	74.609	71.052	67.664	64.437	61.364

Figure 97: Detailed version of Figure 89.

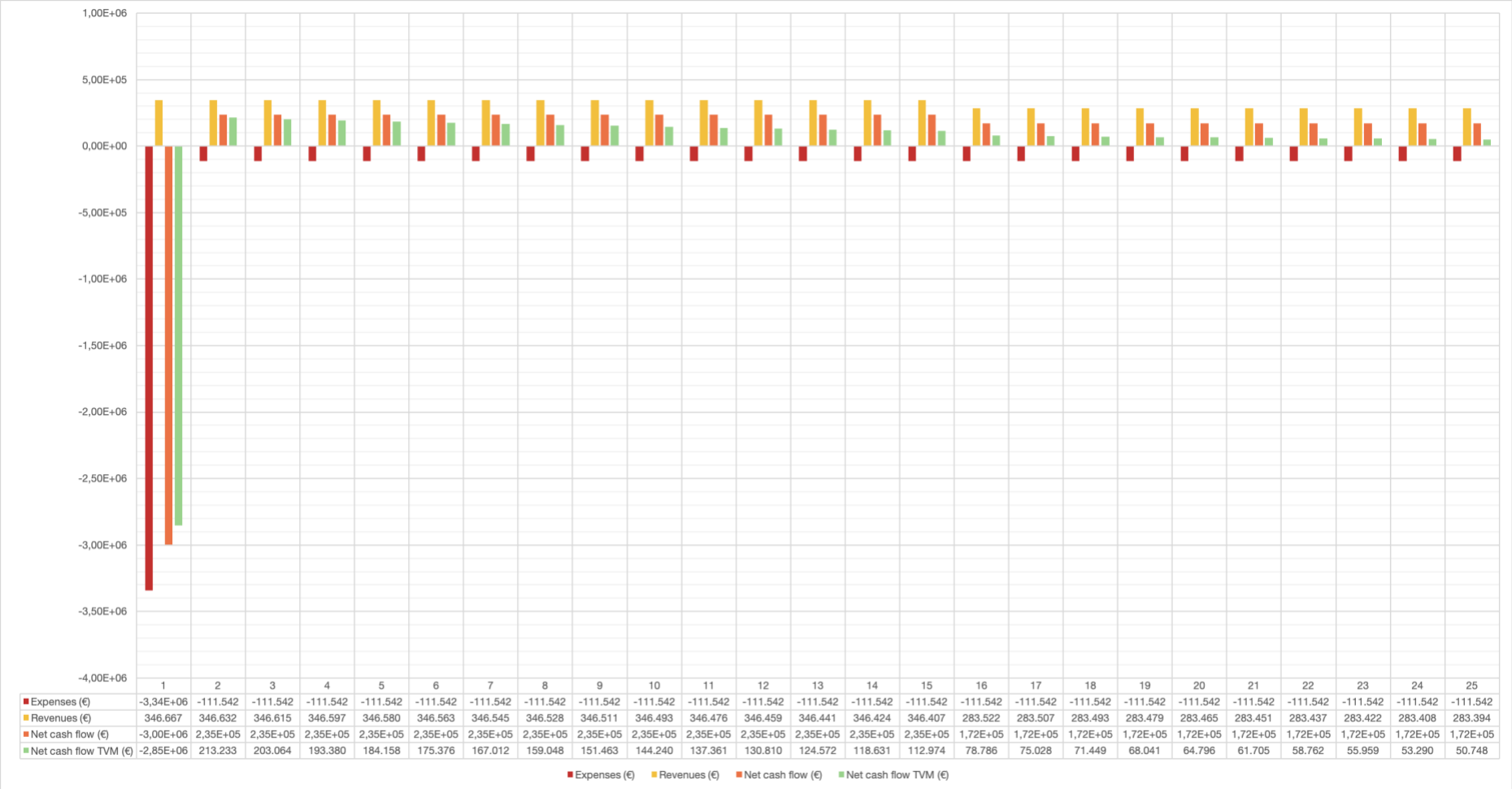

	1	2	3	4	5	6	7	8	9	10	11	12	13	14	15	16	17	18	19	20	21	22	23	24	25
Expenses (€)	-3,34E+06	-111.542	-111.542	-111.542	-111.542	-111.542	-111.542	-111.542	-111.542	-111.542	-111.542	-111.542	-111.542	-111.542	-111.542	-111.542	-111.542	-111.542	-111.542	-111.542	-111.542	-111.542	-111.542	-111.542	-111.542
Revenues (€)	346.667	346.632	346.615	346.597	346.580	346.563	346.545	346.528	346.511	346.493	346.476	346.459	346.441	346.424	346.407	283.522	283.507	283.493	283.479	283.465	283.451	283.437	283.422	283.408	283.394
Net cash flow (€)	-3,00E+06	2,35E+05	2,35E+05	2,35E+05	2,35E+05	2,35E+05	2,35E+05	2,35E+05	2,35E+05	2,35E+05	2,35E+05	2,35E+05	2,35E+05	2,35E+05	2,35E+05	1,72E+05	1,72E+05	1,72E+05	1,72E+05	1,72E+05	1,72E+05	1,72E+05	1,72E+05	1,72E+05	1,72E+05
Net cash flow TVM (€)	-2,85E+06	213.233	203.064	193.380	184.158	175.376	167.012	159.048	151.463	144.240	137.361	130.810	124.572	118.631	112.974	78.786	75.028	71.449	68.041	64.796	61.705	58.762	55.959	53.290	50.748

Figure 98: Detailed version of Figure 90.